DEVELOPMENT, ANALYSIS, AND APPLICATION OF A WELL BY WELL METHOD FOR ESTIMATING SURFACE HEAT FLOW FOR REGIONAL GEOTHERMAL RESOURCE ASSESSMENT

A Thesis

Presented to the Faculty of the Graduate School

of Cornell University

in Partial Fulfillment of the Requirements for the Degree of

Master of Science

by

George Raymond Stutz

August 2012

ABSTRACT

The potential to utilize widespread low-grade geothermal resources of the Northeastern U.S. for thermal direct use and combined heat and power applications can be realized using technologies embodied in Enhanced Geothermal Systems (EGS). In lower grade regions, accurate knowledge of small variations in temperature gradient will be crucial to the economic viability of EGS development. To accurately map local temperature variations, resource assessments have relied largely on bottom hole temperature (BHT) measurements, primarily from oil and gas wells. As the volume of BHT data grows due to increased drilling activity, the ability to quickly analyze and incorporate additional data is critical. To accomplish this task, a thermal model was developed that is a refined and streamlined version of work previously started at Southern Methodist University (SMU) to map out the heat flow of the entire nation. The model developed for this work expands on their contributions and makes it much easier to incorporate the large amounts of data collected. Also, by being developed in Visual Basic for Applications, an Excel add-on, it is hoped that the model will help researchers at all levels of academia, government, and private industry look to EGS as a possible energy source.

In order to facilitate EGS project placement and design, the model was used to draw a more complete picture of geothermal resources in the Northeastern United States, with a particular focus on New York and Pennsylvania, by incorporating thousands of new temperature-depth data collected as a result of continuing drilling for unconventional natural gas in the region. This project follows the entire evolution of an organic geothermal resource study from data collection to map production. Well data in the form of archived oil and gas well logs were collected from SMU, the Pennsylvania Geological Survey, the New York State Museum, and the New York State Department of Environ-

mental Conservation. Using these new data, a series of maps covering the Appalachian Basin of New York and Pennsylvania were produced that show variations in subsurface thermal gradient and surface heat flow.

The increased spatial accuracy and resolution compared to earlier geothermal maps of the Northeast U.S. illuminate better spatial variations in the resource quality and have a much smaller degree of uncertainty in both extent and magnitude. The maps indicate that the temperatures required for direct-use applications are available at technically viable drilling depths over a majority of the region. Smaller hot spot areas of higher than average heat flow are found in the Pennsylvania counties of Indiana, McKean, Lawrence, and Warren, as well as Cayuga County in New York. These anomalies represent the most ideal candidates for further exploration and characterization of their EGS potential.

The model was then subjected to rigorous uncertainty analysis using Oracle Crystal Ball, a commercially available Monte Carlo simulator. This work integrated increasing complexity in the sedimentary cover of the Appalachian basin to test the precision of the predicted temperature at 6 km under Steuben County, NY. The results indicate that while the model does have inherent limitations that the user must be mindful of, it predicts temperature to a degree of precision and accuracy that is reasonable given its original purpose of incorporating very large datasets in an efficient manner.

BIOGRAPHICAL SKETCH

George Stutz was born August 11, 1985 in Denver, Colorado, the only child of Herbert and Sharon Stutz. He graduated from Iver C. Ranum High School in Denver in 2004 where he competed in football, track and field, and Knowledge Bowl, a statewide interdisciplinary academic competition. After high school he attended the Colorado School of Mines (CSM). Majoring in petroleum engineering, he received a Bachelor of Science Degree in 2008. While at CSM he joined the Order of the Engineer and was admitted to Pi Epsilon Tau, the Petroleum Engineer Honor Society, for his high academic record within his chosen major. Additionally he was an active student member of the Society of Petroleum Engineers (SPE) and the American Association of Drilling Engineers (AADE), holding an officer's position in AADE as a senior. In the summer of 2006, George worked at Questar Exploration and Production as an engineering intern. This was followed by a summer in Oklahoma City working for Devon Energy Company, again as an engineering intern.

Upon graduating, George accepted a full time petroleum engineering position with Questar Exploration and Production and moved to Pinedale, WY. He would spend the next year in the field learning about natural gas production, drilling, and completions processes. Following this year in the field, he relocated to Denver where he became a production and reservoir engineer on the Pinedale asset team.

George entered the graduate program in the Earth and Atmospheric Sciences Department at Cornell University in 2010 to pursue a MS degree under the guidance of Jefferson Tester and Teresa Jordan. George spent the summer of 2011 as an intern with Shell exploration and Production Company in New Orleans, Louisiana. At Shell he worked as a geology intern on the Mars Team. This dissertation represents the culmination of research completed during George's two years at Cornell University.

This document is dedicated to all my friends and family who have provided support.

ACKNOWLEDGEMENTS

Countless people have helped me during my time at Cornell, including fellow graduate students, professors, university staff, personal friends outside of school, past coworkers, and my family. All of these people have given me help, guidance and the courage to return to graduate school in the first place.

First and foremost I would like to thank Jefferson Tester, my principal advisor at Cornell University. Jeff has been the source of much encouragement, feedback, and personal and financial support over the last two years. It was through his tutelage that I have become a better researcher, scientist, and critical thinker. In addition to Jeff, Teresa Jordan, my secondary advisor, has been a great source of knowledge and support. Her expertise as a geologist and knowledge of the geology specific to the Northeastern United States has been invaluable the last two years. I have enjoyed working with Terry both in and out of the classroom, and there is no doubt none of this would have been possible without her.

Next I would like to say thank you to Andrea Aguirre, Elaina Shope, and Tim Reber. It has been a great experience to work directly with all of you on this project for the last two years. The lessons, both formal and informal, that I have learned from you will help me forever as a student and person. Also there is no denying that if it were not for the four of us working together, none of this would have been completed to as high of quality or in the same time frame. It has been a pleasure to share my time at Cornell with you.

I would also like to sincerely thank Krysta Biniek for her un-wavering support over the last several years. She is the biggest reason for my graduating from the Colorado School of Mines and making the leap back into graduate school. Without her constant support I never would have imagined I could attend a university such as Cornell. Over the last two years it was continued encouragement that got me through grad school.

It was her presence that kept me at it and has led directly to this dissertation and to graduating once again.

Next I would like to thank my family who have offered their time, support, and of course finances over the years. I would not be here today without them.

To all the friends I have made at Cornell, Southern Methodist University, and everyone at the schools and government organizations we have worked with over the last two years. Specifically David Blackwell, Maria Richards, Mitchell Williams, Zach Frone, Joe Batir, Ryan Dingwall, and Cathy Chickering at SMU, this work is due in large part to your help and patience.

Finally thank you to all the wonderful staff and facility at Cornell that I have not mentioned thus far. Everyone in the EAS department was willing to provide great instruction and guidance over the last two years. I could not have asked for a better group to work with. Special thanks to Savannah Sawyer in the EAS main office.

TABLE OF CONTENTS

Biographical Sketch . . . iii
Dedication . . . iv
Acknowledgements . . . v
Table of Contents . . . vii
List of Tables . . . ix
List of Figures . . . x

1 MOTIVATION AND APPROACH 1
1.1 Motivation . . . 1
1.2 Approach and Methods . . . 2
1.2.1 Data Collection . . . 4
1.2.2 BHT Corrections . . . 4
1.2.3 Sedimentary Thickness Scaling . . . 5
References . . . 9

2 A WELL BY WELL METHOD FOR ESTIMATING SURFACE HEAT FLOW FOR REGIONAL GEOTHERMAL RESOURCE ASSESSMENT 11
2.1 Motivation and Scope . . . 11
2.2 Existing Methodology for Heat Flow Estimation . . . 14
2.3 New Method For Heat Flow And Subsurface Temperature Estimation . . . 19
2.3.1 Estimating Surface Heat Flow . . . 19
2.3.2 Modeling Temperature at Depth . . . 25
2.4 Example Case Evaluated . . . 28
2.5 Conclusions and Future Work . . . 38
References . . . 40
Appendix . . . 44

3 UNCERTAINTY ANALYSIS OF THE THERMAL MODEL TO PREDICT HEAT FLOW AND SUBSURFACE TEMPERATURE 48
3.1 Motivation and Background . . . 48
3.2 Sample Well Selection . . . 50
3.3 Uncertainty in Temperature Reading . . . 53
3.4 Variability in Individual Formation Thickness . . . 56
3.5 Variability in Thermal Conductivity . . . 58
3.6 Variability in Total Sediment Thickness . . . 64
3.7 Property Variation in Relation to Case Study Selections . . . 68
3.8 Case 1 . . . 69
3.8.1 Sensitivity to Input Parameters . . . 69
3.8.2 Case 1 Uncertainty . . . 70
3.9 Case 2 . . . 76
3.9.1 Refined Subdivision of Stratigraphic Units . . . 76
3.9.2 Scaling to the Tully . . . 79

3.9.3 Sensitivity to Input Parameters 80
3.9.4 Case 2 Uncertainty 80
3.10 Case 3 86
3.10.1 The Hamilton Group 87
3.10.2 The Syracuse Formation 88
3.10.3 The Queenston Formation 91
3.10.4 Case 3 Uncertainty 94
3.11 Additional Uncertainties 99
3.11.1 Basement Rock Thermal Conductivity 99
3.11.2 Basement Radiogenic Heat Generation 100
3.12 Accuracy Validation 102
3.13 Conclusions and Future Work 104
References 106

4 Conclusions and Outcomes **110**

5 Appendix **112**

LIST OF TABLES

3.1 Well information for the 6 wells selected for uncertainty analysis in Steuben County, New York. 51
3.2 COSUNA Stratigraphic Column as applied in Case 1 57
3.3 Statistical Summary Data for Case 1 75
3.4 Revised Stratigraphic Column for Case 2 77
3.5 Data on the well files from ESOGIS consulted to construct the Case 2 Stratigraphic Column 78
3.6 Statistical Summary Data for Case 2 85
3.7 Statistical Summary Data for Case 3 98

LIST OF FIGURES

1.1 Comparison of equilibrium temperature to bottom hole temperature data 6
1.2 The thickness of the sedimentary units within the Appalachian Basin of New York and Pennsylvania 7

2.1 Geologic conductivity and radioactivity models for calculation 18
2.2 Well data input for processing and calculation of heat flow and temperature 21
2.3 Stratigraphic column from COSUNA (1985) representing the thickness and conductivity data for Pennsylvania Section 17 23
2.4 Scaling of thickness to anticipated well location. 24
2.5 Chart of 5 equilibrium wells (PA-6, PA-7, PA-8, PA-9, and PA-11) and 11 nearby BHT point wells (labeled by API number) calculated using the VBA thermal modeling routine 31
2.6 Chart of 5 equilibrium wells (P-6, P-7, P-8, P-9, and P-11) and 11 nearby BHT point wells (labeled by API number) calculated using the VBA thermal modeling routine to 10 km depth 32
2.7 Modeled output of geothermal properties for a selection of wells in Westmoreland County, PA 33
2.8 Map of calculated heat flow from well BHT data for NY and PA 34
2.9 Map of wells located in Westmoreland County, PA processed as an example in this study. 35
2.10 Map of anticipated depth to the 80 °C isothermal surface 37
2.11 Decision for Thermal Model Temperature Prediction 44

3.1 Map of New York showing the location of the 6 Steuben County wells being analyzed 52
3.2 Map of a Section of Western New York showing location of the 6 selected wells in Steuben County (marked in black) and the wells with formation tops and other data consulted from the ESOGIS (2012) website 53
3.3 Example BHT Variability for Well #00170 55
3.4 Maps of North America during the Cretaceous and the Devonian 60
3.5 Scan of thermal conductivity data (Zoth and Haenel, 1988) 62
3.6 Limestone Thermal Conductivity Distribution Function 63
3.7 Sandstone Thermal Conductivity Distribution Function 63
3.8 Shale Thermal Conductivity Distribution Function 64
3.9 Histogram and Cumulative Distribution Function for the limestone lithology 65
3.10 Histogram and Cumulative Distribution Function for the sandstone lithology 66
3.11 Histogram and Cumulative Distribution Function for the shale lithology 67
3.12 Total Sediment Thickness Modeled Distribution Function for 10,000 trial Monte Carlo Simulation 68

3.13 Sensitivity diagrams for the 6 modeled wells in Steuben County, NY Case 1 73
3.14 Box and whisker plot for the Case 1 uncertainty 76
3.15 Sensitivity diagram for each of the 6 wells in Steuben County, NY Case 2 84
3.16 Box and whisker plot for the Case 2 uncertainty 86
3.17 Total drilled depth correlated box and whisker plot for the Case 2 uncertainty 87
3.18 Appalachian Basin Black Shale Thermal Conductivity Distribution Function 89
3.19 Halite Thermal Conductivity Distribution Function 90
3.20 Dolomite Thermal Conductivity Distribution Function 90
3.21 Syracuse Formation Total Thermal Conductivity Distribution Function 91
3.22 Hematite Thermal Conductivity Distribution Function 92
3.23 Queenston Total Thermal Conductivity Distribution Function 93
3.24 Diagram of sensitivity of the calculated surface heat flow to the parameters tested for the 6 modeled wells in Steuben County, NY Case 3 . . 97
3.25 Box and whisker plot for the Case 3 uncertainty 99
3.26 Histogram of basement rock heat generation (μW/m^3) from measurements in California, Nevada, and Oregon compared to calculated values by Shope et al. (2012). 101
3.27 Cumulative distribution functions for basement rock heat generation from measurements in CA, NV, and OR compared to calculated values by Shope et al. (2012). 102

CHAPTER 1

MOTIVATION AND APPROACH

1.1 Motivation

The primary goal of this work is to present tools and techniques to map the geothermal resource potential of broad regions in order to provide support for developers of geothermal energy by reducing the cost and risk associated with resource identification and exploration. These costs and risks are one prohibitive block to wider adoption of geothermal energy exploitation, especially Enhanced or Engineered Geothermal Systems (EGS), in large areas of the United States. Currently maps and other assessments of geothermal energy are both incomplete and inadequate over many parts of the country and are sometimes inaccurate. They lack the detailed spatial granularity needed to move development forward. The tools presented here support developers of geothermal energy by helping to overcome this pitfall.

As hydrocarbons lose popularity due to their depletable nature as well as increased social and political pressure, the will for more environmentally benign energy sources will increase. By completing this work, geothermal energy will be better positioned as an option, not only for electricity generation, but also for direct thermal usage. Several previous thermal assessments have identified that the energy available from EGS systems may be enormous (Armstead and Tester, 1987; Rowley, 1982; Mock et al., 1997; Tester et al., 1994; Sass, 1993). However, these previous works did not take into account detailed geologic information and therefore are simplified by necessity. Later works, namely Blackwell and Richards (2004), Tester et al. (2006), and Blackwell et al. (2007), did incorporate such information and therefore represented a much more precise assessment of geothermal resources, yet issues still remained with these new ap-

proaches. This thesis was undertaken in an attempt to resolve some of those remaining issues. The main issues addressed are, first, related to efficient handling of large amounts of data, and second, to the consequences of simplifications that may be adopted in order to be efficient.

Additionally, the majority of previous research and development has focused on the use of geothermal for large-scale electric generation. Expansion of geothermal as a direct thermal energy source is a secondary goal of the author and fellow researchers at Cornell University. Much of the discussion within the following Chapters addresses this, and many of the maps and dialogue depict low grade resources, such as the 80 °C isotherm in Figure 2.6. By developing these tools that not only map out heat flow but can predict temperature over a wide range of depths, costs and risk are reduced, to the betterment of the prospects for EGS use.

All goals were to be met under DOE Contract #DE-EE0002852 whose principal investigator was David Blackwell at Southern Methodist University (SMU). During the course of research at Cornell University, several of the members travelled to SMU to gain first hand experience of how SMU had been approaching its assessment work in the past. The overall objective following this meeting was to use the collected well data from wells in states within the northeastern United States, primarily from oil and gas production, to generate a revised heat flow and temperature at depth maps for these areas based on the techniques and methods of SMU.

1.2 Approach and Methods

To accurately map local temperature variations with depth and local geothermal gradient, resource assessments have relied largely on bottom hole temperature (BHT) mea-

surements, primarily from oil and gas exploration and development. The four students on this project, Andrea Aguirre, Timothy Reber, Elaina Shope, and myself, assembled data for over 5,000 new BHT points for incorporation into existing maps. Collectively we have been known as the Geothermal Resource Assessment (GRA) group within the Tester Lab. The overall objective of the GRA group was to gather well data, primarily from oil and gas production, on wells in states within the northeastern United States and turn that data into revised heat flow and temperature at depth maps for these areas based on the techniques and methods of Southern Methodist University (Blackwell et al., 2007). This thesis documents my contributions to this process.

The second chapter of this thesis was originally presented at the 37th Annual Stanford Geothermal Workshop January 30 to February 1, 2012 as a companion paper to Shope et al. (2012). Chapter 2 contains details of the techniques utilized to process the well data and construct the maps in Shope et al. (2012). These techniques were developed by building on the work of Southern Methodist University, and many of the co-authors are from the Geothermal Laboratory at that university. As the volume of BHT data grows due to increased drilling activity, the ability to quickly analyze and incorporate additional data is critical. Incorporating this number of new BHT points collected by the GRA group using previous techniques may have taken weeks to months. Chapter 2 presents an approach to quickly and efficiently incorporate additional well data into existing geothermal resource maps. The Shope et al. (2012) work, of which I am a participant, contains a more complete discussion of the precursory research. Summarized below are selected topics that are detailed by Shope et al. (2012) that set the stage for the subsequent chapters.

The final thesis chapter is an individual work meant to analyze the uncertainty and issues that still remain with the model brought forth in Chapter 2. The model, which

we designed, has resulted in a large reduction in processing time for large data sets, however uncertainty is still a concern. If the results are very uncertain, it will compromise the quality of the analysis and little will have been gained. For that reason the input parameters and their effect on the outputs, namely surface heat flow and subsurface temperature, are analyzed in Chapter 3. The focus is primarily on how the complexity of the sedimentary section is addressed and how uncertain predicted temperatures at depth are. Additionally, assumptions pertaining to the properties of the basement are briefly analyzed.

1.2.1 Data Collection

The data on which all our assessment studies are based comes from archived oil and gas well logs held by SMU, the Pennsylvania Geological Survey, the New York State Museum, and the New York State Department of Environmental Conservation (NYSDEC, 2011). The well set was filtered, especially with regard to total depth and perceived quality, leaving a set with BHT measurements for depths greater than 600 meters, totalling 814 data points in New York and 3,771 data points in Pennsylvania, all of which are irregularly spaced.

1.2.2 BHT Corrections

In oil and gas operations, true ”equilibrated” BHT measurements are not obtained, requiring that the BHT data be calibrated to wells of similar depth that are at thermal equilibrium. Preferably these wells will have been drilled in a very similar manner within the same field or region. In practice, BHT corrections are commonly empirical

and likely robust within a single oil field or single sedimentary basin. The majority of empirical corrections attempt to estimate the thermal deviation as a function of depth, utilizing several correction coefficients.

A second-order polynomial relationship proposed by Harrison et al. (1983), based on data from the state of Oklahoma, is used in these studies. The resultant δT value is a correction factor that can be added to the BHT from a geophysical log header to yield a corrected equilibrium temperature. Fortunately there exist fourteen thermally equilibrated Spicer wells in New York and Pennsylvania, for which the Harrison correction adequately adjusted BHTs for wells in excess of 1000 meters (Shope et al., 2012).

1.2.3 Sedimentary Thickness Scaling

The area of study is located in the northern Appalachian Basin where sedimentary thicknesses range from 0 to 10 km, increasing steadily to the southeast and reaching maximum thicknesses along the western edge of the Appalachian Mountain range. A map of the total sedimentary thickness from the AAPG Basement of North America (1978) was used to generate a 3D surface representing depth to basement rock over the aerial extent of the wells in this study (Figure 1.2).

In order to better represent the conductivity at a specific location, it was necessary to refine the total sedimentary thicknesses at each well location. For this study, the Correlation of Stratigraphic Units of North America (COSUNA) was used to produce stratigraphic columns for each well (AAPG, 1985). COSUNA provides stratigraphic information over the states of interest with each COSUNA column covering typically 5 $+/-$ counties (1,000 to 10,000 km^2). Additionally it provides lithology data, which is required to estimate conductivity.

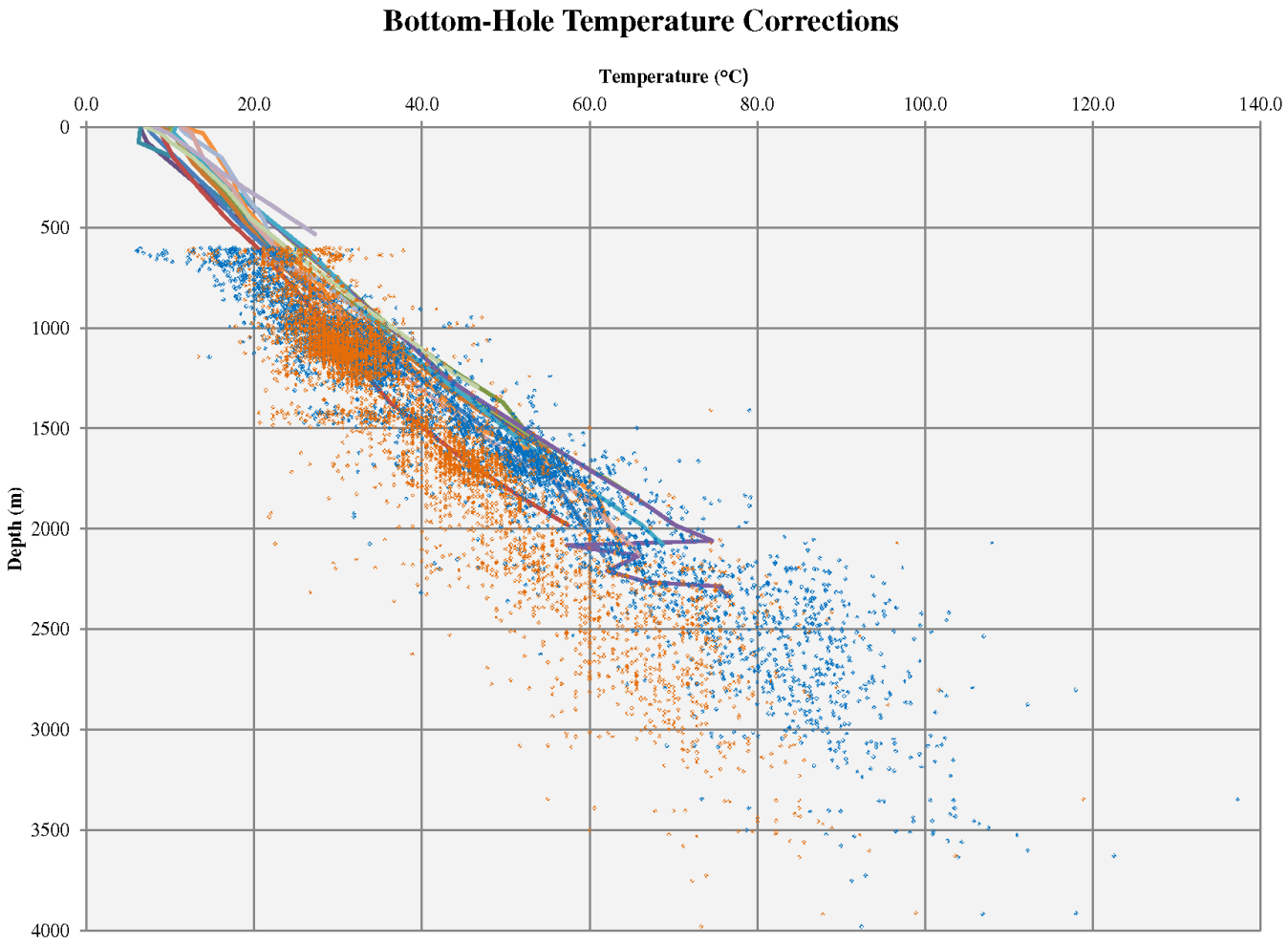

Figure 1.1: Comparison of equilibrium temperature to bottom hole temperature data from 14 equilibrated wells (the thick continuous lines) are compared to Harrison-corrected (blue) and uncorrected (orange) bottom hole temperatures (data sources: SMU; PA Geological Survey; NYS Museum; NYSDEC, 2011). Each dot represents one well data point in the Cornell database utilized in this thesis.

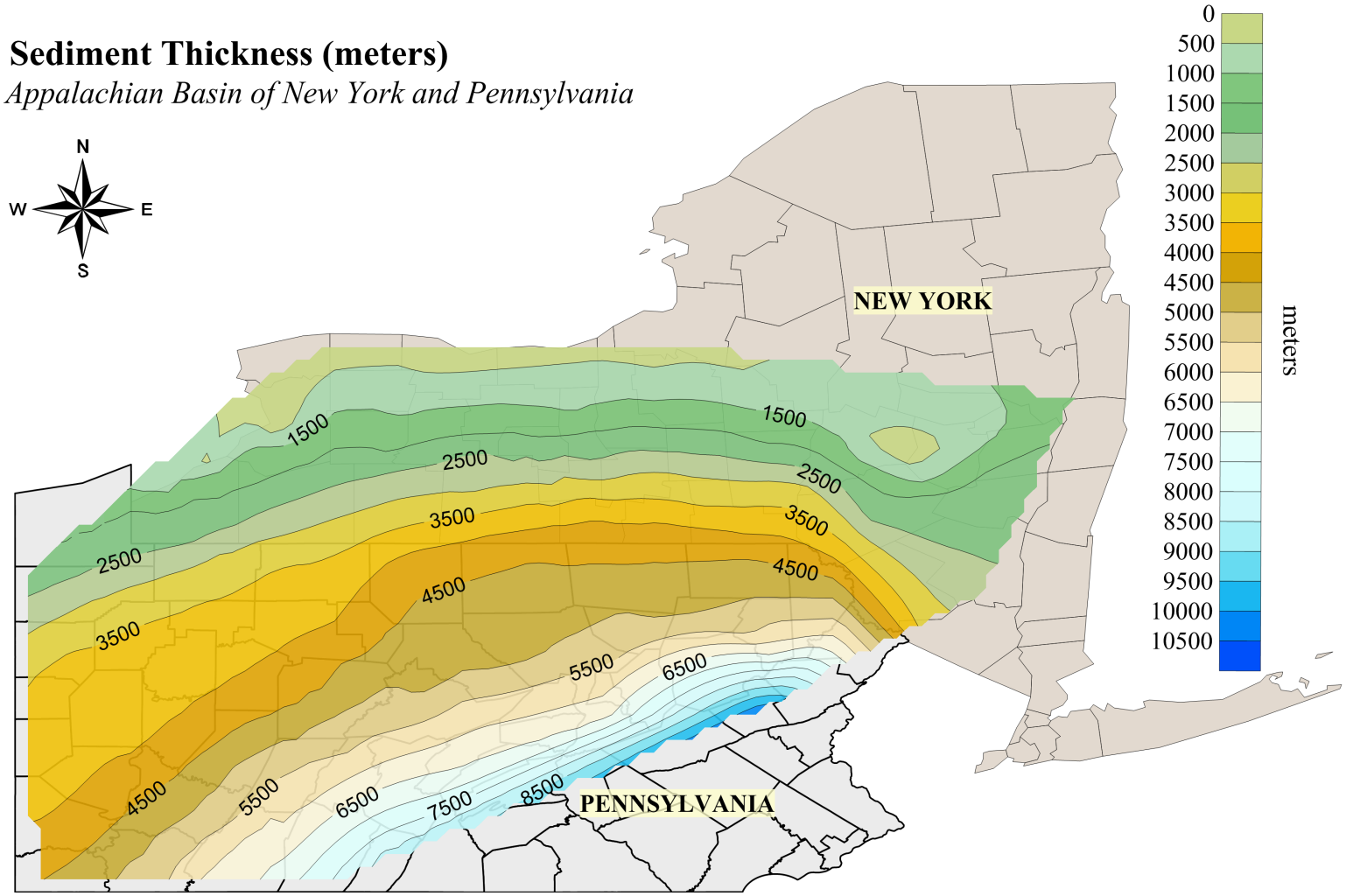

Figure 1.2: The thickness of the sedimentary units within the Appalachian Basin of New York and Pennsylvania, representing the depth from the surface to the underlying basement rock, from AAPG (1978). Using this map, the sedimentary thickness at a given well location was predicted.

Given the location of an individual well (latitude and longitude), the 3D surface (Figure 1.2) was used to interpolate the depth to the basement. The resulting value was applied as a scaling factor to the overall thickness of the COSUNA stratigraphic section. The average thermal conductivity to a given well depth was then calculated using the procedure described in Chapter 2, Section 2.3.1.

REFERENCES

Armstead, H. C. H. and J. W. Tester, (1987), *Heat Mining* E and F. N. Spon, London.

Blackwell, D. D., Negraru, P. T., and Richards, M. C. (2007), "Assessment of the Enhanced Geothermal System Resource Base of the United States," *Natural Resources Research*, 15, December 2006, 283-308.

Blackwell, D. D., Batir, J., Frone, Z., Park, J., and Richards, M. (2010), "New geothermal resource map of the northeastern US and technique for mapping temperature at depth," *Geothermal Resources Council Transactions*, Volume 34. Document ID 28663.

Harrison, W. E., Luza, K. V., Prater, M. L., and Chueng, P. K. (1983), "Geothermal resource assessment of Oklahoma", *Special Publication 83-1*, Oklahoma Geological Survey, 1983.

Mock, J. E., J. W. Tester, and P. M. Wright, (1997), "Geothermal energy from the Earth: Its potential impact as an environmentally sustainable resource." Annual Review Energy Environment, 22, 305-56.

Rowley, J. C. (1982), "Worldwide geothermal resources." In Handbook of Geothermal Energy, Eds. L. H. Edwards et al., Gulf Publishing Co., Houston, Texas.

Sass, J. (1993), "Potential of hot dry rock geothermal energy in the eastern United States," USGS Open File Rep., USGS, Washington, DC, pp. 93-377.

Shope, E. N. et al. (2012), "Geothermal Resource Assessment: A Detailed Approach to Low-Grade Resources in the States of New York and Pennsylvania," *37th Stanford Geothermal Workshop*, Stanford, CA, January 30 February 1, 2012.

Tester, J. W., H. J. Herzog, Z. Chen, R. M. Potter, and M. G. Frank, (1994), ”Prospects for universal geothermal energy from heat mining.” Sci. Glob. Secur., 5, 99-121.

CHAPTER 2

A WELL BY WELL METHOD FOR ESTIMATING SURFACE HEAT FLOW FOR REGIONAL GEOTHERMAL RESOURCE ASSESSMENT

Chapter 2 contains the full text of a paper presented at the 37th Annual Stanford Geothermal Workshop January 30 to February 1, 2012. I was the lead author, with large input by a group, students and faculty, from both Cornell and SMU. The co-authors were George Stutz[1,2], Mitchell Williams[3], Zachary Frone[3], Timothy J. Reber[1,2], David Blackwell[3], Teresa Jordan[1,2], and Jefferson W. Tester[1,2].

This team effort was completed with funding and other assistance from the U.S. Department of Energy (contract # DE-EE0002852), the National Science Foundation's Integrative Graduate Education and Research Traineeship (IGERT) grant, and Cornell's Atkinson Center for a Sustainable Future, whose support made this research possible. Additionally we would also like to recognize the Pennsylvania and New York State Geology departments for their data contributions.

2.1 Motivation and Scope

The process developed in the study utilizes the techniques of mapping potential geothermal resources adopted by the Southern Methodist University (SMU) Geothermal Laboratory and new functional routines to rapidly calculate the estimated surface heat flow, temperature at various depths, and other properties from large quantities of oil and gas well data (Blackwell et al., 2010). In addition, this technique permits incorporation of a more accurate estimate of sediment thickness at each well location and can utilize

[1]Cornell Energy Institute, Cornell University, Ithaca, NY 14853, USA
[2]Cornell Department of Earth and Atmospheric Sciences, Cornell University, Ithaca, NY 14853, USA
[3]SMU Huffington Department of Earth Sciences, Geothermal Laboratory, Dallas, TX, 75275, USA

these estimates of thickness in subsequent calculations, greatly increasing their accuracy. The combination of improved accuracy and speed in incorporating additional data will enable more flexibility in analyzing potential Enhanced Geothermal System (EGS) resources. The resulting maps will aid in locating small temperature gradient variations that may be required for any proposed EGS system in a lower grade region.

The economic success of any potential low grade EGS system in the United States will depend on locating geothermal anomalies at a spatial scale sufficient to establish relative high grade areas large enough to act as a functional heat production system. In the Eastern United States particularly, due to the relative low grade of potential geothermal energy resources, the accuracy and spatial resolution of maps of localized heat flow variations are of greater importance than in conventional, hydrothermal dominated areas where gradients are generally much higher. East of the Rocky Mountains, deep sedimentary basins, such as the Appalachian basin, may provide the best targets for potential EGS exploitation. Installing an EGS reservoir in a sedimentary basin assumes the ability to drill to sufficient depth to reach usable temperatures as defined by the anticipated end use of the thermal energy. To minimize the depth to the EGS reservoir, the first major step is to discover areas of relative high thermal gradient by regional mapping of heat flow and subsurface temperature.

Given the sparseness of conventional heat flow measurements in many regions of the US, mapping and modeling of subsurface temperatures has been time consuming. Additionally, sparse data has severely limited the ability to locate variations in the average heat flow that are spatially small enough to pinpoint additional exploration investment, yet broad enough to result in economically viable EGS systems. To fill in the large spatial gaps in conventional heat flow data, researchers have incorporated oil and gas data.

Oil and gas wells are routinely drilled into sedimentary basins, creating large datasets of BHT measurements and geological information for analysis. In regions with low thermal gradients (20-40 °C/km), such as the Eastern United States, the cost and difficulty of drilling to a reservoir at sufficient depth may make any project technically or economically infeasible (Mock et al., 1997; Tester et al., 2006; IPCC, 2011). Therefore, to maximize the chance of success in such regions, maximum information must be extracted from these datasets, seeking understanding of small variations in heat flow and temperature gradient. Requisite for improving accurate understanding of the magnitudes and three-dimensional spatial scale of favorable thermal anomalies is access to new data, and analytical methods for efficient addition of new data to existing regional geothermal maps. Ongoing oil and gas exploration drilling provides a stream of new data, whose locations are dictated by criteria unrelated to EGS assessment. The focus of this study is to provide a new method to use this data to quickly and accurately calculate estimated surface heat flow and predict subsurface temperature profiles for use in EGS resource assessments.

This Chapter describes the means by which the thermal modeling process has been streamlined and given improved accuracy while increasing the speed with which large amounts of data can be incorporated and used to improve data synthesis. The generalized method is independent of the data source and is intended to allow for user discretion when choosing inputs. One well could be processed with very precise data, or as is more likely, thousands of wells with best available data could be analyzed in minutes. The addition of either type of data should provide maps with higher granularity, thereby reducing uncertainty and risk in EGS exploration. This automation process utilizes Microsoft Excel and user defined functions written in the Visual Basic for Applications (VBA) language. The resulting models provide routines with sufficient accuracy and speed to quickly and efficiently incorporate massive amounts of data into geothermal

mapping. Presented here is a discussion of the equations used, the scientific basis behind them, and a specific review of how the programs and procedures have been applied in Southwestern Pennsylvania.

2.2 Existing Methodology for Heat Flow Estimation

In 2007 the Geothermal Laboratory at the Southern Methodist University (SMU) Huffington Department of Earth Sciences published their work, "Assessment of Enhanced Geothermal System Resource Base of the United States" (Blackwell et al., 2007). This document provided a framework which incorporated oil and gas data into EGS resource evaluations. The maps produced, and subsequent revisions, utilized BHT data, mainly from the oil and gas industry, as a primary data source. More than 2,000 rotary rigs were active in the U.S. as of September 2011, resulting in continued rapid growth in the quantity of BHT data. As a consequence, there is a need for reliable and simple methods to incorporate each new well data points. The BHT measurements obtained from these wells can then be used to help validate and refine resource assessment models, such as SMU's.

As discussed by Blackwell et al. (2007; 2010) and Shope et al. (2012), BHT data are commonly of very low quality. Because measurements are taken very shortly after cessation of drilling operations, the temperature presented on geophysical logs does not represent a true formation value. For this reason a correction must be applied. Entire publications have been devoted to analyzing the validity of the numerous equations and methods proposed to adjust BHT data to thermal equilibrium (Deming, 1989). The model presented in this study is independent of the technique used to adjust BHT data to thermal equilibrium. It is assumed that the BHT points input into the model have

been adequately adjusted by the user through whichever technique was determined to be most appropriate.

The corrected BHT's are used to calculate an average temperature gradient for that well. The equilibrium gradient is calculated as:

$$\left(\frac{dT}{dz}\right) = \frac{T_{BHT} - T_S}{z} \tag{2.1}$$

Where T_{BHT} is the corrected temperature, T_S is the average annual surface temperature, both in °C, and z is the true vertical depth of the log measurement in meters.

The resulting corrected gradient can then be utilized to calculate surface heat flow, assuming 1D vertical conduction of heat through the rock column as:

$$Q_s = k\left(\frac{dT}{dz}\right) \tag{2.2}$$

Where gradient is in °C/km, thermal conductivity k is in W/m/K, and heat flow Q_s is in mW/m^2. Given that the depth of the well is small compared to the distance of significant structural changes in geology, and precluding recent volcanism or other changes that will negate the assumption of steady-state heat flow, this 1D case will be accurate.

To apply Equation (2.2), thermal conductivity values from the surface to the well depth must be established. Conductivity values for various lithologies have been the focus of several publications including Joyner et al. (1960), Blackwell and Steele (1989), Beach et al. (1989), and Gallardo and Blackwell (1999). If the well is in crystalline basement rocks, it may be appropriate to assume a single k for the entire well section. However, oil and gas wells, the main source of data in these assessment studies, are

drilled into basins with thick sedimentary covers with highly variable lithologies and, therefore, conductivities. Utilizing a unit thickness and thermal conductivity, a thermal resistance R can be defined as:

$$R = \frac{h}{k} \tag{2.3}$$

Where h is the unit thickness in meters, and k the unit conductivity in W/m/K. The resistance for each unit is added to calculate the total resistance from the surface to the well depth. The resistance of the deepest lithology the well reached is calculated via a linear interpolation to account for the fraction of the lithology penetrated. By dividing the total thermal resistance ($\sum R$) by the total well depth (z_w), the thermal conductivity ($\bar{k}$) from the ground surface to that depth is:

$$\bar{k} = \frac{z_w}{\sum R} \tag{2.4}$$

This average conductivity can then be used directly in Equation (2.2), yielding a surface heat flow, unless the well penetrates below 4 km. Thermal conductivity is a function of temperature and pressure, both of which in a first order sense increase in a predictable manner with depth. Consequently, conductivity asymptotically approaches a constant value at sufficient depth. According to Blackwell et al. (2007) this depth for sedimentary rocks is at or near 4 km. Therefore regardless of lithology, any well penetration below this depth is treated as a single unit with constant k. For further detail see Blackwell et al. (2007).

Once the heat flow and average conductivity are determined, the subsurface temperature $T(z)$ at a particular depth z in meters in a basement terrain, igneous or metamorphic rocks at surface, can be estimated by:

$$T(z) = T_s + Q_m \frac{z}{k} + \frac{A_b b^2 \left(1 - exp(\frac{z}{b})\right)}{k} \tag{2.5}$$

Quantitatively Equation (2.5) represents the anticipated temperature T, at depth z, given mantle heat flow Q_m, average conductivity k, radiogenic heat contribution A_b, the characteristic thickness of the heat producing layer b in meters, and the surface temperature T_s (Blackwell et al. 2007). A more complete discussion of this equation can be found later in the text.

Equation (2.5) can be modified to predict the temperature within basins containing thick sedimentary covers given more specific information of the lithologies, differing thermal conductivities, and highly variable radiogenic heat production.

Blackwell et al. (2007) also proposed that each well can be classified into one of four broad categories of geological settings. These categories are divided according to the depth of the sedimentary cover as shown in Figure 2.1, the four divisions being 1) no sediment cover (basement at surface), 2) sediments less than 3 km thick, 3) sediment thickness between 3 and 4 km, and 4) sediment thickness greater than 4 km.

The division at 3 km in Figure 2.1, column B, represents a relatively thick sedimentary cover where it is believed that such a thickness would only occur over attenuated or eroded crust, resulting in a decreasing thickness of the primary radioactive heat production layer, represented by b in Equation (2.6). The thickness of this layer is estimated via:

$$If z_{sed} < 3000\ m\ then$$

$$b = 10,000$$

$$Else$$

$$b = 13,000 - z_{sed} \tag{2.6}$$

Blackwell (1971) states that b typically ranges from 7.5 km to 10 km. As shown in Equation (2.6), the base case here is taken to be b=10 km. The final division at 4 km represents the constant thermal conductivity layer as discussed previously.

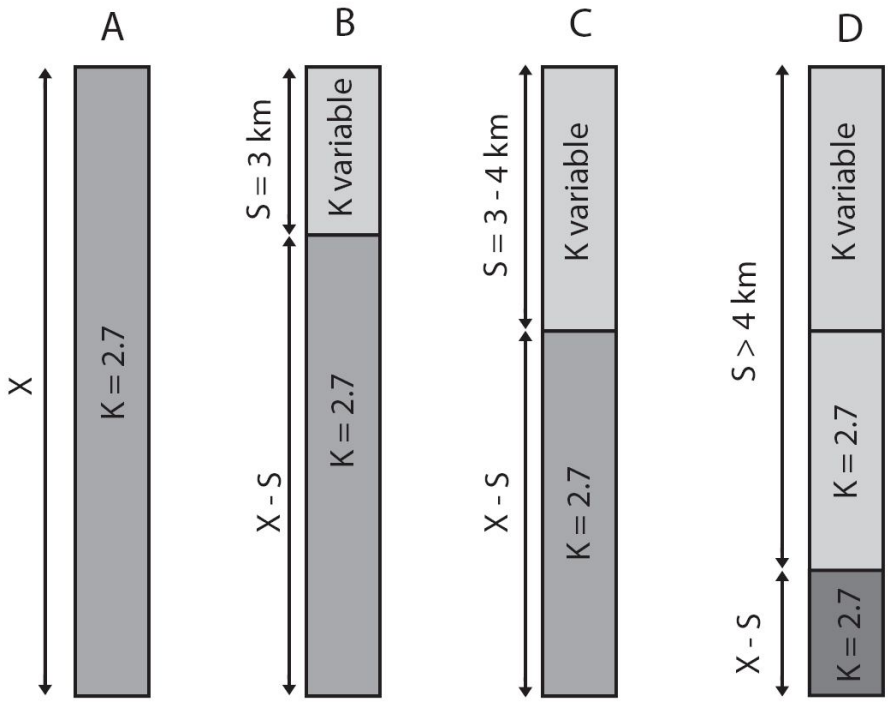

Figure 2.1: Geologic conductivity and radioactivity models for calculation

SMU's use of geological information yields a more comprehensive analysis of possible EGS resources when compared to previous works. Incorporation of data of this type reduced the need to simplify estimation, a necessity in earlier works. Additionally the study concluded that the resource potential for the United States is quite large and that EGS systems may hold promise nationwide. However current maps lack the spatial granularity to identify small to moderate regions of aberrantly high thermal gradients in regions of the eastern US.

2.3 New Method For Heat Flow And Subsurface Temperature Estimation

2.3.1 Estimating Surface Heat Flow

The general framework for correcting to thermal equilibrium, anticipating average thermal conductivity to total well depth, calculating surface heat flow, and finally predicting temperature at depth, follows the basic procedure as outlined above.

Following earlier conventions, Microsoft Excel and Microsoft Access were utilized to store the large number of BHT data points and to perform the calculations. Therefore, Excel was the natural choice for continued development calculations. Prior work without use of Visual Basic for Applications (VBA) inevitably had to make simplifications due to the amount of data processed. For example, given time and other limitations, large groups of wells were divided by depth to basement and placed in 500 m bins. A scaled sedimentary section was then utilized for all wells within that grouping, i.e. all wells believed to have sediment cover between 4,000 and 4,500 m would be assumed to be 4,250 m. Additionally, earlier calculations of average thermal conductivities to the well depth and to the desired depth where temperature was estimated were simplified in various ways to aid in calculation.

The methods presented in this Chapter utilize the ability of VBA as an Excel add-on to manipulate the existing data and quickly calculate the desired values. Two gross simplifications, rounding sediment thickness and simplifying conductivity estimates, were removed in these models. The base sheet for calculation and processing of data (Figure 2.2) illustrates information for 11 wells in Westmoreland County, Pennsylvania, which will be used as an example of the thermal modeling process.

Desired inputs are marked in yellow and include well information, basement conductivity, deep (>4 km) sediment conductivity, and a specified isotherm of interest. Depths for temperature estimation are marked in blue and can be updated to be any set of values of interest to the user. All unmarked columns are calculated and filled in by the processing macros.

Although the presented example shows constant surface temperature, mantle heat flow, and sediment column radiogenic heat production values, this model allows for individual values to be input for each BHT point. This may be critical if, for example, the area being modeled has large topographic relief resulting in highly variable average surface temperatures or contains a known amount of shale or other horizons of higher than average radiogenic heat production capability. In addition to predicting temperature at the specified depths, the model iteratively solves for the depth to the input isothermal surface at each BHT location. This surface can be used to analyze the depth to the specified temperature based on the anticipated use of the thermal energy.

The second Excel sheet accepts the data for the stratigraphic column (Figure 2.3), in which each unit is a proxy for a rock horizon with a specific thermal conductivity. In addition to providing BHT data, wells drilled for oil and gas exploration are a source of abundant data about stratigraphic units and thus can be very useful in analyzing temperature distributions. However, the full use of all the publicly available non-interpreted well log data would greatly slow the incorporation of the new BHT data into a preliminary exploration program.

Calculate

Basement Conductivity (W/m/K)	2.7
Deep Sediment Conductivity (W/m/K)	2.7
Isotherm (°C)	80

Identifier (API/Name)	BHT (°C)	Well Depth (m)	Mantle Heat Flow (mW/m2)	Depth to Basement (m)	Avg. Surface Temperature (°C)	Sediment Radiogenic Heat Generation (μW/m^3)	Basement Radiogenic Heat Generation (μW/m^3)	Gradient (°C/km)	Heat Flow (mW/m2)	Average Conductivity To Well Depth (W/m/K)	Temperature Estimation at Depth (°C at m)						Depth to Specified Isotherm (m)
											1500	3000	4500	6000	7500	10000	
37129202870000	85	2346	30	5369	9	1											
37129203880000	89	2547	30	4780	9	1											
37129215570000	86	2558	30	5314	9	1											
37129239710000	66	2207	30	5320	9	1											
37129225960000	31	1177	30	4860	9	1											
37129237810000	30	1127	30	4876	9	1											
37129241990000	31	1127	30	4865	9	1											
37129243130000	30	1117	30	4832	9	1											
37129243700000	27	1171	30	4869	9	1											
37129245160000	37	1252	30	4518	9	1											
37129247300000	34	1201	30	4514	9	1											

Figure 2.2: Well data input for processing and calculation of heat flow and temperature

Thus for this example, we sought an efficient method to incorporate stratigraphic data, using the assumption that lateral extrapolation of stratigraphic columns would be valid over some distance. As a result, Figure 2.3 represents an idealized or average column for a large area, and a thickness factor must be developed to scale the column to the well location. The specific data depicted in the example are from the Correlation of Stratigraphic Units of North America (COSUNA) (AAPG, 1985).

To scale the representative section, the anticipated depth to igneous or metamorphic basement rock for each well had to be determined (Figure 2.2 Depth to Basement (m)). In this example, a map of the thickness of sedimentary cover from the AAPG Basement of North America (1978) was used to interpolate the depth to basement at each well location.

The interpolated sedimentary cover depth was then divided by the total thickness of the stratigraphic section to calculate a scaling factor (Figure 2.4). Each unit in the stratigraphic section was then multiplied by this factor to yield an anticipated thickness at each well.

Finally a representative thermal conductivity for each unit is required for calculation. In this study, each unit was given a thermal conductivity based on a 60/40 mix of the primary and first secondary lithology from the USGS (2011) description, with the conductivities for each lithology type from Beardsmore and Cull (2001).

In addition to gradient, surface heat flow, and average thermal conductivity to well basement, the anticipated radiogenic heat generation of the underlying basement terrain, A_b, is calculated. A_b is determined from the surface heat flow Q_s, the mantle heat flow Q_m, and the radiogenic heat generation in the sediments A_s, via:

Unit Indentifier	Thickness (m): Min	Max	Assumed	Conductivity
*Un-named	81	359	220	3.34
Monogahela OR Uniontown/Pittsburgh	74	108	91	2.22
Conemaugh OR Casselman/Glenshaw	264	264	264	1.60
Allegheny	85	85	85	2.91
Pottsville	54	63	58.5	3.25
Mauch Chunk	135	142	138.5	2.15
Greenbrier	0	72	36	3.10
Burgoon/Rockwell OR unnamed/Shenango	164	224	194	2.91
Venango OR Catskill OR Hampshire	272	670	471	3.17
Chadakoin/Bradford OR Lock Haven	150	910	530	3.05
Brallier	697	1060	878.5	2.25
Harrell	140	140	140	1.02
Tully	20	20	20	2.45
Mahantango	73	73	73	1.98
Marcellus	37	37	37	1.52
Selinsgrove	3	6	4.5	2.45
Huntersville Chert	32	32	32	2.33
Needmore Shale	7	7	7	2.12
Ridgeley Sandstone	30	30	30	3.42
Licking Creek OR Shriver	12	39	25.5	2.08
Mandata shale	7	7	7	1.43
Corriganville limestone	3	3	3	2.45
New Creek limestone	3	3	3	2.45
Keyser formation	15	39	27	2.45
Tonoloway	6	36	21	2.31
Wills Creek	130	221	175.5	2.26
Lockport OR McKenzie	0	100	50	1.90
Clinton group	100	223	161.5	2.51
Tuscarona formation	45	133	89	4.60
Queenston OR Juniata/Bald Eagle	290	487	388.5	3.34
Reedsville shale	233	233	233	2.15
Antes formation	54	54	54	1.72
Coburn formation	75	75	75	2.50
Salona formation	39	39	39	2.01
Nealmont	78	78	78	2.50
Benner (also called "Linden Hall)	36	54	45	2.70
Snyder	14	39	26.5	3.35
Hatter	36	60	48	3.35
Loysburg	34	51	42.5	3.35
Beekmantown Gp	652	704	678	3.35
Gatesburg	246	332	289	3.35
Warrior Fm	134	134	134	3.35

Figure 2.3: Stratigraphic column from COSUNA (1985) representing the thickness and conductivity data for Pennsylvania Section 17

Unit Indentifier	COSUNA Thickness (m)	Well Thickness (m)
*Un-named	220	197
Monogahela OR Uniontown/Pittsburgh	91	81
Conemaugh OR Casselman/Glenshaw	264	236
Allegheny	85	76
Pottsville	58.5	52
Mauch Chunk	138.5	124
Greenbrier	36	32
Burgoon/Rockwell OR unnamed/Shenango	194	174
Venango OR Catskill OR Hampshire	471	421
Chadakoin/Bradford OR Lock Haven	530	474
Brallier	878.5	786
Harrell	140	125
Tully	20	18
Mahantango	73	65
Marcellus	37	33
Selinsgrove	4.5	4
Huntersville Chert	32	29
Needmore Shale	7	6
Ridgeley Sandstone	30	27
Licking Creek OR Shriver	25.5	23
Mandata shale	7	6
Corriganville limestone	3	3
New Creek limestone	3	3
Keyser formation	27	24
Tonoloway	21	19
Wills Creek	175.5	157
Lockport OR McKenzie	50	45
Clinton group	161.5	144
Tuscarona formation	89	80
Queenston OR Juniata/Bald Eagle	388.5	347
Reedsville shale	233	208
Antes formation	54	48
Coburn formation	75	67
Salona formation	39	35
Nealmont	78	70
Benner (also called "Linden Hall)	45	40
Snyder	26.5	24
Hatter	48	43
Loysburg	42.5	38
Beekmantown Gp	678	606
Gatesburg	289	258
Warrior Fm	134	120
Total (m):	**6003**	**5369**
Well Total Thickness (m):	**5369**	
Scalign Factor:	**0.894**	

Figure 2.4: Scaling of thickness to anticipated well location. Data for well API # 37129202870000 from Table 1. The total thickness of the COSUNA section is 6003 m, while the total sedimentary cover at the well is anticipated to be 5369 m. This results in a scaling factor of 0.894

$$A_b = \frac{Q_s - Q_m - A_s z_s}{b} \tag{2.7}$$

Where the assumption of 1D steady state conduction is maintained. As a result, surface heat flow is only a product of mantle heat flow and in-situ radioactive decay from the surface to the effective crust mantle interface.

2.3.2 Modeling Temperature at Depth

The modeling of subsurface temperatures is based on the observation of a linear relationship between observed surface heat flow, Q_s, and radiogenic heat production (A) when measured at or near the surface of plutonic rock intrusions. This relationship can be estimated as:

$$Q_s = Q_o + Ab \tag{2.8}$$

Equation (2.8) has been confirmed for many geologic provinces including the Eastern United States, the Sierra Nevada, Scandinavia, the Basin and Range, and the Eastern Canadian Shield. As a consequence, an exponential source model can be assumed for the radiogenic basement as:

$$A(z) = A_o exp\left(-\frac{z}{b}\right) \tag{2.9}$$

Where $A(z)$ is the radiogenic heat generation in μW/m^3 at depth z in meters, given initial heat generation A_o in μW/m^3 and the scale constant for the depth of the heat

generation layer b in meters. This linear relationship and exponential model of heat production has been found to be a typical approximation in many studies and publications (Birch et al., 1968; Roy et al., 1968; Lachenbruch, 1968, 1970; Blackwell, 1971; Allen and Allen, 2005, Blackwell et al., 2007). Given the exponential model, b, as determined by the slope described by Equation (2.8), is not a physical thickness, but a bound below which heat entering the system will be mantle heat flow only, i.e. no radiogenic contribution.

A single uniform layer of thickness b and radiogenic heat production A has also been proposed. In this uniform case, b may represent the physical thickness of the radiogenic body. The primary argument in favor of Equation (2.9) is that Equation (2.8) is maintained during differential erosion (Lachenbruch, 1968 and Blackwell, 1971). In either model, as discussed earlier, b must be reduced for sediment covers greater than 3 km (Blackwell et al., 2007). This assumption is reflected in the temperature calculations in this model by direct subtraction of additional sedimentary thickness from b according to Equation (2.6).

The steady state 1D conduction Equation (2.10) is used to solve for temperature at depth when Equation (2.8) is substituted for the generalized source term $g(z)$:

$$-k\frac{d^2T}{dz^2} = g(z) \tag{2.10}$$

$$-k\frac{d^2T}{dz^2} = A_o exp\left(-\frac{z}{b}\right) \tag{2.11}$$

By integrating and applying the boundary condition, that as depth z approaches infinity $Q = Q_m$, Equation (2.11) becomes:

$$\frac{dT}{dz} = \frac{Q_m}{k} - \frac{A_o b exp\left(-\frac{z}{b}\right)}{k} \tag{2.12}$$

By integrating Equation (2.12) and applying the boundary condition $T(0) = T_s$, Equation (2.12) will reduce to Equation (2.5). However if the sedimentary cover is not fully penetrated, i.e. $X < zsed$, then Equation (2.11) would be replaced with:

$$-k\frac{d^2T}{dz^2} = A_s \tag{2.13}$$

Where A_s is the uniform radiogenic heat production in sediments. Following the same integration scheme and applying the boundary condition that Q at $z = 0$ is Qs and $T(0) = T_s$, Equation (2.13) becomes:

$$T(z) = T_o + Q_s\frac{z}{k} - \frac{A_s z^2}{2k} \tag{2.14}$$

From these generalized solutions to the steady state 1D conduction equation, all equations in the Chapter 2 Appendix were derived to handle temperature calculations for any combination of geological and thermodynamic inputs. This decision process and calculations are run in VBA through a series of nested IF statements, as visually represented by the decision tree in the Appendix for this chapter.

In the Chapter Appendix, terms described as before basement, meaning thickness between the BHT point and above basement rocks, are introduced and signified by the subscript *bb*. This is a generalized term to account for the incremental temperature and thermal conductivity between the well depth and a depth of interest that is smaller than the sediment thickness. Thermal conductivity for this incremental depth (k_{bb}) was calculated using a thickness weighted average approach via:

$$\bar{x} = \left[\sum_{i=1}^{n} k_i * dh_i \right] / h_t \tag{2.15}$$

Where k_i and h_i are the individual unit thickness and conductivity, and h_t is the total column thickness. In this model the conductivity of the column to the depth of interest, conductivity to the well depth and their respective thicknesses are used to solve for the k_{bb} value in Equation (2.15). This is completed in an attempt to match as closely as possible the observed BHT.

Additionally the model will iteratively solve for a specified depth to an isothermal surface of the users choosing. Determination of this surface enables basic techno-economic analyses of potential EGS resources as the drilling depth to the level of thermal energy desired in each location can be estimated.

2.4 Example Case Evaluated

To demonstrate the new method described above, eleven wells in Westmoreland County, PA were analyzed (see Figure 2.2 and 2.3). Westmoreland County lies in the central part of the Appalachian basin, a deep foreland basin containing up to 10 km of sedimentary strata over a variable and poorly understood basement complex. Basins such as this have some of the best potential for EGS exploitation outside of hydrothermal locales.

As discussed earlier in the Existing Methodology section, BHTs must be corrected to thermal equilibrium. Commonly, given typical data constraints with publicly available oil and gas well information, an empirical correction factor will be used, such as demonstrated by Harrison et al. (1983), Blackwell et al. (2007), Frone and Blackwell (2010), and Shope et al. (2012).

The Harrison correction is a second order polynomial function of depth in meters. Based on empirically adjusting BHT data to equilibrium temperature proxies in a study in the state of Oklahoma, the resultant ΔT value in °C is a correction factor that can be added to the BHT from a geophysical log header to yield an estimated equilibrium temperature.

The Harrison correction equation utilized in this example is:

$$\Delta T = -16.51 + 0.018z - 2.34E10^{-6}z^2 \tag{2.16}$$

By selecting the textbox Calculate, the macro titled RunCalc() will execute and model the subsurface temperature regime based on the geological and thermodynamic properties inputs (Figures 2.2 and 2.3). VBA was a good choice for this model, as it is able to use IF statements to make decisions, read inputs, manipulate data and cease when all wells are processed.

Previous work identified a potential geothermal anomaly in Westmoreland County. The method presented in this Chapter for processing well data is for the specific purpose of mapping and locating such anomalies. Consequently it serves as an excellent test case. The degree of spatial refinement in this county, and several others in New York and Pennsylvania, are discussed in more detail by Shope et al. (2012).

To validate the accuracy of this model and the assumptions that went into it, the results were compared to temperature data published by Spicer (1964). These wells are taken to represent actual thermal equilibrium in the area, as the wells were drilled without mud circulation, which changes the borehole temperature. A total of 5 wells were within Westmoreland or bordering Allegheny County. Figure 2.5 shows these 5 wells, PA-6, 7, 8, 9, and 11 (their Spicer data set designations), as well as the thermal

modeling results for the nearest 11 new oil and gas wells. The model was also used to predict temperatures to a depth of 10 km, as shown in Figure 2.6.

With a lack of equilibrium well data to this depth, validation of the model is lacking. In lieu of such data, published information of temperature with depth was used. With similar assumptions, Q_m=30 mW/m^2 and T_s=10 °C, Allen and Allen (2005) present a series of models utilizing a similar 1D conduction assumption and various radiogenic heat production conditions that result in temperatures of approximately 170-270 °C at 10 km. The temperatures at this depth were predicted to be between 150 °C and 300 °C when calculated using the model presented here.

This model was then applied to 4,585 wells with BHT readings across Pennsylvania and New York. The exact source and precursory processing of this data and additional maps are discussed in depth by Shope et al. (2012). The resulting heat flow map over the sedimentary basin regions of these two states is shown in Figure 2.8. In Figure 2.8, areas on the scale of 100 km^2 can be seen with heat flow 15-20 mW/km^2 above an average background of 50 mW/km^2 previously not evident in earlier studies.

Based on the data collected and presented by Shope et al. (2012), there may be a geothermal anomaly in Westmoreland County of sufficient magnitude and spatial area to be a potential EGS site. Figure 2.9 shows a detailed thermal map of southwest Pennsylvania in Figure 2.8. The locations of the five Spicer wells and the 11 wells in Figures 2.5 and 2.6 are shown in red and black respectively.

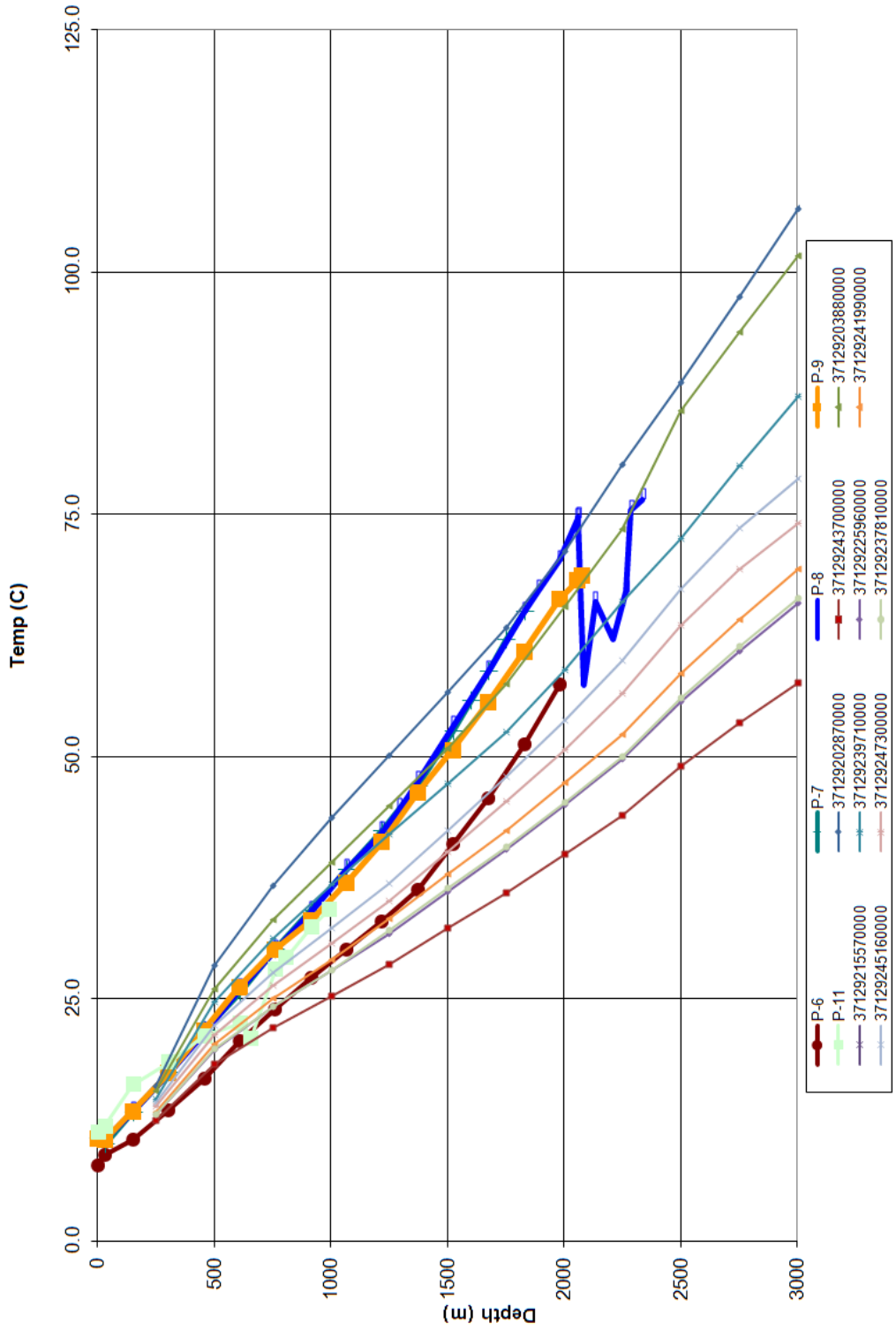

Figure 2.5: Chart of 5 equilibrium wells (PA-6, PA-7, PA-8, PA-9, and PA-11) and 11 nearby BHT point wells (labeled by API number) calculated using the VBA thermal modeling routine

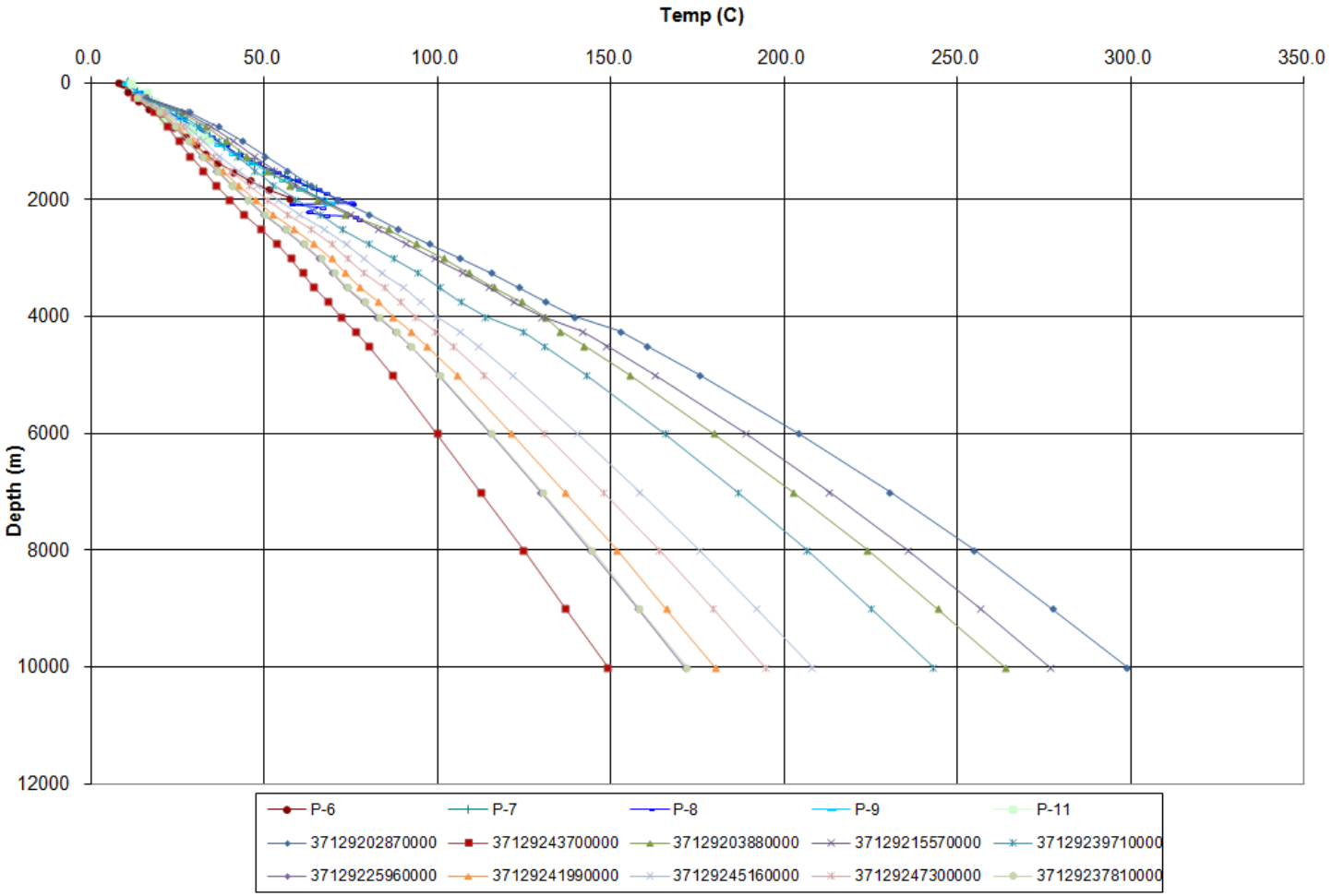

Figure 2.6: Chart of 5 equilibrium wells (P-6, P-7, P-8, P-9, and P-11) and 11 nearby BHT point wells (labeled by API number) calculated using the VBA thermal modeling routine to 10 km depth

Calculate

Basement Conductivity (W/m/K)	2.7
Deep Sediment Conductivity (W/m/K)	2.7
Isotherm (oC)	80

Identifier (API/Name)	BHT (°C)	Well Depth (m)	Mantle Heat Flow (mW/m2)	Depth to Basement (m)	Avg. Surface Temperature (°C)	Sediment Radiogenic Heat Generation (μW/m^3)	Basement Radiogenic Heat Generation (μW/m^3)	Gradient (°C/km)	Heat Flow (mW/m2)	Average Conductivity To Well Depth (W/m/K)	Temperature Estiamtion at Depth						Depth to Specified Istotherm (m)
											7000	8000	9000	10000	5000	6000	
37129202870000	85	2346	30	5369	9	1	6.2	32.2	82.7	2.57	230	255	277	299	175	204	2249
37129203880000	89	2547	30	4780	9	1	4.7	31.3	73.8	2.36	202	224	244	264	155	180	2456
37129215570000	86	2558	30	5314	9	1	5.3	30.1	76.3	2.53	213	235	257	277	162	189	2414
37129239710000	66	2207	30	5320	9	1	4.1	25.7	66.4	2.59	187	206	225	243	143	166	2719
37129225960000	31	1177	30	4860	9	1	1.4	18.4	46.3	2.52	130	144	158	171	100	115	3771
37129237810000	30	1127	30	4876	9	1	1.4	18.6	46.4	2.49	130	144	158	172	100	116	3764
37129241990000	31	1127	30	4865	9	1	1.7	19.6	48.9	2.49	137	152	166	180	105	121	3587
37129243130000	30	1117	30	4832	9	1	1.4	18.4	45.9	2.49	129	143	156	170	99	114	3806
37129243700000	27	1171	30	4869	9	1	0.6	15.8	39.7	2.51	112	125	137	149	87	100	4510
37129245160000	37	1252	30	4518	9	1	2.8	22.5	57.9	2.58	158	175	192	208	121	140	2927
37129247300000	34	1201	30	4514	9	1	2.3	21.0	53.9	2.56	148	164	179	194	113	131	3244

Figure 2.7: Modeled output of geothermal properties for a selection of wells in Westmoreland County, PA

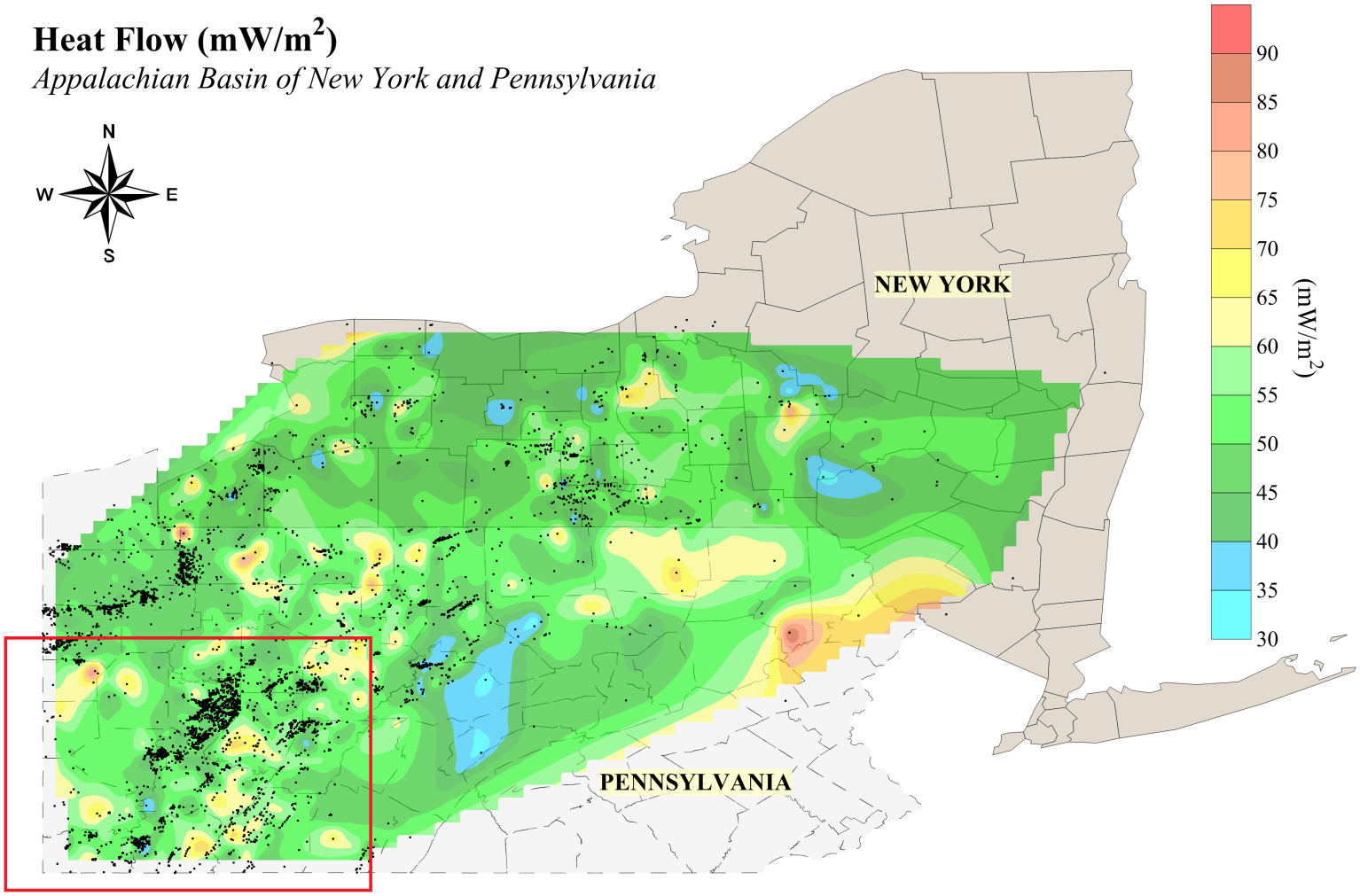

Figure 2.8: Map of calculated heat flow from well BHT data for NY and PA. Area marked in red in detailed in Figure 2.9.

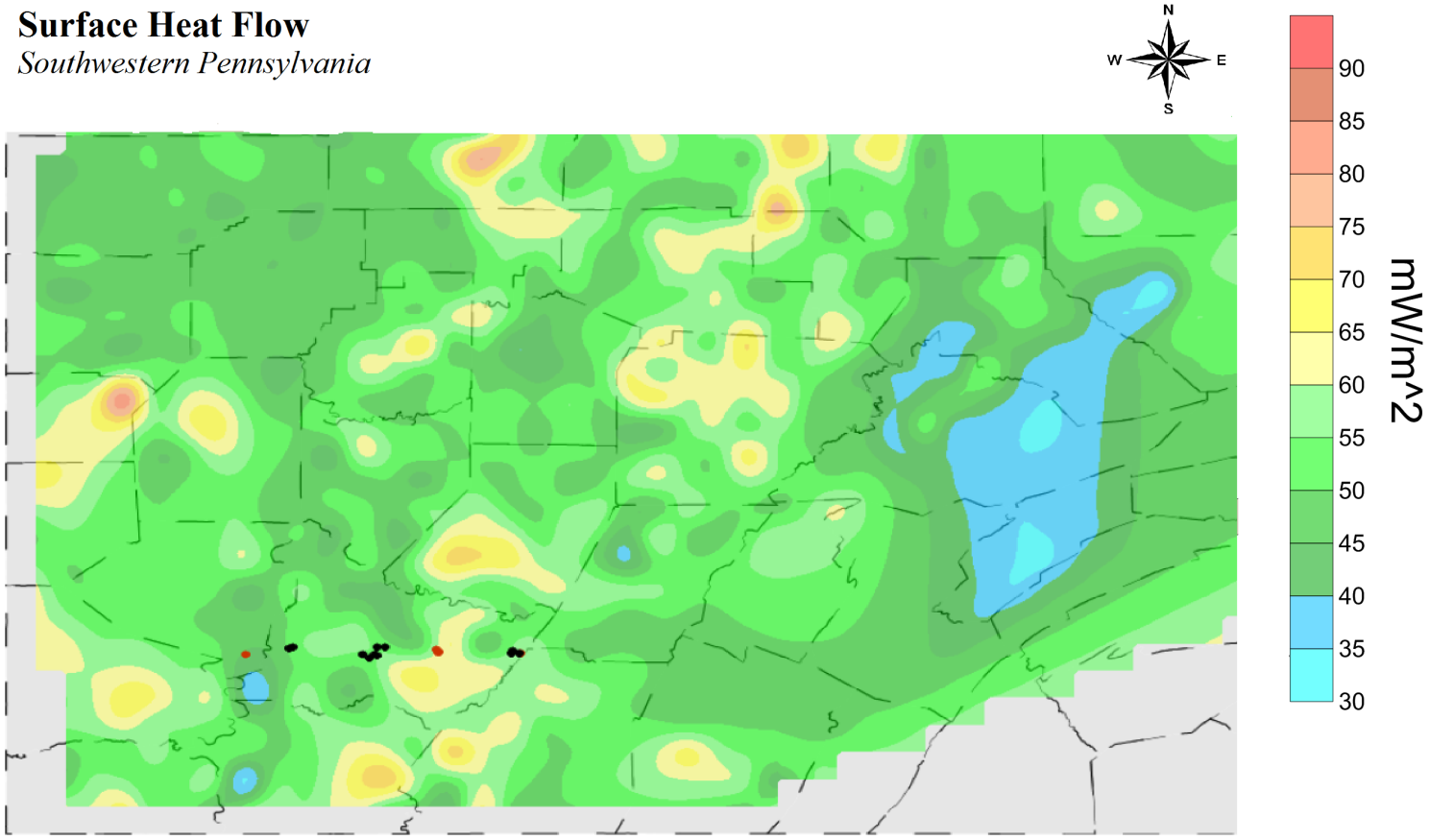

Figure 2.9: Map of wells located in Westmoreland County, PA processed as an example in this study. The locations of the five Spicer wells and the 11 wells in Figures 2.5 and 2.6 are shown in red and black respectively

According to Fox et al. (2011), about 25% of the U.S. annual primary energy demand is consumed as thermal energy at or below 100 °C. This provides an opportunity for lower grade EGS to economically provide direct thermal energy for these low to mid temperature applications. In the example presented here, 80 °C was analyzed in the model. Energy consumption up to this temperature is estimated to be approximately 19 EJ/yr for the U.S. (Fox et al. 2011). The resulting isothermal surface at 80 °C is shown in Figure 2.10.

Different temperature values based on the intended use of the thermal energy can be specified by the user. As a result, this modeling method will aid in specific economic analyses as drilling depths can be estimated.

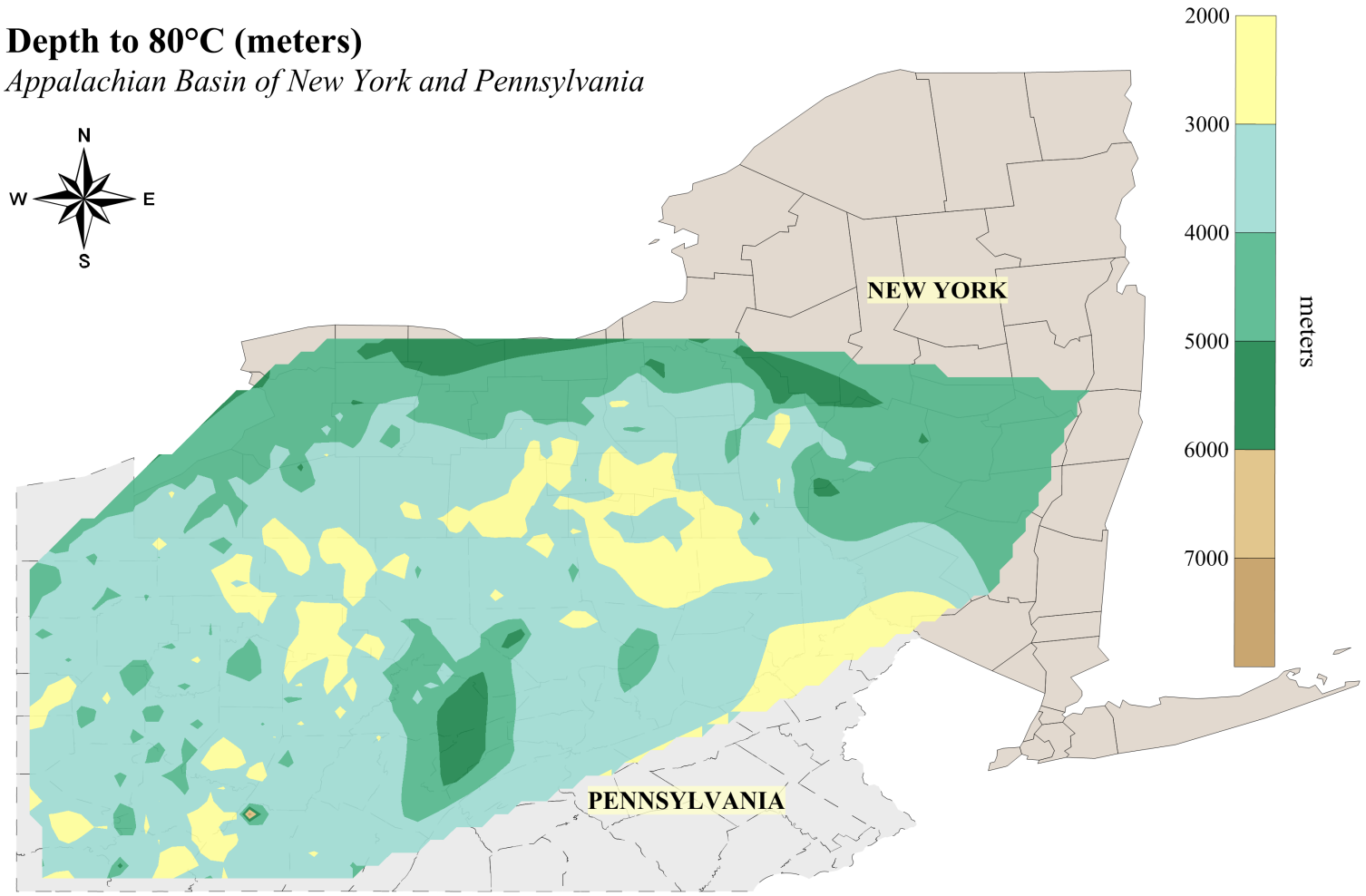

Figure 2.10: Map of anticipated depth to the 80 °C isothermal surface

2.5 Conclusions and Future Work

The quality of EGS resource assessment has been improved by the progressive public availability of oil and gas borehole temperature data. These well data created a need for the development of more efficient analytical tools to incorporate large amounts of BHT and borehole depth data into geothermal resource assessments. The thermal modeling tool constructed in VBA in this study has resulted in improved accuracy and large processing time reductions allowing researchers to shift their efforts from implementing cumbersome calculations to evaluating raw data and model assumptions.

New borehole temperature data for Westmoreland County, PA was used to successfully validate our new method of thermal modeling. We demonstrated that the calculations and techniques accurately predict temperature over the depth ranges of existing equilibrium data. The computational approach described in this study was then applied to a large data set in the Northeastern United States, substantiating the ease and rapidity of the processing techniques described here (Shope et al., 2012).

Prior to this model, establishment of thermal maps using more than 4,000 BHT measurements could take several person months of work. Using the techniques and programs shown in this Chapter, the same group of wells may take a single researcher only weeks to process. Additionally, the enhanced automation allows removal of simplifications in previous well processing methods, with the consequence that the new techniques result in more precise and accurate results.

Additionally, it is believed that EGS in relatively low heat flow regions will have 60% or more of their capital cost consumed by drilling and completion of the geothermal wells (Tester et al., 2006). Therefore, the depth at which usable geothermal heat can be recovered will be the main economic hurdle to adoption of lower grade geothermal as an

alternative energy source. Utilizing a geothermal temperature depth contour map, such as the one shown in Figure 2.10, will allow for cost minimization, as it provides accurate representation of where the shallowest depths to reach a specified rock temperature may be found in the area of interest. As a result, the model will help academic, governmental, and civilian investigators consider the use of EGS as a potential energy resource in previously under explored regions.

For future work, some of the simplifying assumptions will be removed to allow for more region-specific inputs. In doing so, the model has the potential to have a higher accuracy than that shown in this Chapter.

REFERENCES

AAPG (1978), Basement map of North America: American Association of Petroleum Geologists, scale: 1:5,000,000.

AAPG (1985), Correlation of Stratigraphic Units of North America Project, The American Association of Petroleum Geologists, 1985.

Allen, P. A., and Allen, J. R. (2005), *Basin Analysis: Principles and Applications*. Malden, MA: Blackwell Publishing. Print.

Beach, R. D. W., Jones, F. W., and Majorowicz, J. A. (1989), "Heat Flow and heat generation estimates for the Churchill basement of the Western Canadian basin in Alberta, Canada," Geothermics, 16, 1-16.

Beardsmore, G. R., and Cull, J. P. (2001), *Crustal Heat Flow: A Guide to Measurement and Modeling*, New York: Cambridge University Press, 2001. Print.

Birch, F., Roy, R. F., and Decker, E. R. (1968), "Heat flow and thermal history in New England and New York," *in* Studies of Appalachian Geology: Northern and Maritime, Zen, E., White, W. S., Hadley, J. B., and Thompson, Jr., J. B., eds., Interscience, New York, p. 437451.

Blackwell, D. D. (1971), The thermal structure of the continental crust, *in* The Structure and Physical Properties of the Earths crust, Heacock, J. G., ed., American Geophysical Union Geophysics Monograph, v. 14, p. 169184.

Blackwell, D. D., and Steele, J. L. (1989), "Thermal Conductivity of sedimentary rock-measurement and significance," *in* Thermal History of Sedimentary Basins: Methods and Case Histories, Naeser, N. D., and McCulloh, T. H., eds., Springler Verlag,

New York, 13-36.

Blackwell, D. D., Negraru, P. T., and Richards, M. C. (2007), "Assessment of the Enhanced Geothermal System Resource Base of the United States," *Natural Resources Research*, 15, December 2006, 283-308.

Blackwell, D. D., Batir, J., Frone, Z., Park, J., and Richards, M. (2010), "New geothermal resource map of the northeastern US and technique for mapping temperature at depth," *Geothermal Resources Council Transactions*, Volume 34. Document ID 28663.

Bullard, E. C. (1947), "The Time Necessary For a Borehole to Attain Temperature Equilibrium," *Geophysical Journal International*, Volume 5, May 1947, 127-130.

Deming, D. (1989), "Application of Bottom-Hole Temperature Corrections in Geothermal Studies," *Geothermics*, 18, Issues 5-6, 1989, 775-786.

Deming, D., and Chapman, D. S. (1988), "Heat Flow in the Utah-Wyoming Thrust Belt from analysis of bottom-hole temperature data measured in oil and gas wells," *Journal of Geophysical Research*, 93, 13657-13672.

Fox, D. B., Sutter, D., and Tester, J. W. (2011), "The Thermal Spectrum of Low-Temperature Energy Use in the United States," Ithaca, NY: Cornell University. Print.

Frone, Z., and Blackwell, D. D. (2010), "Geothermal Map of the Northeast United States and the West Virginia Thermal Anomaly," *Geothermal Resources Council Transactions*, Volume 34, 2010.

Gallardo, J., and Blackwell, D. D. (1999), "Thermal Structure of the Anadarko Basin,

Oklahoma," *American Association of Petroleum Geologists Bulletin*, 83, no. 2, February, 1999, 333-361.

Harrison, W. E., Luza, K. V., Prater, M. L., and Chueng, P. K. (1983), "Geothermal resource assessment of Oklahoma," *Special Publication 83-1*, Oklahoma Geological Survey, 1983.

Horner, D. R. (1951), "Pressure Build-up in Wells," *3rd World Petroleum Congress*, The Hague, NL, World Petroleum Congress, May 28 June 6, 1951.

IPCC (2011), IPCC Special Report on Renewable Energy Sources and Climate Change Mitigation, Prepared by Working Group III of the Intergovernmental Panel on Climate Change [O. Edenhofer, O. et al. eds)]. Cambridge University Press, Cambridge, United Kingdom and New York, NY, USA, 1075 pp.

Joyner, W.B. (1960), "Heat flow in Pennsylvania and West Virginia," *Geophysics*, 25, 1225-1241.

JPT (2011), "World Rotary Rig Count," *Journal of Petroleum Technology (JPT)*, 63, Dec. 2011.

Kehle, R. O. (1972), "Geothermal Survey of North America," *1972 Annual Progress Report for the AAPG*, 23, p. 1973.

Lachenbruch, A. H. (1968), "Preliminary geothermal model for the Sierra Nevada," *Journal of Geophysical Research*, 73, 69776989.

Lachenbruch, A. H. (1970). "Crustal temperature and heat production: Implications of the linear heat flow relation," *Journal of Geophysical Research*, 75, 32913300.

Mock, J. E., Tester, J. W., and Wright, P. M. (1997), "Geothermal Energy from the

Earth: Its Potential Impact as an Environmentally Sustainable Resource," *Annual Review of Energy and the Environment*, 22, 305-356.

Roy, R. F., Decker, E. R., Blackwell, D. D., and Birch, F. (1968), "Heat flow in the United States," *Journal of Geophysical Research*, 73, 5207-5221.

Shope, E. N. et al. (2012), "Geothermal Resource Assessment: A Detailed Approach to Low-Grade Resources in the States of New York and Pennsylvania," *37th Stanford Geothermal Workshop*, Stanford, CA, January 30 February 1, 2012.

Spicer, H.C. (1964), "A compilation of deep Earth temperature data: USA 1910-1945," *U.S. Geological Survey Open File Report*, 64-147.

Tester, J. W. et al. (2006), The future of geothermal energy: Impact of enhanced geothermal systems (EGS) on the United States in the 21st century, Massachusetts Institute of Technology, DOE Contract DE-AC07-05ID14517 Final Report.

USGS (2011), "Geologic Maps of US States," *USGS Mineral Resources On-Line Spatial Data*. Web. Fall 2011. http://tin.er.usgs.gov/geology/state/

Appendix

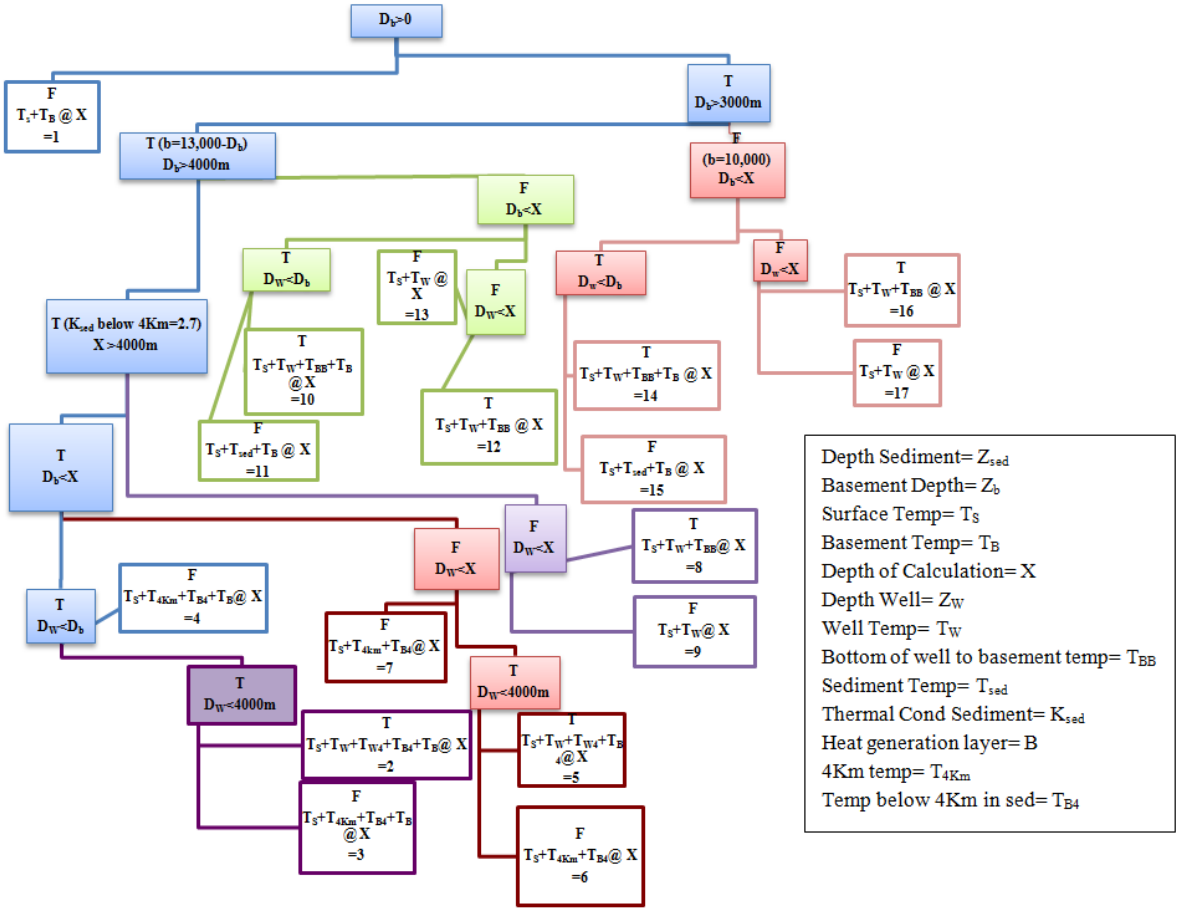

Figure 2.11: Decision for Thermal Model Temperature Prediction (Blackwell et al., 2010)

1. $$= T_S + \left[\frac{Q_S X}{K} - A_S \frac{X^2}{2K} \right]$$

2. $$= T_S + \left[\frac{Q_S Z_W}{K} - A_S \frac{Z_W^2}{2K} \right] + \left[\frac{Q_S (4 - Z_W)}{K_{bb}} - A_S \frac{(4 - Z_W)^2}{2K_{bb}} \right] + \left[\frac{(Q_S - A_S)(Z_B - 4)}{K_{sed>4km}} - A_S \frac{(Z_B - 4)^2}{2K_{sed>4km}} \right] + \left[\frac{Q_m (X - Z_B)}{K_b} + A_b (b)^2 \left(\frac{1 - e^{-\frac{X - Z_B}{b}}}{K_b} \right) \right]$$

3. $$= T_S + \left[\frac{4Q_S}{K} - A_S \frac{4^2}{2K} \right] + \left[\frac{(Q_S - A_S)(Z_B - 4)}{K_{sed>4km}} - A_S \frac{(Z_B - 4)^2}{2K_{sed>4km}} \right] + \left[\frac{Q_m (X - Z_B)}{K_b} + A_b (b)^2 \left(\frac{1 - e^{-\frac{X - Z_B}{b}}}{K_b} \right) \right]$$

4. $$= T_S + \left[\frac{4Q_S}{K_{ave}} - A_S \frac{4^2}{2K_{ave}} \right] + \left[\frac{(Q_S - A_S)(Z_B - 4)}{K_{sed>4km}} - A_S \frac{(Z_B - 4)^2}{2K_{sed>4km}} \right] + \left[\frac{Q_m (X - Z_B)}{K_b} + A_b (b)^2 \left(\frac{1 - e^{-\frac{X - Z_B}{b}}}{K_b} \right) \right]$$

5. $$= T_S + \left[\frac{Q_S Z_W}{K} - A_S \frac{Z_W^2}{2K} \right] + \left[\frac{Q_S (4 - Z_W)}{K_{bb}} - A_S \frac{(4 - Z_W)^2}{2K_{bb}} \right] + \left[\frac{(Q_S - A_S)(X - 4)}{K_{sed>4km}} - A_S \frac{(X - 4)^2}{2K_{sed>4km}} \right]$$

6. $$= T_S + \left[\frac{4Q_S}{K} - A_S \frac{4^2}{2K} \right] + \left[\frac{(Q_S - A_S)(X - 4)}{K_{sed>4km}} - A_S \frac{(X - 4)^2}{2K_{sed>4km}} \right]$$

7. $$= T_S + \left[\frac{4Q_S}{K} - A_S\frac{4^2}{2K}\right] + \left[\frac{(Q_S - A_S)(X-4)}{K_{sed>4km}} - A_S\frac{(X-4)^2}{2K_{sed>4km}}\right]$$

8. $$= T_S + \left[\frac{Q_S Z_W}{K} - A_S\frac{{Z_W}^2}{2K}\right] + \left[\frac{Q_S(X-Z_B)}{K_{bb}} - A_S\frac{(X-Z_B)^2}{2K_{bb}}\right]$$

9. $$= T_S + \left[\frac{Q_S X}{K} - A_S\frac{X^2}{2K}\right]$$

10. $$= T_S + \left[\frac{Q_S Z_W}{K} - A_S\frac{{Z_W}^2}{2K}\right] + \left[\frac{Q_S Z_{bb}}{K_{bb}} - A_S\frac{{Z_{bb}}^2}{2K_{bb}}\right] + \left[\frac{Q_m(X-Z_B)}{K_b} + A_b(b)^2\left(\frac{1-e^{-\frac{X-Z_B}{b}}}{K_b}\right)\right]$$

11. $$= T_S + \left[\frac{Q_S Z_B}{K_{ave}} - A_S\frac{{Z_B}^2}{2K_{ave}}\right] + \left[\frac{Q_m(X-Z_B)}{K_b} + A_b(b)\left(\frac{1-e^{-\frac{X-Z_B}{b}}}{K_b}\right)\right]$$

12. $$= T_S + \left[\frac{Q_S Z_W}{K} - A_S\frac{{Z_W}^2}{2K}\right] + \left[\frac{Q_S(X-Z_B)}{K_{bb}} - A_S\frac{(X-Z_B)^2}{2K_{bb}}\right]$$

13. $$= T_S + \left[\frac{Q_S(X-Z_W)}{K_{bb}} - A_S\frac{(X-Z_W)^2}{2K_{bb}}\right]$$

14. $$= T_S + \left[\frac{Q_S Z_W}{K} - A_S \frac{{Z_W}^2}{2K} \right] + \left[\frac{Q_S Z_{bb}}{K_{bb}} - A_S \frac{{Z_{bb}}^2}{2K_{bb}} \right] + \left[\frac{Q_m (X - Z_B)}{K_b} + A_b (b)^2 \left(\frac{1 - e^{-\frac{X - Z_B}{b}}}{K_b} \right) \right]$$

15. $$= T_S + \left[\frac{Q_S Z_B}{K_{ave}} - A_S \frac{{Z_B}^2}{2K_{ave}} \right] + \left[\frac{Q_m (X - Z_B)}{K_b} + A_b (b)^2 \left(\frac{1 - e^{-\frac{X - Z_B}{b}}}{K_b} \right) \right]$$

16. $$= T_S + \left[\frac{Q_S Z_W}{K} - A_S \frac{{Z_W}^2}{2K} \right] + \left[\frac{Q_S (X - Z_W)}{K_{bb}} - A_S \frac{(X - Z_W)^2}{2K_{bb}} \right]$$

17. $$= T_S + \left[\frac{Q_S X}{K} - A_S \frac{X^2}{2K} \right]$$

CHAPTER 3

UNCERTAINTY ANALYSIS OF THE THERMAL MODEL TO PREDICT HEAT FLOW AND SUBSURFACE TEMPERATURE

3.1 Motivation and Background

As stated in Chapter 2, one of the advantages of the model developed is that it allows researchers to spend more time on data analysis, instead of data processing and handling. But the question remains how accurately this model predicts temperature at depth. For this analysis, both accuracy and precision are investigated.

Uncertainty, broadly speaking, is a measure of precision which is thoroughly evaluated here. According to Blackwell et al. (2007), the temperature at depth calculations are expected to have an uncertainty of approximately 10%, but Williams and DeAngelo (2011) estimated that uncertainty at 6 km was more likely in the range of 15-20% or higher. The result will be increases in drilling depth to reach a specified temperature due errors in estimating temperature at depth. This will result in increased cost, potentially putting future projects out of the realm of economic possibility.

Accuracy is the more difficult to gauge and is only covered briefly here. The difficulty in evaluating the accuracy of the model arises from a lack of equilibrium or actual full well temperature data for comparison. Therefore accuracy will be investigated in two ways: how closely the model matches the assumed corrected bottom hole temperature (BHT) and a plausibility calculation on temperature using average thermal properties.

For this reason the model proposed here, and previously applied in New York and Pennsylvania, will be analyzed to estimate the uncertainty of the modeled temperatures

at 6 km, focusing specifically on uncertainty in the properties of the sedimentary section. Further progress and refinement to the model will be best served by analyzing which of the remaining assumptions and simplifications induce the most uncertainty in the resulting temperature at depth. This work focuses on the uncertainty of three main model input properties: the well log BHT, the thickness of each geologic formation in the sedimentary section, and the thermal conductivity of each sedimentary geologic formation.

The approach used is to vary these properties according to modeled distribution functions and utilize a Monte Carlo simulation to predict the resultant temperatures at 6 km depth. The range of variation of the properties was selected based on the nature of confidence in their absolute values from the inputs as outlined in Chapter 2 and Shope et al. (2012). Commercially available software for Monte Carlo Analysis was applied to analyze the variation in calculated surface heat flow for a subset of wells in Steuben County, New York. The software selected for the task was Oracle Crystal Ball, a spreadsheet-based application capable of modeling risk and uncertainty. The resulting output was then run through the model developed in Chapter 2 to predict temperature at 6 km.

Presented here are the results of the formal analysis of uncertainty in the range of modeled temperatures at depth for three Cases. Each Case will incorporate increasing complexity as detailed below and contain 10,000 randomly generated trials using the Monte Carlo simulator. This increasing complexity was used to determine the possible reduction in uncertainty with refined inputs to the existing model. For this study uncertainty will be taken to be the percent variation of the P95 and P5 values from the mean temperature at 6 km predicted from Monte Carlo simulated data for each well. The primary properties explored in each case are measured wellbore BHT, individual formation

thickness, formation thermal conductivity, total sediment thickness, formation thickness scaling, and mineral and lithology variations.

3.2 Sample Well Selection

For this study, six wells from Steuben County, New York were selected for Monte Carlo simulation. In the Cornell well database, Steuben County has 143 wells that have survived review and processing as described in detail by Shope et al. (2012). This is a relatively large number for a single county in the state of New York. Additionally the geology is relatively simple, i.e. subsurface bedding is near horizontal and free of potential known or unknown large-scale faults or folds. Counties with much higher well count can be found, especially in Pennsylvania, but the closer the wells are to the Appalachian mountain front, the more likely that faulting, fracturing, or other deformation will be present. This would add a degree of complexity not addressed in this work.

The next selection criterion was depth to basement or total sediment thickness, one of the inputs in the Chapter 2 thermal model. This value ranges from around 2,500 m to 4,200 m in Steuben County. Wells that had sediment thickness within 5% or 200 m of 4,000 m were selected. The affects of individual formation thickness and thermal conductivity will likely be more evident with a thicker total sedimentary section.

Based on this criterion, 31 wells of the original 143 in the county remained. Six wells were then selected at random that spanned the range of total drilled depth of 1177 m to 3560 m. Basic data for these wells can be seen in Table 3.1. In the majority of this work, the wells are sorted by ascending total depth in meters. Whenever the wells are discussed by a simple numeric designation 1-6, this refers to this sorting by depth with well 6 being the deepest. Their locations are shown in Figures 3.1 and 3.2.

Table 3.1: Well information for the 6 wells selected for uncertainty analysis in Steuben County, New York.

Well Number	Identifier (API/Name)	API/Short Name	Base Case Uncorrected BHT (°C)	Well Depth (m)	Shope et al. (2012) Temp (°C) @ 6 km
1	31101001700000	00170	40	1177	135.9
2	31101231900000	23190	45	1776	132.4
3	31101230400000	23040	42	2287	129.5
4	31101230380000	23038	73	3206	148.1
5	31101228610000	22861	78	3206	145.4
6	31101229630000	22963	86	3560	146.4

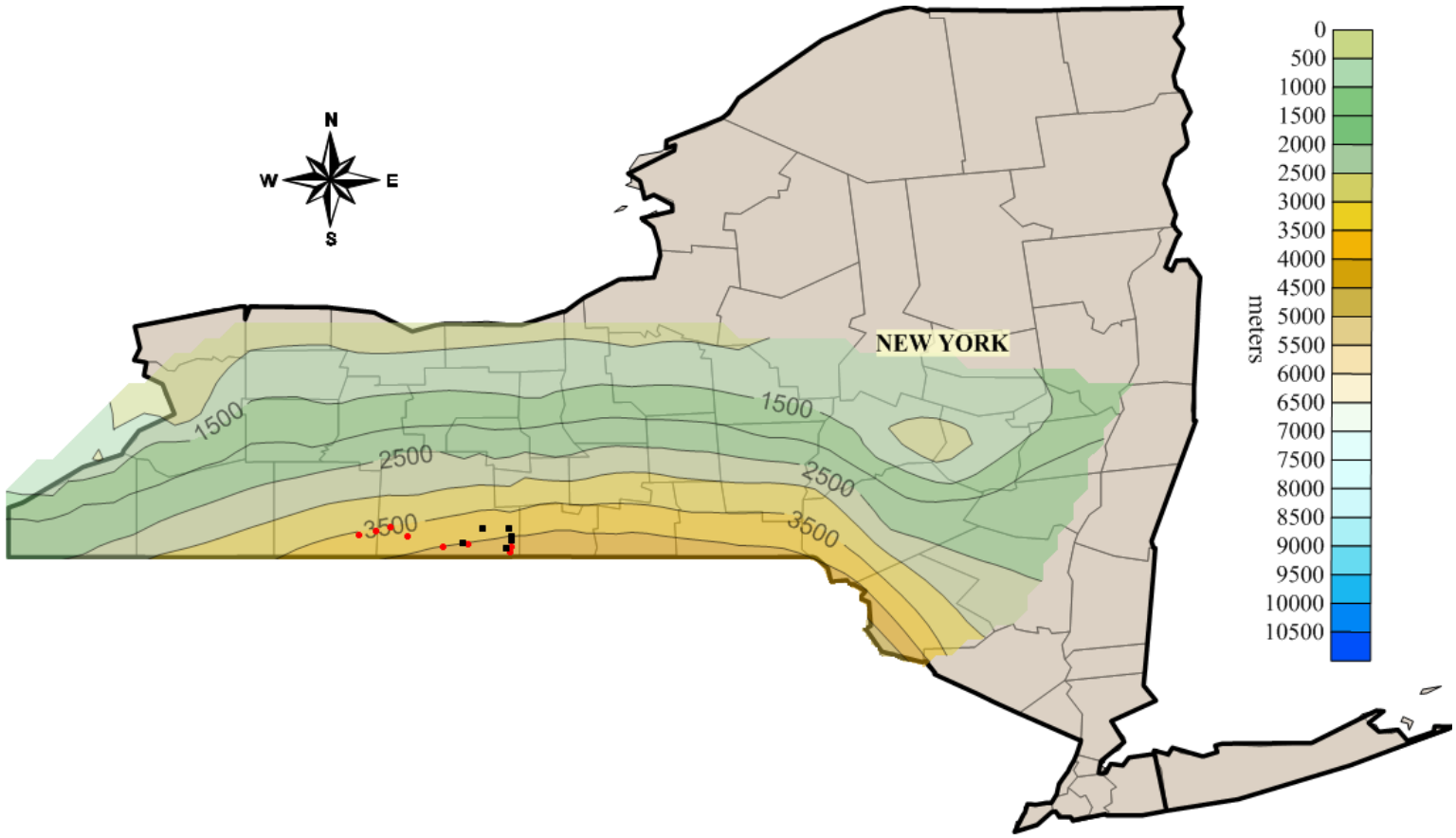

Figure 3.1: Map of New York showing the location of the 6 Steuben County wells being analyzed (marked in black) and the wells consulted for formation tops and other data from the ESOGIS (2012) website for Case 2 and 3 (wells marked in red). Contours are depth to basement below sea level (AAPG, 1978). Brown areas in Northern New York and Eastern New York either are outside of the Appalachian Basin or have basement at surface. These areas do not have sediments 5000m deep as the slight color variation may indicate.

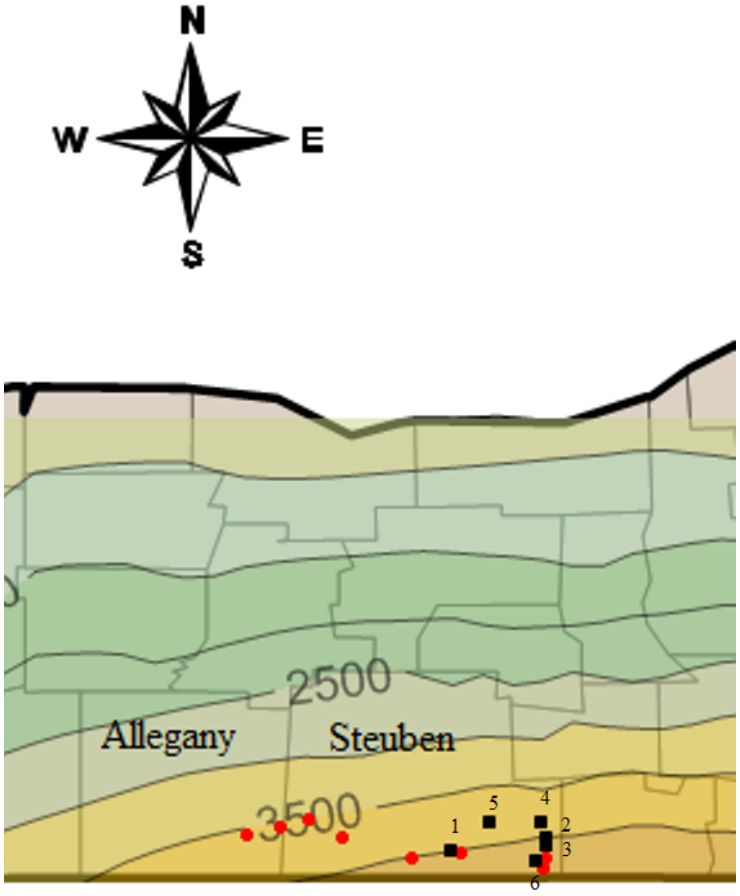

Figure 3.2: Map of a Section of Western New York showing location of the 6 selected wells in Steuben County (marked in black) and the wells with formation tops and other data consulted from the ESOGIS (2012) website for Case 2 and 3 (marked in red). Wells in both data sets are marked only in black; please see Case 2 for more detail. Contours are depth to basement (AAPG, 1978) in meters following the same contours as in Figure 3.1. Wells are numbered according to increasing total depth (see Table 3.1).

3.3 Uncertainty in Temperature Reading

The corrected BHT, as used in the model, will have two separate sources of error: the raw measured BHT and the application of a correction to estimate the equilibrium temperature of the virgin rock. The error in the raw measurement is difficult to precisely

quantify but includes tool error, miss-calibration, operator error, and other such events that may affect the uncorrected value (Majorowizc et al., 1980; Reiter and Tovar, 1982; Beach et al., 1986; Blackwell and Richards, 2004). For this study it is assumed that this error will not exceed 5%.

Additionally there will be error inherent in the application of the Harrison et al. (1983) temperature correction. Because the correction is empirically derived from the state of Oklahoma, its use in the states of Pennsylvania and New York may be questionable. By deriving an equation for a specific location, it is implicitly assumed that surface temperature was relatively constant for each well and that the drilling times and techniques over the range of depths to which the correction is being applied are the same.

The similar drilling technique assumption would include intermediate casing setting points, drilling mud rheology, circulation and trip times, and total down time spent on activities such as fishing or mechanical issues that would affect the thermal environment of the wellbore. These assumptions may be fairly accurate over a single producing field, but they begin to break down for an entire sedimentary basin, or as in this case, an entirely different basin.

However, as has been discussed by Shope et al. (2012) and Chapter 2, with a lack of deep equilibrium well temperature logs, there is not currently a more applicable alternative. Additionally, as discussed by Shope et al. (2012), the Harrison equation (Equation 2.16) does seem to provide accurate BHT correction for wells deeper than 1,000 meters in the states of interest (Figure 1.1). For this uncertainty analysis, an arbitrary 5% additional error will be applied to the well temperature, yielding 10% total assumed error.

For well temperature uncertainty, a triangular distribution was selected. This shape was chosen because it can closely match a normal distribution but allows for precise truncation at each end. Additionally, without multiple measurements of temperature in a single well at the same time, the presence of a normal distribution is not substantiated. The observed BHT with the Harrison et al. (1983) correction applied was set as the most likely value with the minimum and the maximum set to +/-10%. Figure 3.3 is an example for well # 00170 that has a measured uncorrected BHT of 38 °C and a corrected value of 42 °C.

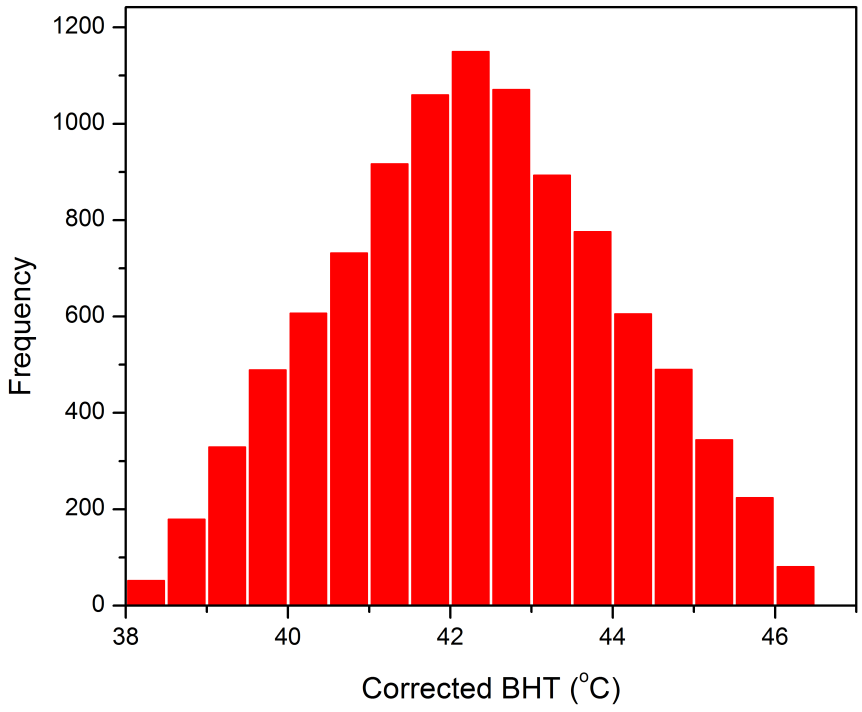

Figure 3.3: Example BHT Variability for Well #00170. This histogram is the modeled distribution function for the 10,000 trial Monte Carlo Simulation.

3.4 Variability in Individual Formation Thickness

As discussed by Shope et al. (2012) and Chapter 2, due to data volume, the spatial variability of individual sedimentary units was not taken into consideration (e.g. thickening, thinning, and pinch outs). Instead, each well was assigned the average thickness over the aerial extent of each Correlation of the Stratigraphic Units of North America (COSUNA) (Orlo, 1985) section and these averages were used in the model presented by the aforementioned author. Each unit was assumed to be present in each well and in the same proportion as in the COSUNA section. Individual formation thickness was then scaled to each well by the methods discussed in Section 1.2.3 and 2.3.1.

If throughout the geologic history of the region all the time intervals displayed the same spatial patterns of variation, this COSUNA-based approach would provide a good approximation of the spatial variability of thickness of rocks from each time period but not necessarily for the individual lithologic formations. But it is well known that over the 300 million years of Appalachian Basin accumulation, the patterns of regional thickness variation differed as a consequence of changing tectonic subsidence patterns (Jacobi, 1981; Quinlin and Beumont, 1984). Therefore, the simplified COSUNA-based approach rather than a well-by-well determination of each formation's thickness creates considerable uncertainty: the actual thickness of each sedimentary unit in an individual well could be any value ranging from the absolute maximum to the absolute minimum of the COSUNA section. Here this uncertainty is analyzed by the application of a rectangular distribution over this range for each unit at each well location. Table 3.2 shows the thickness values as taken from the COSUNA chart for NY28, the section containing Steuben County.

Table 3.2: COSUNA Stratigraphic Column (NY28) as applied in Case 1. For this Case the thickness of each unit is allowed to vary according to a rectangular distribution from the minimum thickness to the maximum thickness.

Formation	**Min Thickness (m)**	**Max Thickness (m)**
Sunfish/Conewango/Conneaut	580	1150
Canadaway	400	550
West Falls	335	762
Sonyea	55	200
Genesee	30	230
Tully	2	6
Hamilton	100	270
Onondaga	24	45
Oriskany	1	20
Becraft	0	15
Kalkberg	0	18
Coeymans	0	30
Manlius	0	12
Rondout	8	14
Bertie	15	20
Camillus	25	40
Syracuse	80	400
Vernon	150	300
Lockport	45	50
Clinton OR Rochester	30	80
Grimsby	18	20
Queenston	256	302
Lorraine	216	280
Utica	35	55
Trenton	198	229
Black River	90	137
Tribes Hill	0	11
Little Falls	20	168
Theresa	20	100
Potsdam	0	107

3.5 Variability in Thermal Conductivity

The main aspect of conductivity that is addressed here is the assumption that each formation is a proxy for a rock type with a single conductivity over the entire area underlying each group of wells. In the case of the New York and Pennsylvania maps presented by Shope et al. (2012), each formation present in the COSUNA column is assumed to have the same exact lithology over the entire area of each section. For example in NY28, the Canadaway Group is listed as undifferentiated and exclusively made of shale over the entire county with an anticipated thickness of 400-550 m.

By applying a single conductivity, we are assuming that the formation is shale, and it does not change appreciably in grain size or mineral content over the 1000's of square kilometers it is applied to. While this is known to be untrue, the uncertainty analysis conducted here determines if the effect is large enough as to render the model output useless. Each geologic formation may have a grain-size dependent lithologic variation (e.g. it can change from shale-dominated to sandstone dominated) or a mineral-dependent variation over some lateral distance (e.g., it may change from shale-dominated (clay minerals) to limestone-dominated (calcite and aragonite dominated)). This scale of variation will be discussed broadly as lithologic variation in this work, with the understanding it contains both grain size and mineralology changes as described.

Each formation may have additional mineralogy variation within what has been dubbed a single lithology (e.g., a sandstone may change from a dominance of quartz grains to a dominance of volcanic lithic fragments with a high proportion of plagioclase and feldspar). Variation of this type will be discussed as mineral variation, which is not to be confused with broader scale mineralogical controls on gross lithologies (i.e. siliciclastic to carbonate mineral variation). By looking at known mineral dispersal

patterns in other formations, we can gauge how large of a variation there will be over the aerial extent of each COSUNA section.

Jones and Blatt (1984) analyzed the mineral content of 116 samples from the Pierre Shale in south central Canada and the north central United States. The Pierre Shale is a large laterally extensive unit that formed in the shallow waters of an inland seaway that split the North American continent during the Late Cretaceous Period. Quartz percentages were determined by x-ray diffraction on the aforementioned 116 samples, 100 of those from surface collection at outcrops and 16 from subsurface sources. While the Pierre is younger in age, this environment would have been very similar to that which formed the Marcellus and other shale units within the Appalachian basin (Figure 3.14).

From their isopach map, Jones and Blatt (1984) conclude that the Pierre Shale was sourced from areas on the western shore. It was found that quartz content varied significantly in an east-west trend, with lower average values being found in the east or farther from the western source area. Quartz values as high as 30% can be found in central Montana, while 5% quartz is common in central North Dakota. On a more relevant spatial scale, Jones and Blatt (1984) found that quartz percentage in parts of Colorado and New Mexico could drop by 10% over short distances, more appropriate for this study of Steuben County. While no comparable mineralogical data exist for Steuben County's shales, it is to be expected that comparable horizontal changes in mineralogy occur.

Additionally, mineralogy and therefore conductivity can change vertically in a unit. With full well logs, this could be addressed for each well. But given the amount of data processed in the previous work, review of this quantity of well logs was infeasible. In the Pierre shale, Jones and Blatt (1984) found standard deviations in excess of 6% on the quartz volume fraction over the vertical thickness of the formation at a given location.

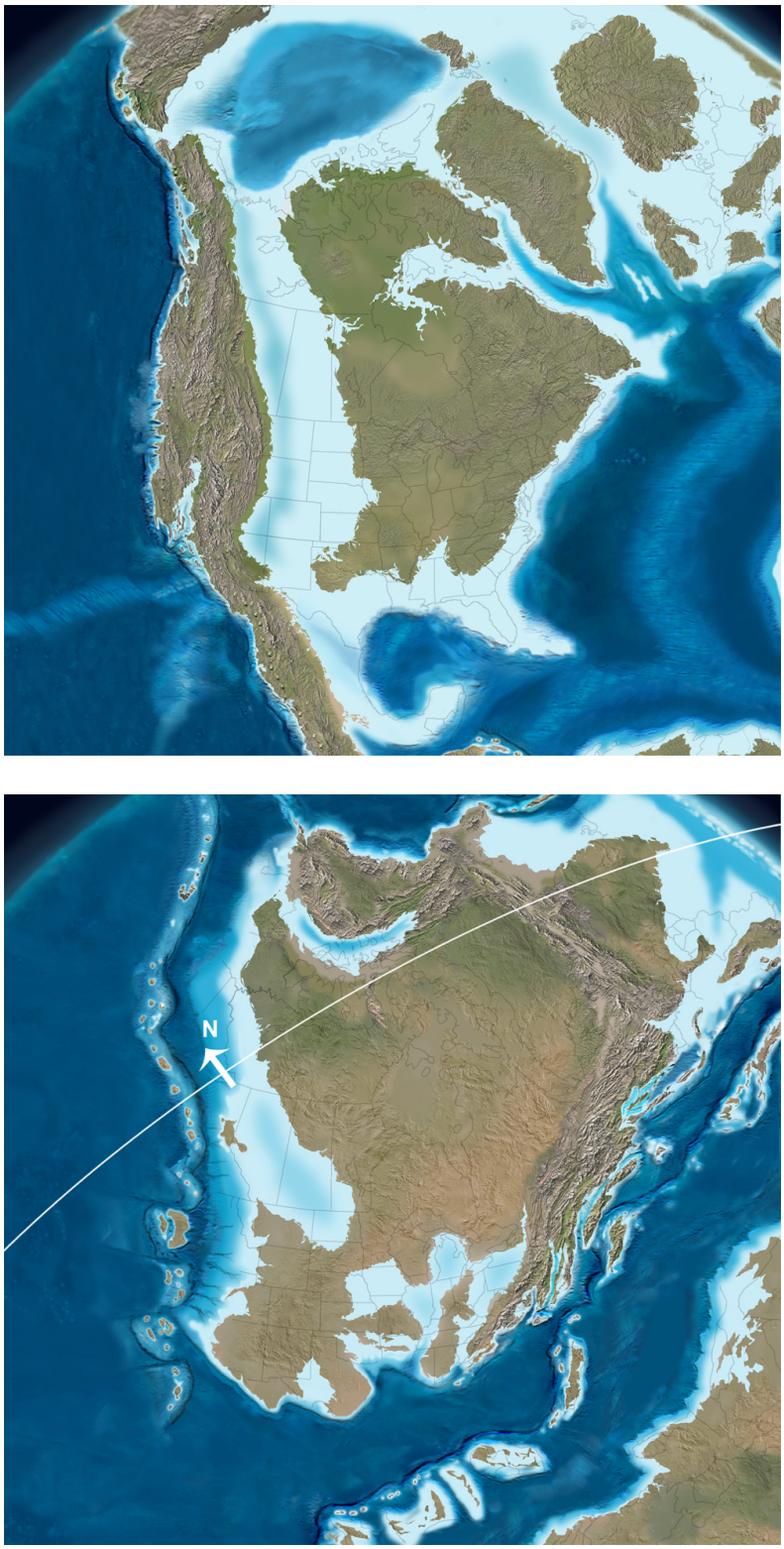

Figure 3.4: Maps of North America during the Cretaceous and the Devonian. The first map shows North America during the Cretaceous 85 Ma when the Pierre Shale (discussed by Jones and Blatt) formed. The second shows the conditions during the Middle Devonian 385 Ma when the Marcellus was formed. Both were formed in shallow inland seas (NAPM, 2012).

This shows the possibility for significant heterogeneity within what has been dubbed a single lithology in the model. The result is a broad range of thermal conductivities for any given classification of lithology. For example Figure 3.5 shows the range of conductivities observed for many lithologies as presented by Zoth and Haenel (1988).

In Case 1 and Case 2 only the "mineral" variation, as defined above, will be taken into consideration for each geological unit by generating a normal distribution of conductivity for each dominate lithology and applying only one of those distributions to each formation. The average thermal conductivity and standard deviation of each lithology type was determined from the Beardsmore and Cull (2001) text, which was the primary source for Shope et al. (2012) and Chapter 2. Each conductivity distribution was then truncated at a maximum and minimum based on the work of Touloukian (1970), Reiter and Tover (1982), and Zoth and Haenel (1988). The result can be seen in Figure 3.6, 3.7, and 3.8, which show the modeled conductivity distribution functions for shale, sandstone, and limestone, the three dominant lithologies in the stratigraphic section. These diagrams represent the distributions as used in the Monte Carlo Simulator for the 10,000 simulations being performed for each Case. Similar distributions were generated for halite, dolomite, and any other necessary lithologies within the section. Cases 1 and 2 mainly probe the potential effect and gains of stratigraphic refinement by the researcher.

The general normal distribution and limits for each lithology was confirmed by reviewing lithology specific data by Touloukian et al. (1970), Beach (1985), Beach et al. (1987), and Zoth and Haenel (1988). Figure 3.9, 3.10, and 3.11 present histograms and cumulative distribution plots for the model as well as the distributions from measurements of thermal conductivity by Beach (1985) on rock samples primarily from Alberta Canada.

TABLE 10.1
Thermal conductivity of different rocks at room temperature Čermák and Rybach (1982), Kappelmeyer and Haenel (1974).

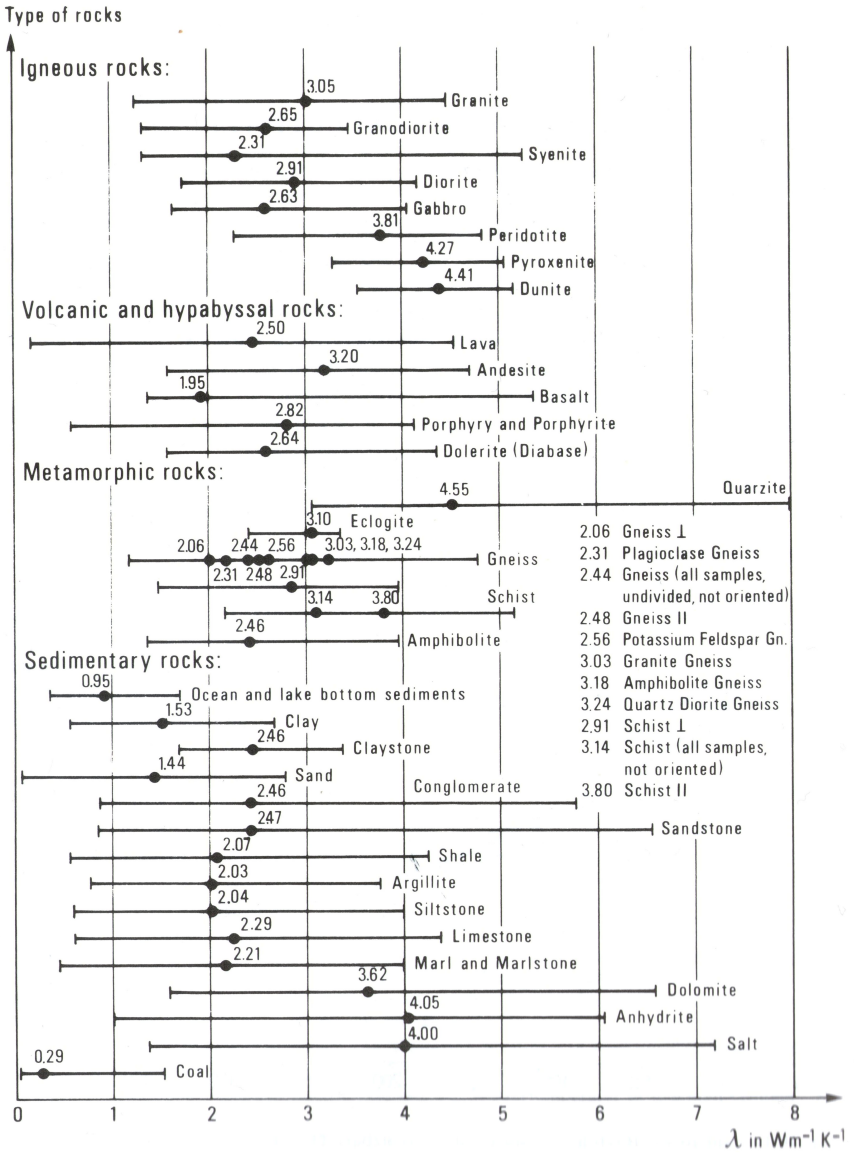

Figure 3.5: Scan of thermal conductivity data, including average and absolute range from measured samples as presented by Zoth and Haenel (1988). This is one of the principal references used to constrain the thermal conductivity distribution function models used in this study.

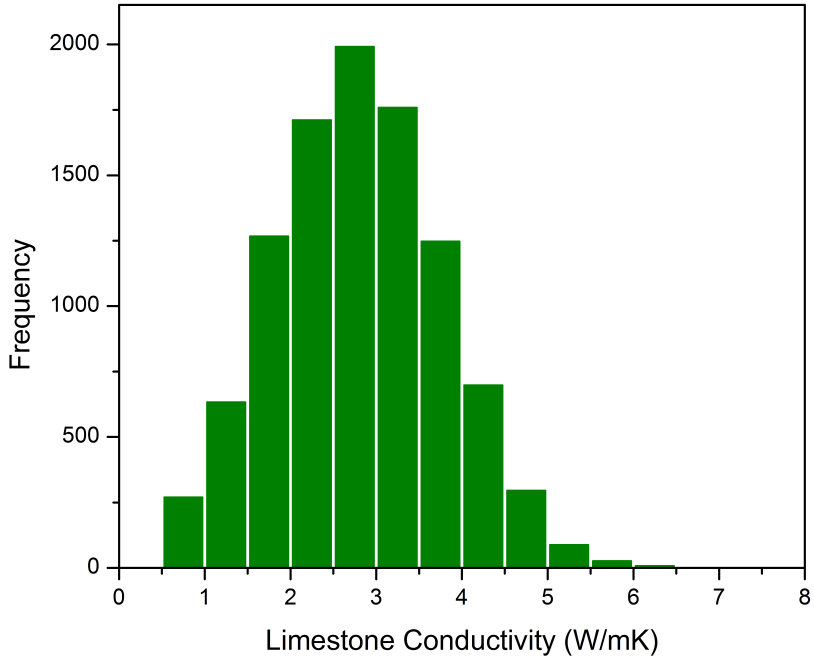

Figure 3.6: Limestone Thermal Conductivity Distribution Function

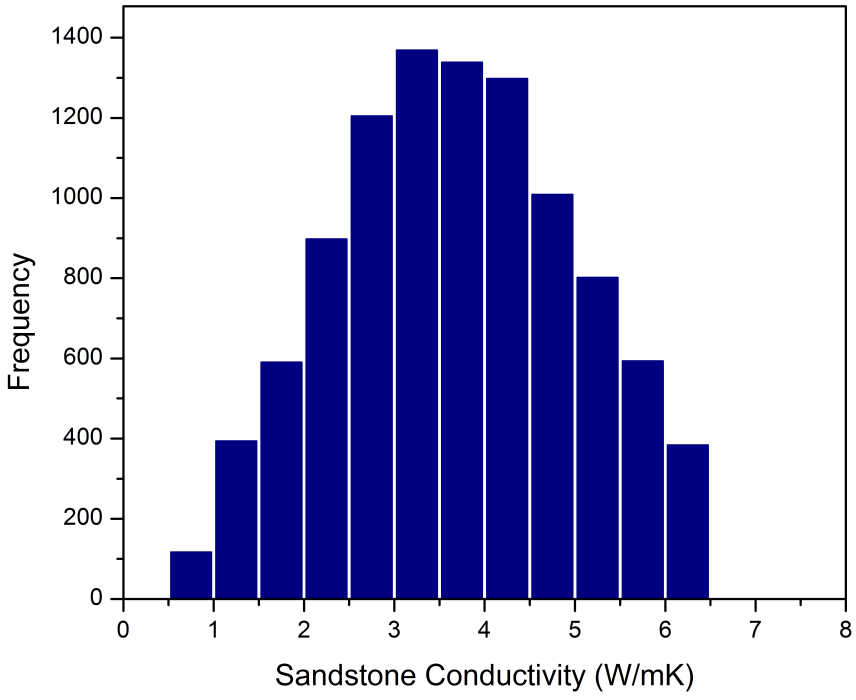

Figure 3.7: Sandstone Thermal Conductivity Distribution Function

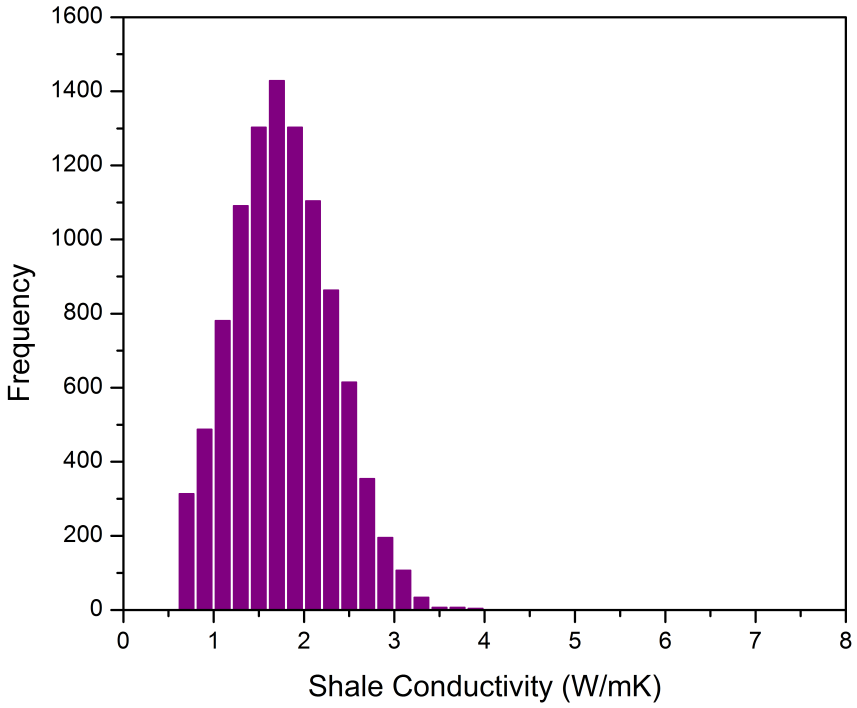

Figure 3.8: Shale Thermal Conductivity Distribution Function

3.6 Variability in Total Sediment Thickness

Because the procedure described by Chapter 2 involves scaling the thickness of all the rock units that lie above the basement, the total thermal resistance of each formation changes as the thickness of the full column. As a result, the uncertainty on the thermal resistance caused by the uncertainty on the thickness of individual rock units needs to be investigated. For all 6 sample wells, the sediment thickness is 4,000 m +/- 200 m; therefore this property was modeled as a triangular distribution with those bounds. The modeled distribution function for the 10,000 Monte Carlo simulations can be seen in Figure 3.12.

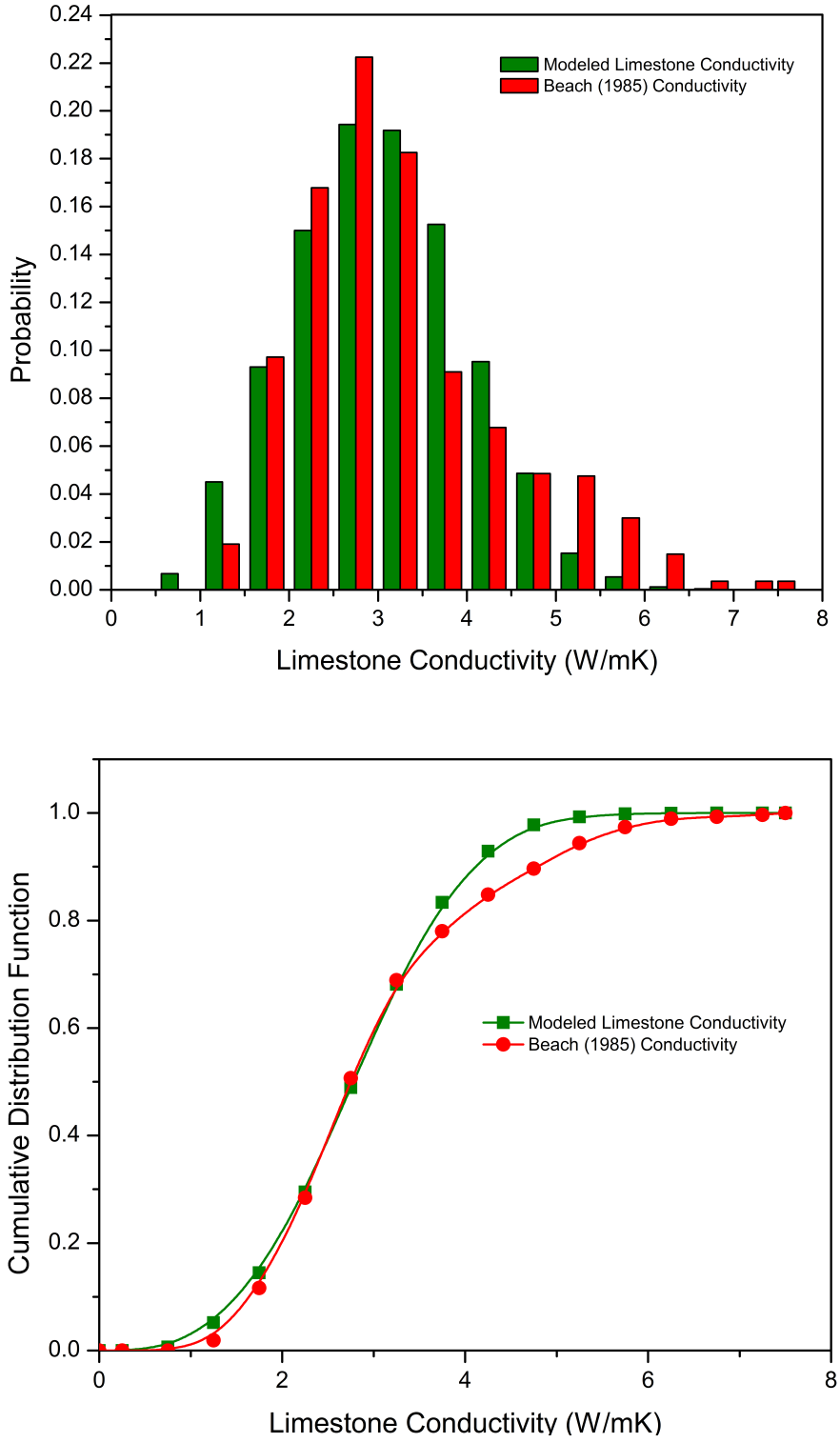

Figure 3.9: Histogram and Cumulative Distribution Function for the limestone lithology. Data displayed in red contains the normal distribution as modeled for this study. Data in green is from Beach (1985) showing a distribution from sample data in Alberta, Canada.

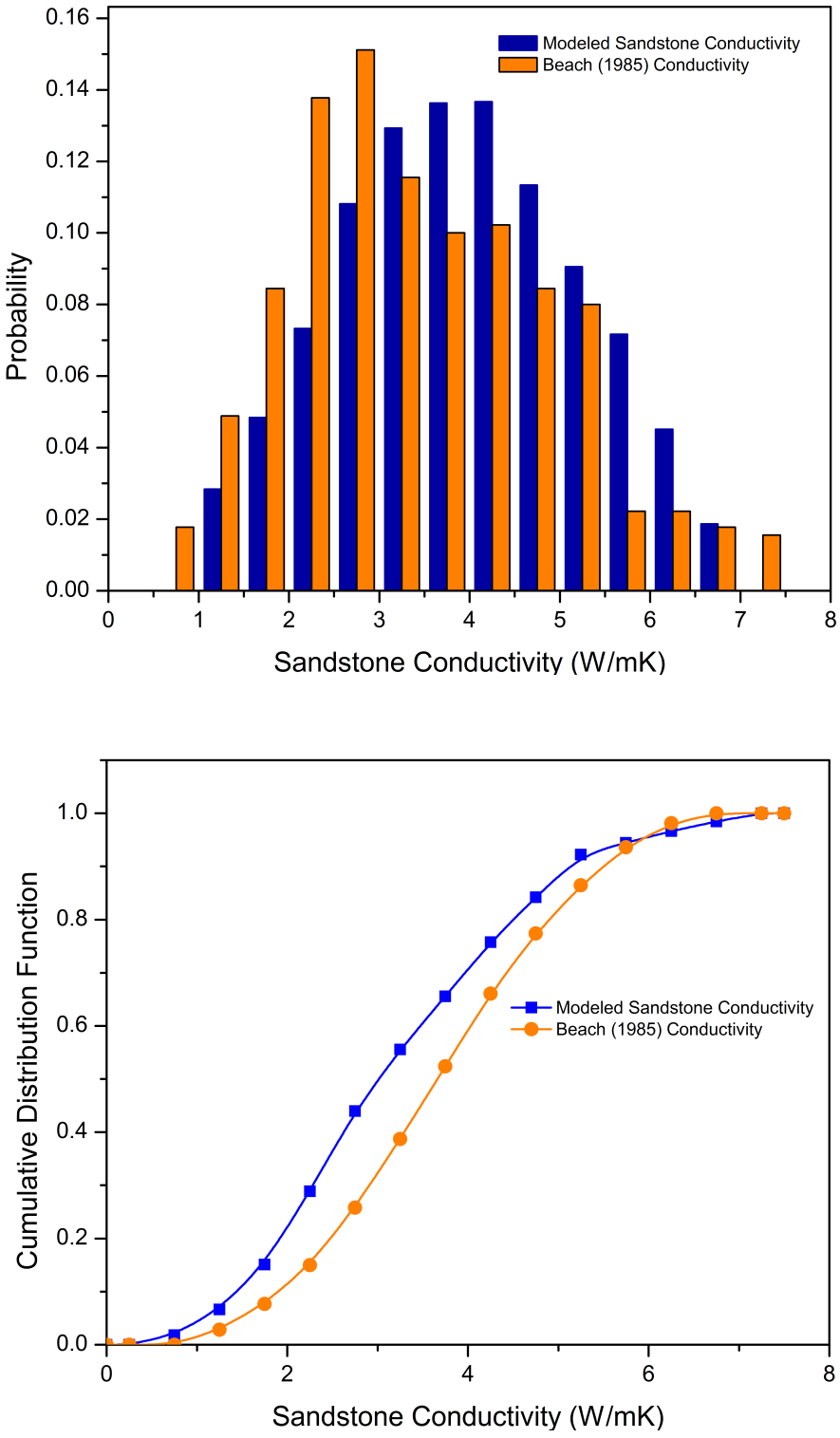

Figure 3.10: Histogram and Cumulative Distribution Function for the sandstone lithology. Data displayed in blue contains the normal distribution as modeled for this study. Data in orange is from Beach (1985), showing a distribution from sample data in Alberta, Canada.

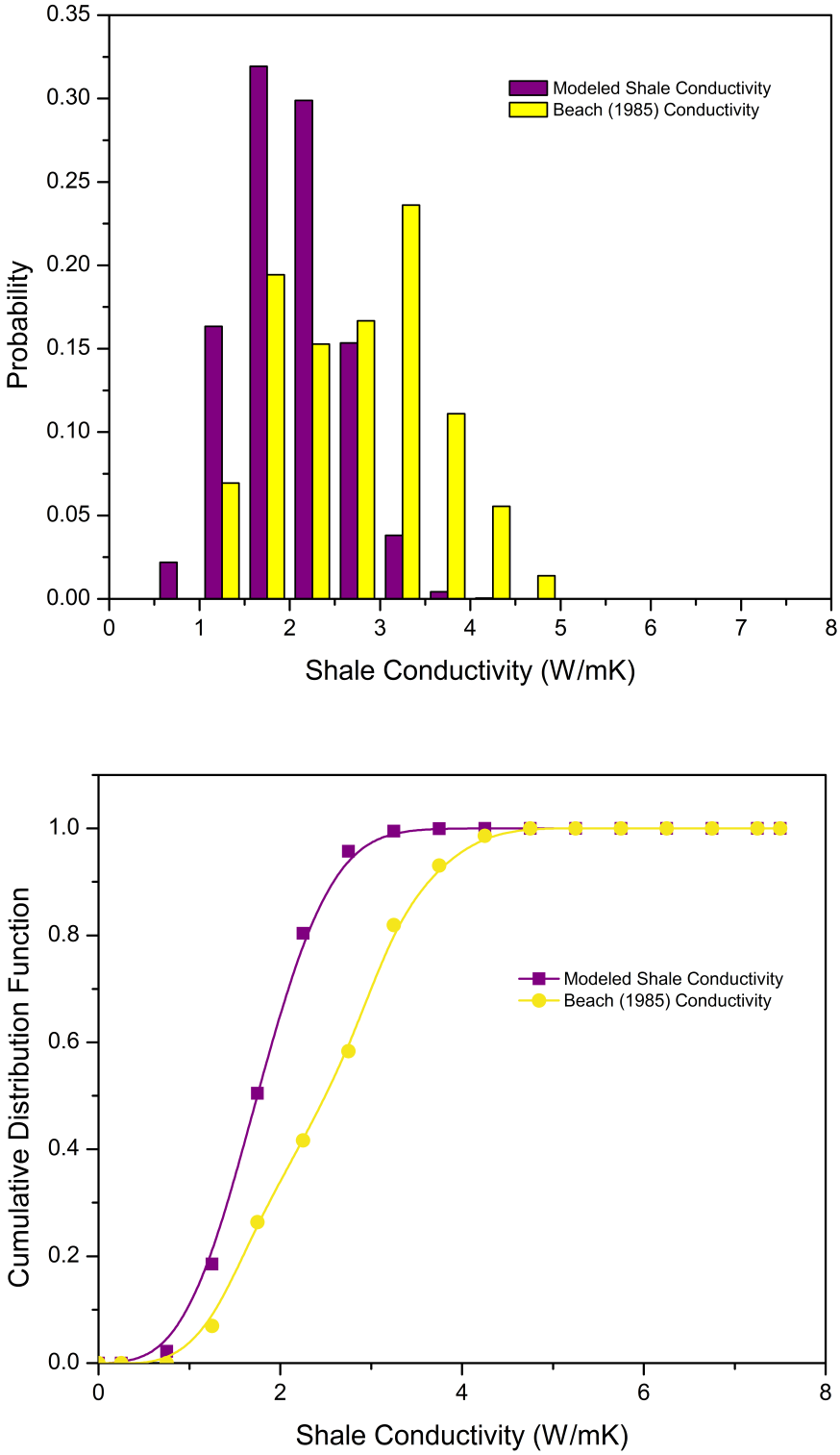

Figure 3.11: Histogram and Cumulative Distribution Function for the shale lithology. Data displayed in purple contains the normal distribution as modeled for this study. Data in yellow is from Beach (1985), showing a distribution from sample data in Alberta, Canada.

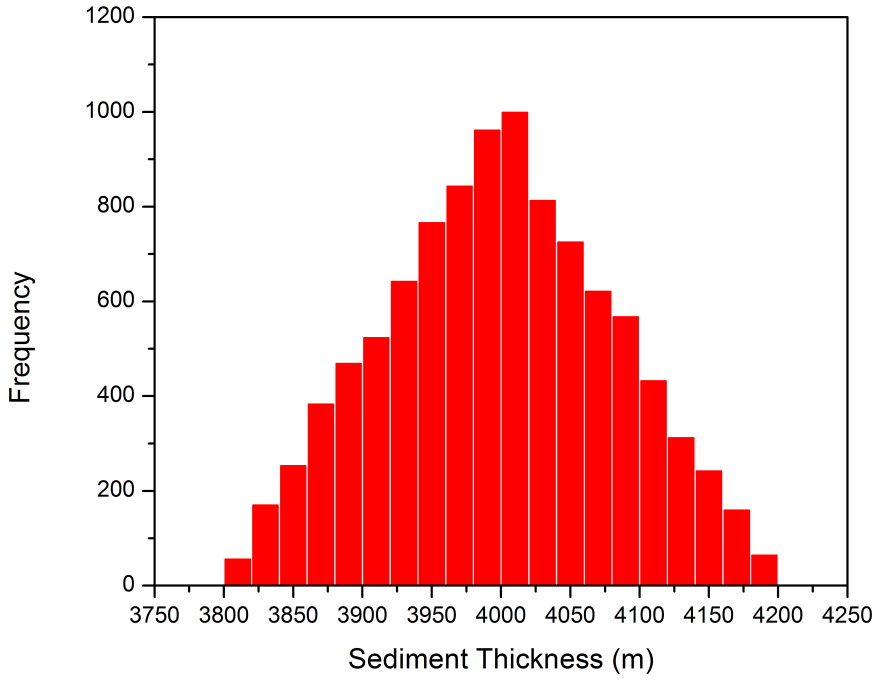

Figure 3.12: Total Sediment Thickness Modeled Distribution Function for 10,000 trial Monte Carlo Simulation. Wells were selected to vary between 3,800 and 4,000 meters of total sediment thickness. This can roughly be seen in Figure 3.1 and 3.2 where the contours depict depth to basement.

3.7 Property Variation in Relation to Case Study Selections

As stated, it was decided that a series of 3 Cases would be developed each with increasing complexity and refinement that would build on the inputs of the previous Cases. The Cases themselves can be thought of as a series, as changes in Case 2 are retained and then expanded in Case 3.

For Case 1 the exact stratigraphic column is shown in Table 3.2. Further, Case 1 will apply the variation and uncertainty of 10% on the BHT, the variation in total sediment thickness in Figure 3.12, and apply a single lithology for each formation along with the appropriate thermal conductivity from modeled distributions in Figures 3.6 to 3.8.

Case 2 differs from Case 1 in two ways. First, it examines the impact of refinement

of the stratigraphic column to eliminate or reduce the size of the undifferentiated units at or near the surface. Second, Case 2 performs the individual unit thickness scaling at an intermediate formation as well as to total sediment thickness. Details of the scaling process can be found in section 1.2.3, 2.3.1, and 3.8.2. In Case 1 it was found that the wells were very rarely predicted to reach total depth in the correct formation. By applying these changes, each well was predicted to reach total depth within a few formations of the actual total depth formation. Details can be found below.

Case 3 again builds on Case 2 by selecting three formations for more specific thermal conductivity estimation. These formations were selected because they are relatively thick compared to others in the section, they are high on the sensitivity diagrams for each well in Case 2, and they are all known to have some special attributes that may make their conductivity significantly different from other formations. Specifics on each formation and how it was treated can be found in Section 3.10.

3.8 Case 1

As previously stated, Case 1 is the simplest and used the modeled property distribution functions shown earlier and the stratigraphic column in Table 3.2.

3.8.1 Sensitivity to Input Parameters

Below are sensitivity or tornado diagrams for each of the 6 wells in order of ascending total depth. A sensitivity or tornado diagram here presents the rank correlation coefficient of each input parameter to the output parameter, which in this case is the modeled surface heat flow. For Case 1 each well output depends on 67 inputs; the correlation

coefficients for the top 15 are shown here.

As can be seen from the sensitivity charts, the geologic units near the top of the stratigraphic column (i.e. the Sunfish, Canadaway, and West Falls Group) in Table 3.2 and their corresponding conductivities have the largest impact on the modeled heat flow for each well. The property that distinguishes these upper units from the lower ones are that they are disproportionately thick, which is an artifact of the lack of knowledge when using the COSUNA sections for the model. It is only in the deeper wells that other units show significant impact on the heat flow and modeled temperatures.

The issue that arises is that each undifferentiated unit will be given a single conductivity for a very thick section and that conductivity may be the end member for each lithology. For example the Sunfish Formation may be assumed to be 1,150 m thick, with a conductivity of 6.5 W/mK, the extreme high value for sandstone. It is unlikely any formation would be uniform enough in a vertical sense to have a single conductivity over 1,150 m of thickness. Case 2 will attempt to divide each formation and alleviate this issue.

3.8.2 Case 1 Uncertainty

Using the thermal model developed by Chapter 2, the uncertainty in temperature at 6 km based on each well can be seen in Table 3.3. The P95 and P5 levels are displayed with their percentage deviation from the mean.

In general the uncertainty decreases with increasing depth of the well used to calculate heat flow. Additionally, the uncertainty is always lower for the P5 value, meaning less risk of finding temperatures lower than expected.

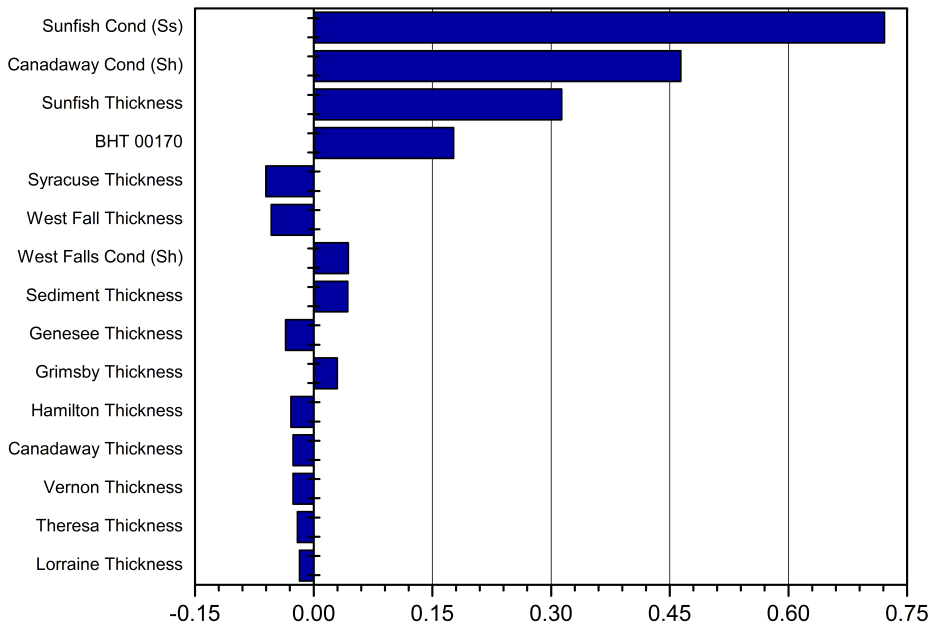

Well # 00170 Sensitivity Case 1

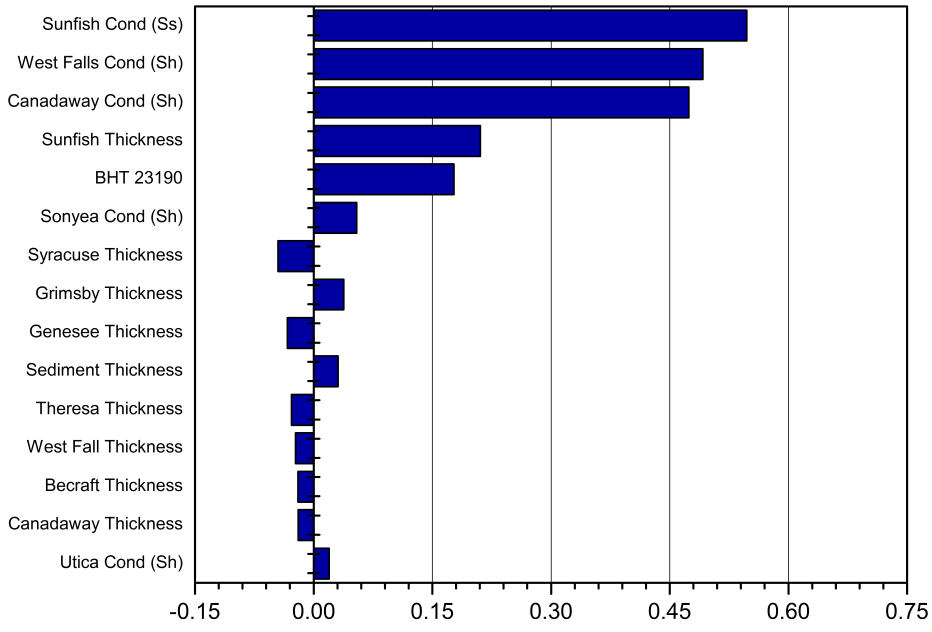

Well # 23190 Sensitivity Case 1

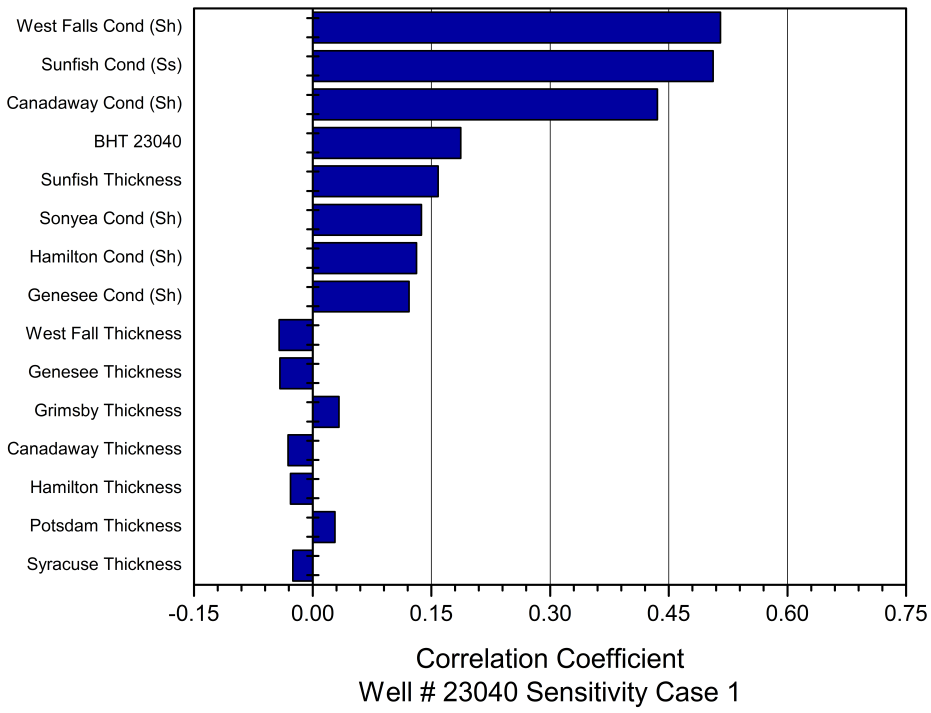
West Falls Cond (Sh)
Sunfish Cond (Ss)
Canadaway Cond (Sh)
BHT 23040
Sunfish Thickness
Sonyea Cond (Sh)
Hamilton Cond (Sh)
Genesee Cond (Sh)
West Fall Thickness
Genesee Thickness
Grimsby Thickness
Canadaway Thickness
Hamilton Thickness
Potsdam Thickness
Syracuse Thickness
-0.15
0.00
0.15
0.30
0.45
0.60
0.75
Correlation Coefficient
Well # 23040 Sensitivity Case 1

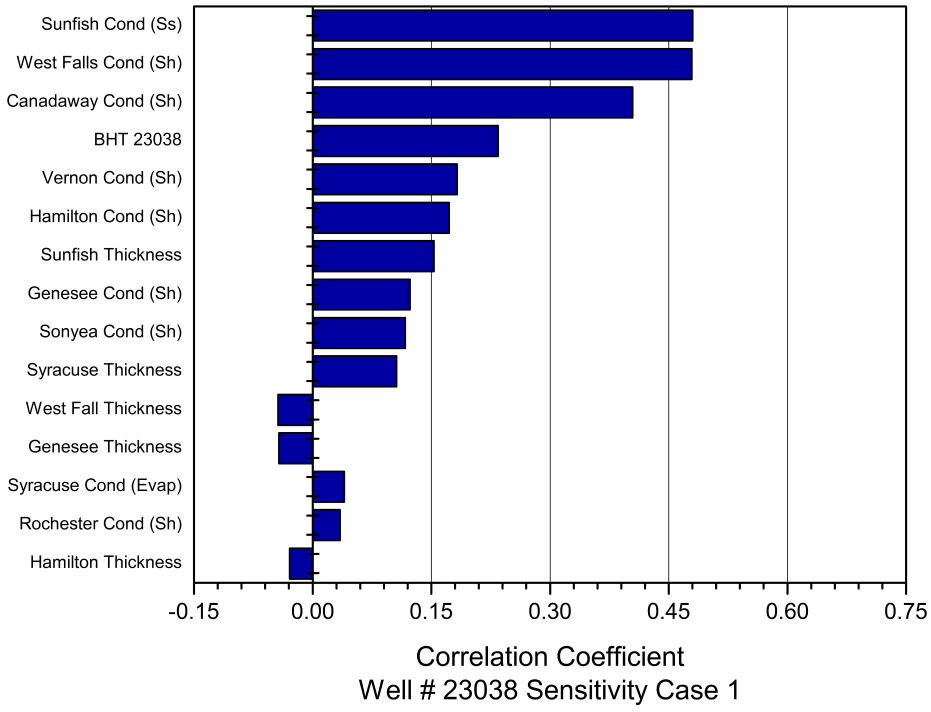
Sunfish Cond (Ss)
West Falls Cond (Sh)
Canadaway Cond (Sh)
BHT 23038
Vernon Cond (Sh)
Hamilton Cond (Sh)
Sunfish Thickness
Genesee Cond (Sh)
Sonyea Cond (Sh)
Syracuse Thickness
West Fall Thickness
Genesee Thickness
Syracuse Cond (Evap)
Rochester Cond (Sh)
Hamilton Thickness
-0.15
0.00
0.15
0.30
0.45
0.60
0.75
Correlation Coefficient
Well # 23038 Sensitivity Case 1

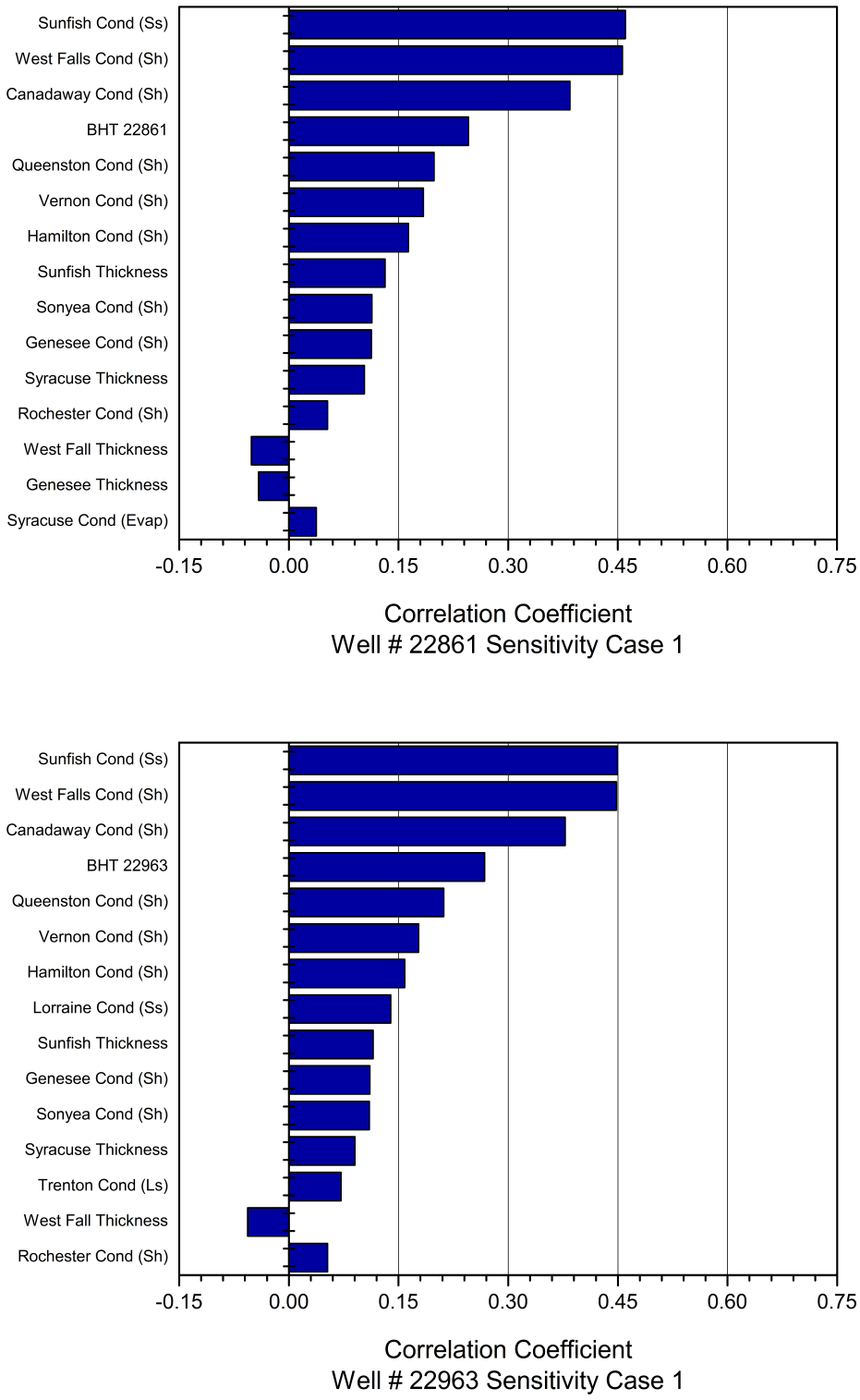

Figure 3.13: Sensitivity diagrams for the 6 modeled wells in Steuben County, NY Case 1. Parameters refer to the thickness and conductivity assigned to each formation (Table 3.2). Abbreviations refer to: Cond = conductivity; BHT = bottom hole temperature; Sh = shale; Ss = Sandstone, Ls = limestone, Evap = halite, Dol = dolomite.

The most striking result is the uncertainty in well #00170, which ranges from 38% to 65%. The absolute range in modeled temperature for this well is 104 to 907 °C. This is due to the fact that the well, at only 1,177 m in depth, can be nearly completely controlled by the thickness (maximum of 1,150 m) and conductivity (assumed sandstone lithology) of the Sunfish Formation. When values close to the end member of each distribution are selected in one of the 10,000 trials in the Monte Carlo simulator, the results may be infeasible. As discussed in Section 3.5, based on the work of Jones and Blatt (1984), it is unlikely a formation would be this homogenous over such a large vertical scale.

Given *a priori* knowledge many of these results could be removed, including values such as 907 °C. However it is left in here to demonstrate the inherent limitations of the current model. Further, with no additional data, the exact way in which to truncate or remove these cases cannot be determined. This demonstrates that there is an irreducible complexity that must be kept in mind by researchers when processing any well, but especially the shallowest wells. A visual representation of the output data in Table 3.3 can be seen in Figure 3.14.

Table 3.3: Statistical Summary Data for Case 1. The mean, standard deviation, P95 and P5 values refer to the anticipated temperature at 6 km based on the BHT data acquired from each well and processed via the model presented by Chapter 2.

Well:	**00170**		**23190**		**23040**		**23038**		**22861**		**22963**	
Depth (m)	1177		1776		2287		2879		3206		3560	
Mean (°C)	212		160		145		157		148		148	
Std. Dev (°C)	65.97		27.35		16.45		15.37		10.95		10.11	
P95 (°C)	335	58%	212	32%	174	20%	183	16%	167	12%	165	11%
P5 (∘C)	131	38%	124	23%	122	16%	136	13%	132	11%	133	10%

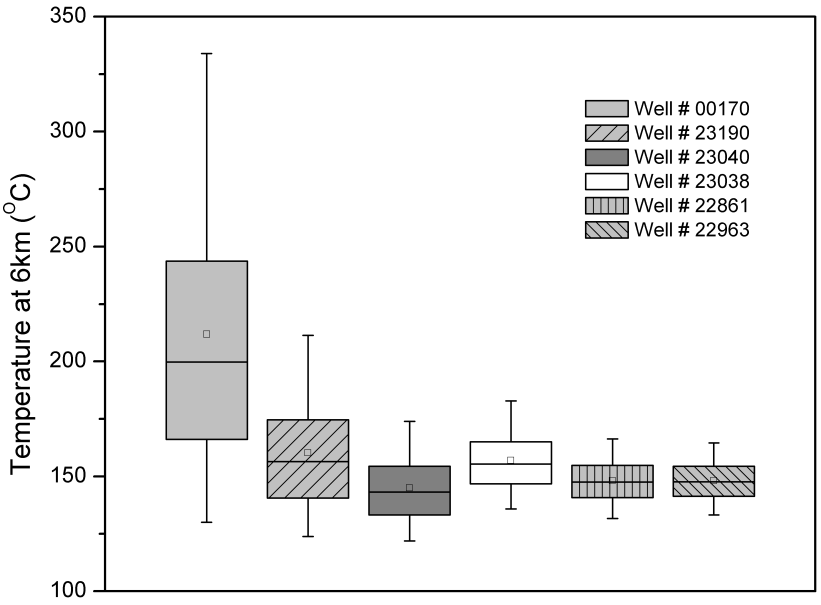

Figure 3.14: Box and whisker plot for the Case 1 uncertainty. Box and whisker plots are graphical representations of descriptive statistics. The box shows the median 50% (i.e. range from P25 to P50), the small square shows the mean, and the whiskers are the P95 and P5 values.

3.9 Case 2

3.9.1 Refined Subdivision of Stratigraphic Units

From the original stratigraphic column (Table 3.2), the Conneaut/Conewango/Sunfish Group, the Canadaway Group, and West Falls Group are broken into 20 smaller units of varying lithology. The new stratigraphic column can be seen in Table 3.4. This column was developed specifically for southern Steuben County. A summary of the wells reviewed from the ESOGIS (2012) database can be seen in Table 3.5.

Table 3.4: Revised Stratigraphic Column for Case 2. All formations below the West Falls Group, starting with the Sonyea, remain the same as in Case 1 (Table 3.2).

Original Group	Formation	Min Thickness (m)	Max Thickness (m)
Sunfish Group	Sunfish Undiff	425	759
	Conewango	140	200
Conneaut Group	Germania	0	21
	Whitesville	10	91
	Hinsdale	5	18
	Wellsville	0	61
	Conneaut Undiff	0	9
Canadaway Group	Cuba	0	12
	Machias	94	121
	Rushford	0	11
	Caneadea	30	85
	Hume	0	10
	Canaseraga	49	91
	South Wales	2	6
	Dunkirk Sh	0	14
	Canadaway Undiff	35	161
West Falls Group	Hanover/Wiscoy	33	80
	Pipecreek Sh	0	8
	Angola Sh/Nunda Fm	60	200
	Rhinestreet	0	60

This new section was determined from review of well log tops from the Empire State Oil and Gas Information System (ESOGIS) (2012) database, the identification and description of each unit by the USGS (2012), and the work of Young and Kreidler (1957), Smith (2002), and Jacobi (2012). The remaining undifferentiated thickness for each group was then determined by subtracting the sum of the minimum and maximum thickness of the new individual units from the thickness range in the original column (Table 3.2) of their respective geologic group. The one exception is the West Falls Group. This formation was found to have a total differentiated thickness close to what would be expected in this location. Therefore additional undifferentiated thickness was not required for the West Falls.

Table 3.5: Data on the well files from ESOGIS consulted to construct the Case 2 Stratigraphic Column including the identified interpreter for each well log set. Although the test wells for this project occur in Steuben County, the shallow units were subdivided for few wells there. Instead, the shallow units were more commonly subdivided for wells in neighboring Allegany County. Therefore two Allegany County wells are included in this compilation. Formation Tops Geologist "Comp Report" refers to tops identified on the completion report as filed by the well operator.

Well (API):	**Total Depth (m)**	**Formation Tops Geologist**
31101000800000	1252	Fralich/ Beinkafner
31101001310000	1298	NYSGS Files/Kreidler/Beinkafner
31003098960000	1416	VanTyne/Rickard/Beinkafner
31003093300000	1511	VanTyne/Rickard/Comp Report
31101239680000	1457	Comp Report
31101239050000	1478	Comp Report
31101232270000	3351	Comp Report
31101231100000	3431	Comp Report
31101229630300	3565	Comp Report
31101001700000	1180	Beinkafner/NYSGS
31101231900000	3000	Comp Report
31101260610000	3518	Comp Report
31101230380000	3084	Comp Report
31101228610000	3208	Slater/Comp Report

Further, the scaled column was checked to verify if the well would be predicted to reach total depth in the appropriate formation. For Case 2, 10,000 new trials using this refined upper section and the original lower section (Table 3.2) were generated. The shallowest well, # 00170 (1177 m), reaches total depth (TD's) in the Oriskany sandstone (ESOGIS, 2012). While the scaling approach here is not perfect, based on the column presented this well is predicted, in most of the Monte Carlo Simulations, to TD in a formation no further than two away from the Oriskany. The same holds true for the deepest well, # 22963 (3560 m), which reaches total depth in the Tribes Hill Formation. Review of the Monte Carlo trials for Case 2 reveals that the scaled column is predicting a TD between the Trenton and Little Falls formations for this deepest well, again only a couple

formations from the actual. Discussing the difference in TD as number of formations would not be a typical way of discussing the difference given that each formation has a variable and different thickness. However in this model each formation is a proxy for a unit with a distinct conductivity. Therefore missing a formation is missing an individual conductivity. Overall the results being only 2 or 3 formations off was much better than expected, given the simplicity of the scaling approach.

3.9.2 Scaling to the Tully

In Chapter 2, section 2.3.1, the method of determining and applying a scaling factor to the stratigraphic section to adjust the unit thickness to the anticipated value at each well location is given in detail. For this uncertainty analysis, the approach was applied to the depth of the Tully Formation as well as to the total sediment thickness.

From the formation tops reviewed in the ESOGIS well database (Table 3.5), it was apparent that the Tully Formation was widespread and occurred at a fairly constant depth below the surface over the area covered by the wells being analyzed. Therefore the new stratigraphic column had two scaling factors developed. One factor scaled everything above the Tully to the average depth to this formation, and another scaled the units below the Tully to the anticipated total sediment thickness. For this case, these factors will be discussed as Thickness to Tully and Sediment Thickness respectively. See Figure 2.4 for an example of how these factors are calculated.

3.9.3 Sensitivity to Input Parameters

Figure 3.15 shows sensitivity charts for each well using the refined geologic column of Case 2 and the two scaling factor methods as discussed. The output for each well depends on 102 inputs in Case 2; only the top 15 are displayed here.

The previous dependence of each well mostly on the dominating undifferentiated formations has largely been alleviated. This is especially true of the deeper wells, where relatively thick formations deeper in the sedimentary section now have greater influence on the modeled heat flow.

3.9.4 Case 2 Uncertainty

The resulting uncertainty based on the refined stratigraphic column can be seen in Table 3.6. Case 2 has brought the largest improvement in the shallowest well, # 00170. This well is no longer subject to large influence by one formation, and as a result the model is now stable to this depth. Additionally, the new stratigraphic column has resulted in the reduction of uncertainty in all wells as evidenced by their P95 and P5 values. These changes are due to the averaging affect of the 20 formations of variable lithologies that replace the three original groups. The thermal conductivity on an average basis over the total thickness of the original groups will now be much closer to the actual average. Uncertainty data for Case 2 is presented in Figure 3.16.

Based on Equations (2.2, 2.3, and 2.4), surface heat flow should be a linear function of both unit thickness and conductivity; however typically conductivities dominate as shown in Figure 3.15. This is mostly due to the fact that the distribution of lithology conductivity has a range of up to a factor of 8 or 9 times the lowest value. The formation

thickness typically ranges by no more than a factor of 2 from the lowest value. With this in mind, by reviewing the stratigraphic column, it is the thickest units whose conductivity is usually near the top in Figure 3.15. Therefore in general it is the confluence of thickness and conductivity that has the greatest effect on the model output.

Based on Figure 3.16 a very distinct pattern appears between mean predicted temperature and the total depth of the well: the predicted temperature increases up to wells 23038 and 22861 and then drops back down for well 22963. This may indicate a systematic bias in prediction based on deeper wells. A cursory look at the spatial relation of the wells organized by total depth in Figure 3.2, the map showing their locations, does not immediately point to a spatial correlation. However the box chart in Figure 3.16 was redrawn including a relative scale for total depth along the x-axis (Figure 3.17). By looking at both their spatial location (Figure 3.2) and their relative total depths, some correlations start to emerge.

First, well # 00170 is both the shallowest and the most aerially distant. Therefore having somewhat dissimilar results (aberrant predicted temperature) is not entirely unexpected. Second, of the remaining five wells a general trend of temperature increasing northward emerges. This trend is most striking between wells # 23038 and # 22861 and wells # 23190 and # 23040. These groups have internally consistent mean temperatures and are relatively close in latitude, wells # 23038 and # 22861 being separated by only 0.0002 degrees. Additionally, it appears well # 22963 may be similar to wells # 23190 and # 23040. These three are the most southerly, with approximately 0.03 degrees of latitude separating well # 22963 from well # 23190 and only 0.025 degrees separating wells # 23190 and # 23040.

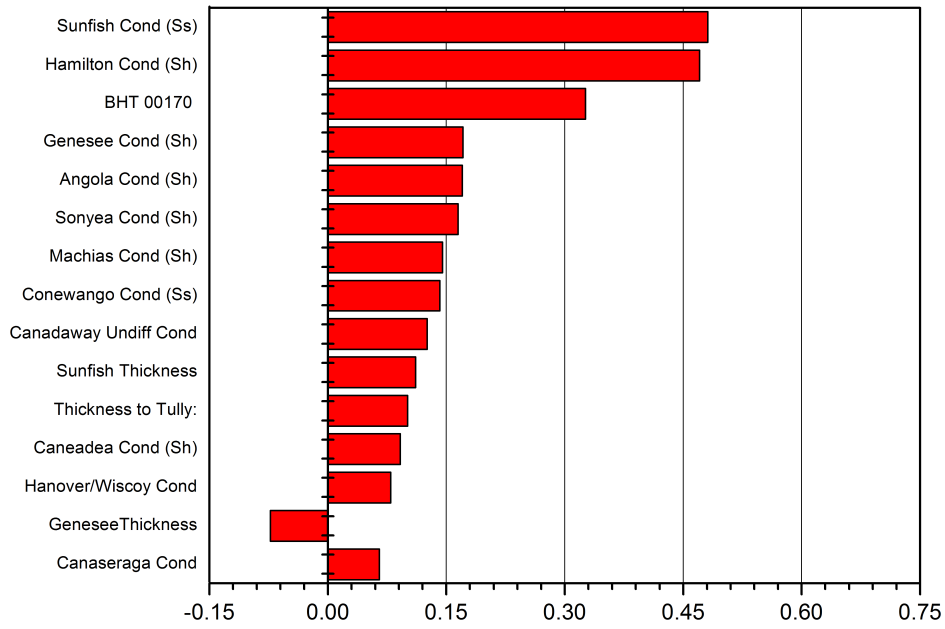

Well #00170 Sensitivity Case #2

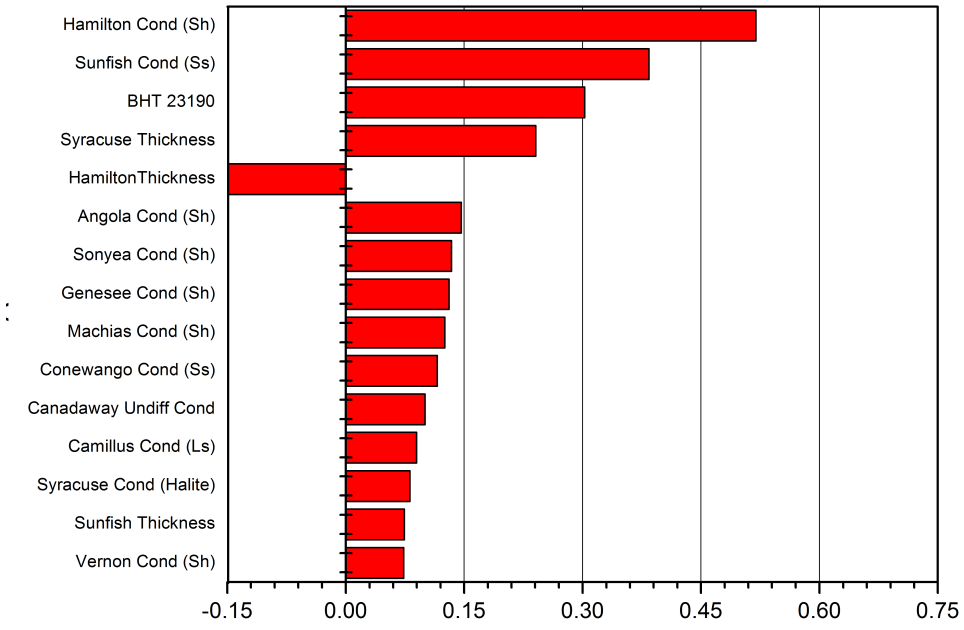

Well #23190 Sensitivity Case # 2

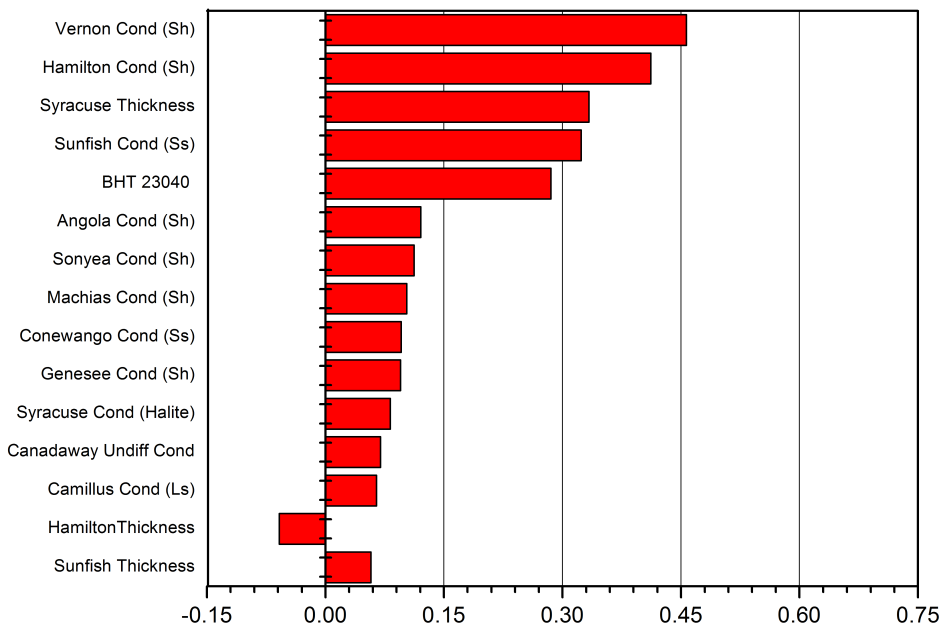

Well #23040 Sensitivty Case #2

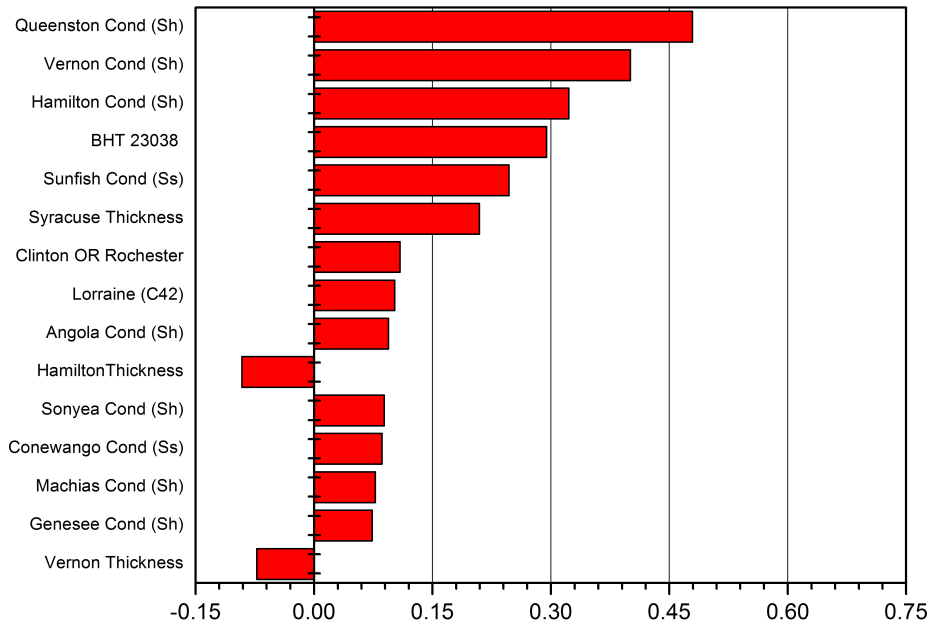

Well #23038 Sensitivity Case #2

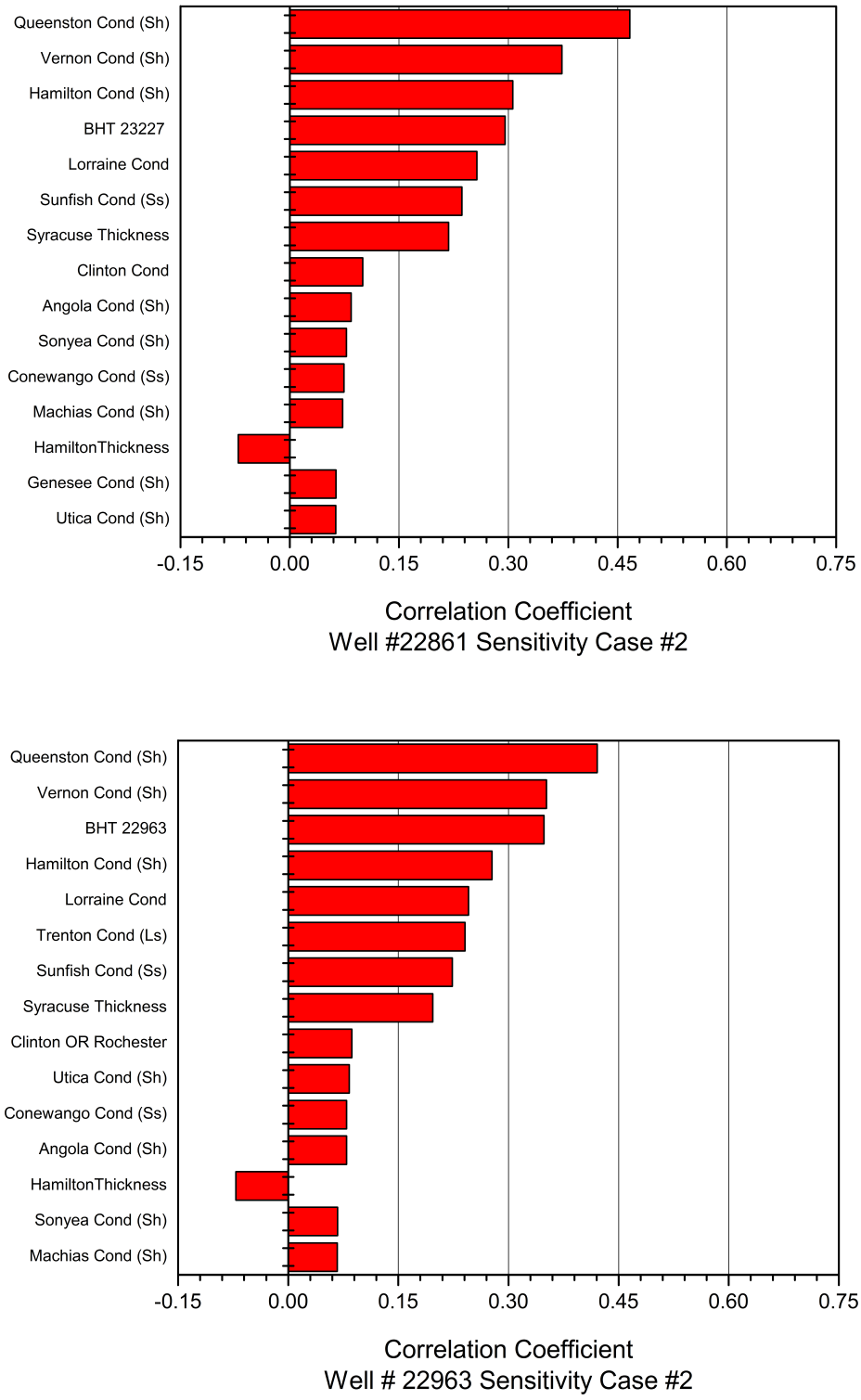

Figure 3.15: The sensitivity is displayed for each of the 6 wells in Steuben County, NY with stratigraphic column and scaling thickness adjustments of Case 2. Abbreviations refer to: Cond = conductivity; BHT = bottom hole temperature; Sh = shale; Ss = Sandstone, Ls = limestone, Evap = halite, Dol = dolomite.

Table 3.6: Statistical Summary Data for Case 2. The mean, standard deviation, P95 and P5 values refer to the anticipated temperature at 6 km based on the BHT data acquired from each well and processed via the model presented by Chapter 2.

Well:	**00170**		**23190**		**23040**		**23038**		**22861**		**22963**	
Depth (m)	1177		1776		2287		2879		3206		3560	
Mean (°C)	136		147		149		160		159		146	
Std. Dev (°C)	17.04		17.93		15.46		11.79		12.51		11.63	
P95 (°C)	166	22%	179	22%	175	18%	178	12%	176	11%	160	10%
P5 (°C)	110	19%	122	17%	128	14%	143	10%	143	10%	132	9%

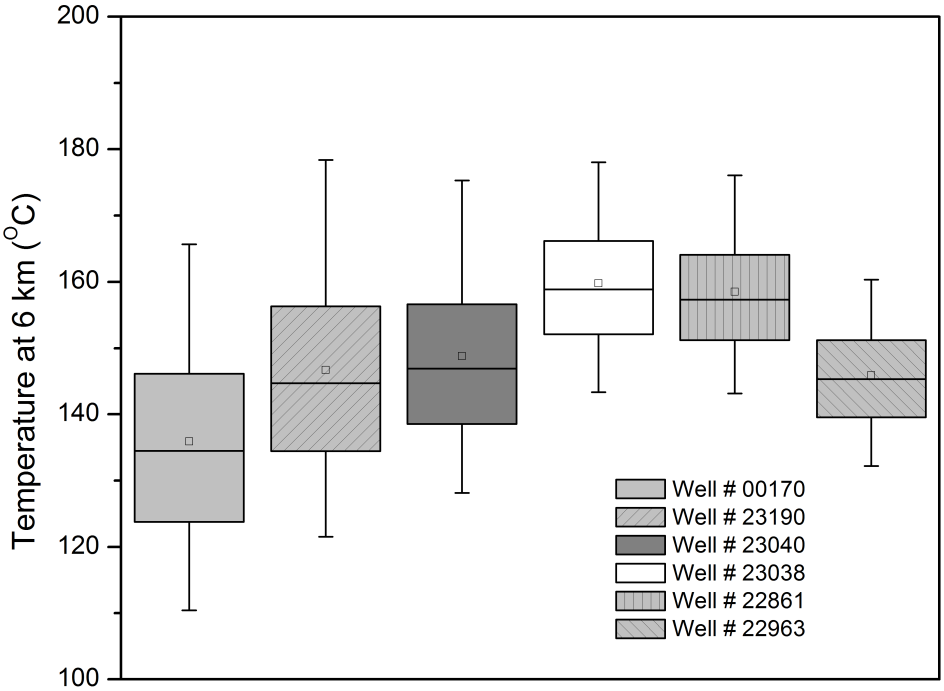

Figure 3.16: Box and whisker plot for the Case 2 uncertainty. The box represents the median 50% (i.e. range from P25 to P50), the small square the mean, and the whiskers the P95 and P5 values, as before.

3.10 Case 3

For Case 3, three geologic formations that are relatively thick compared to others in the stratigraphic column and appear at or near the top of the sensitivity diagrams for Case 2 were selected for further refinement. Moreover these units have particular attributes that would potentially affect their conductivity in such a way as to make them more critical to heat flow models. The three formations are the Hamilton, the Syracuse, and the Queenston.

For the two preceding cases only the lithology variation, as defined in Section 3.5, of each formation was explored using the normal distributions of conductivity for each

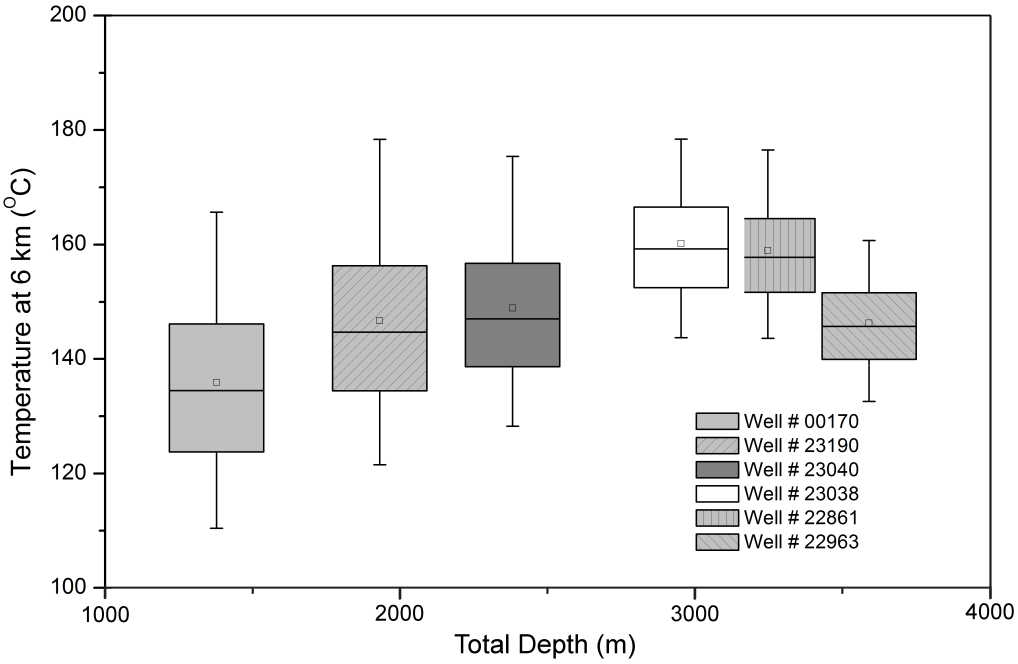

Figure 3.17: Total drilled depth correlated box and whisker plot for the Case 2 uncertainty

lithology. For Case 3 the mineralogy variation, also as defined in Section 3.5, will be analyzed by applying a volume fraction scheme where the Syracuse and Queenston units will be some mix of three lithologies. The Hamilton is treated in a different manner as described below.

3.10.1 The Hamilton Group

The Hamilton is a Devonian age group of formations that are primarily shale, the most recognizable of which is the Marcellus. The group also includes the Moscow, Ludlowville, and Skaneateles shale formations. Based on the same well formation tops reviewed in Case 2 (Table 3.5), the Marcellus is the only shale that is typically individually indentified, while the remaining Hamilton Group is left undifferentiated. The

formation tops reveal that the Hamilton ranges in thickness from 230 to 280 meters over the area of interest (ESOGIS, 2012). Therefore the original range in thickness of 100 to 270 meters applied in Case 1 and Case 2 was removed for the Case 3 tests.

Additionally the Marcellus was broken out from the group and allowed to vary in thickness from 15 to 22 meters. Because the Marcellus is a highly organic-rich black shale, its conductivity is expected to be different from the gray to light black and sometimes limestone bearing shales of the remaining Hamilton group formations. According to Cercone et al. (1996), the much lower conductivity of black shale and coals in the Appalachian basin may help to explain the high oil and gas maturity in parts of the basin. This work, specifically in the Appalachian basin, showed organic rich black shale as having an average conductivity of 0.9 +/- 0.05 W/mK, which is nearly half the average for all shale according to Beardsmore and Cull (2001). Dark grey shale, such as the remaining Hamilton Group, also has a conductivity slightly lower than average (Cercone et al. 1996), but because the exact nature of the remaining shale groups in this location could not be verified, the original shale conductivity distribution was applied.

Furthermore, because the Utica is an additional well known organic-rich black shale in the section, the lower average conductivity was applied to it as well. The upper and lower bounds of the black shale remain the same as the shale distribution in Figure 3.2. Figure 3.18 shows the modeled distribution function for the black shale thermal conductivity applied to the Marcellus and Utica formations.

3.10.2 The Syracuse Formation

In the original work by Shope et al. (2012), the Syracuse Formation was identified as a mixed evaporite and shale unit, with the evaporite minerals dominated by halite. For the

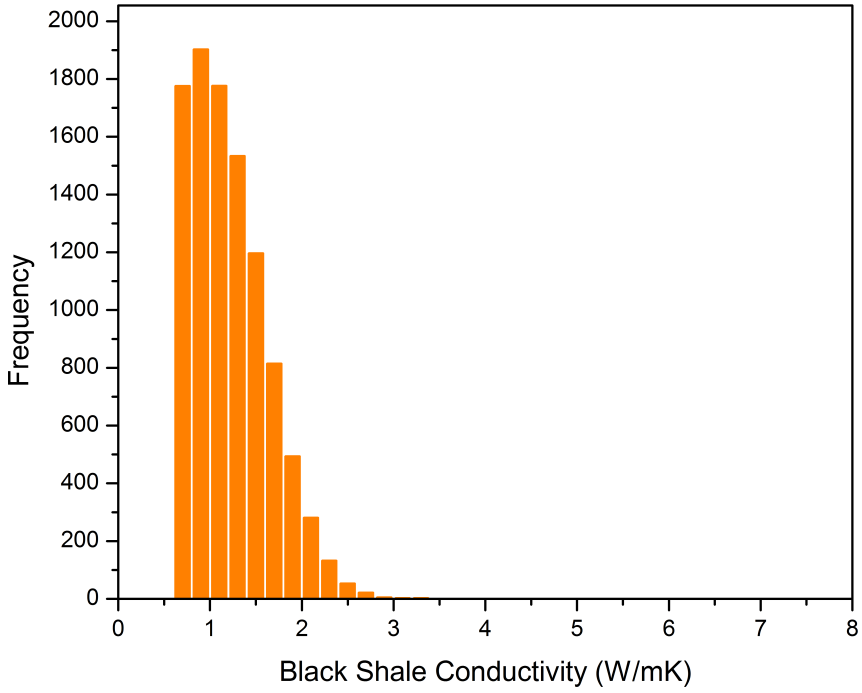

Figure 3.18: Appalachian Basin Black Shale Thermal Conductivity Distribution Function

Case 1 and 2 uncertainty models, it was given a halite conductivity distribution (Figure 3.19). For Case 3 this generalized lithology description will be refined.

Based on the work of Smith et al. (2005), a percentage model containing halite, shale, and dolomite was constructed for the Syracuse Formation. For this analysis the Syracuse Formation was allowed to vary from 54% to 60% salt, as the Smith et al. (2005) work identified a more shale-rich section near the base that was not considered when they stated that the Syracuse in South-Central New York would likely contain a minimum of 60% halite. The shale fraction was varied between 30 and 40% with the remainder assumed to be dolomite. A volume weighted total conductivity was then calculated by combining the percentage of each lithology and their respective conductivity distributions. The result of this was the overall thermal conductivity distribution for the Syracuse which can be seen in Figure 3.21.

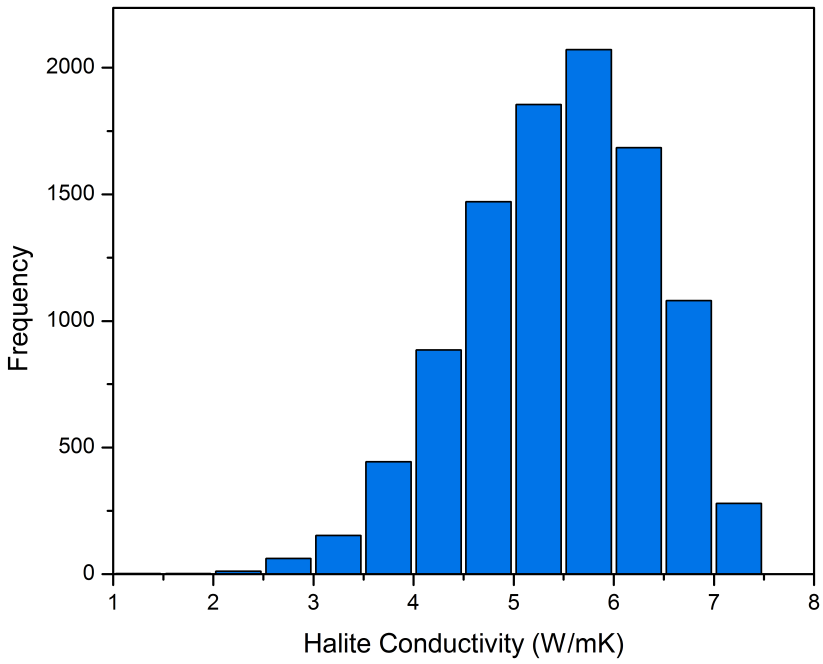

Figure 3.19: Halite Thermal Conductivity Distribution Function

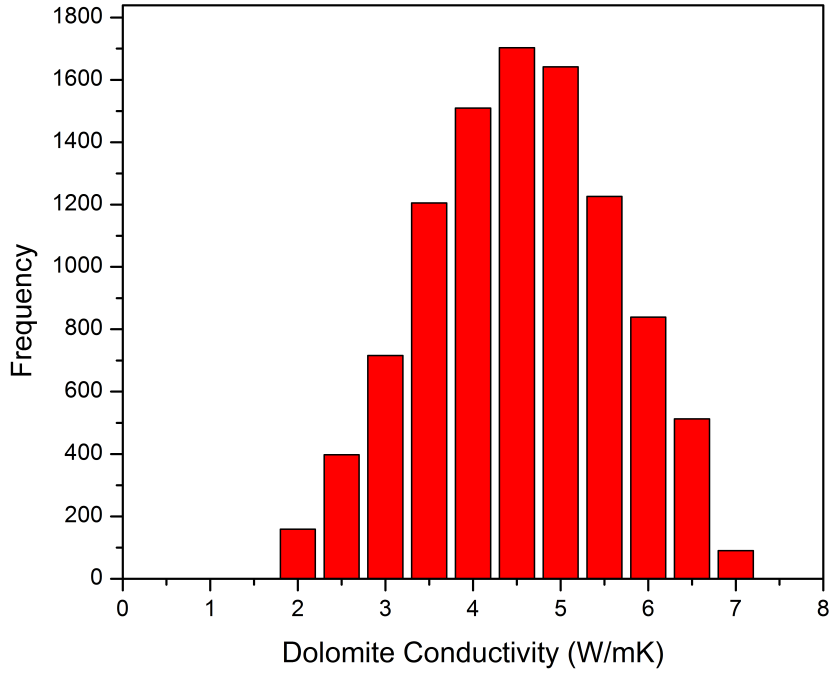

Figure 3.20: Dolomite Thermal Conductivity Distribution Function

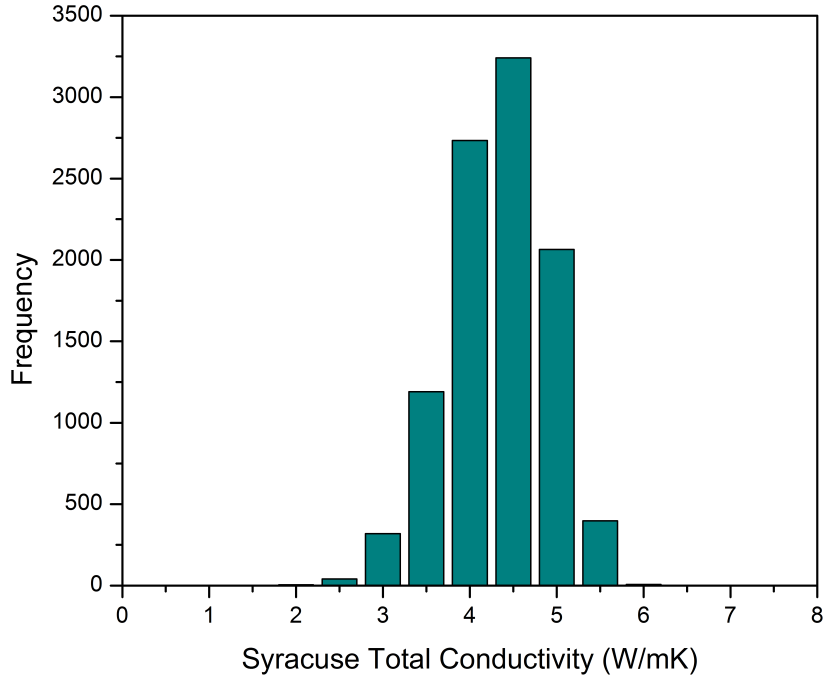

Figure 3.21: Syracuse Formation Total Thermal Conductivity Distribution Function

3.10.3 The Queenston Formation

In the original model, the Queenston was assumed to be a sandstone-dominated unit with a thickness ranging from 256 to 302 meters. For this case the lithology of the Queenston will be refined to include sandstone, hematite, and shale.

Hematite, as an iron bearing mineral, may significantly impact the overall conductivity of the unit. According to Tamulonis (2010), hematite is present in the Queenston Formation at fractions up to 22%. This analysis was done on a core from north-central New York State approximately 100 km distant from the wells being analyzed in this study. However, visual inspection of outcrops in Tamulonis (2012) reveal the presence of hematite still in large quantities at similar distances in varying directions. Therefore, for Case 3 the hematite fraction was set to between 10 and 20%.

Based on the log tops analyzed in Case 2, the Queenston is expected at around 2,000

meters in depth where the temperature is predicted to be between 50 and 70 °C by the model. Molgaard and Smeltzer (1971) developed an empirical equation for the temperature dependent thermal conductivity of hematite in the range of 67 to 400 °C. Although the temperature range for this study extends below the lower limit of 67 °C (340 K), conductivity values derived from the Molgaard and Smeltzer (1971) approach are believed to be more representative of the conductivity at depth than using the room temperature low pressure value of 12.42+/-1.74 as given by Clauser and Huenges (1995). The result is that hematite conductivity was allowed to range uniformly between 6.12 and 6.24 W/mK, as shown in Figure 3.22.

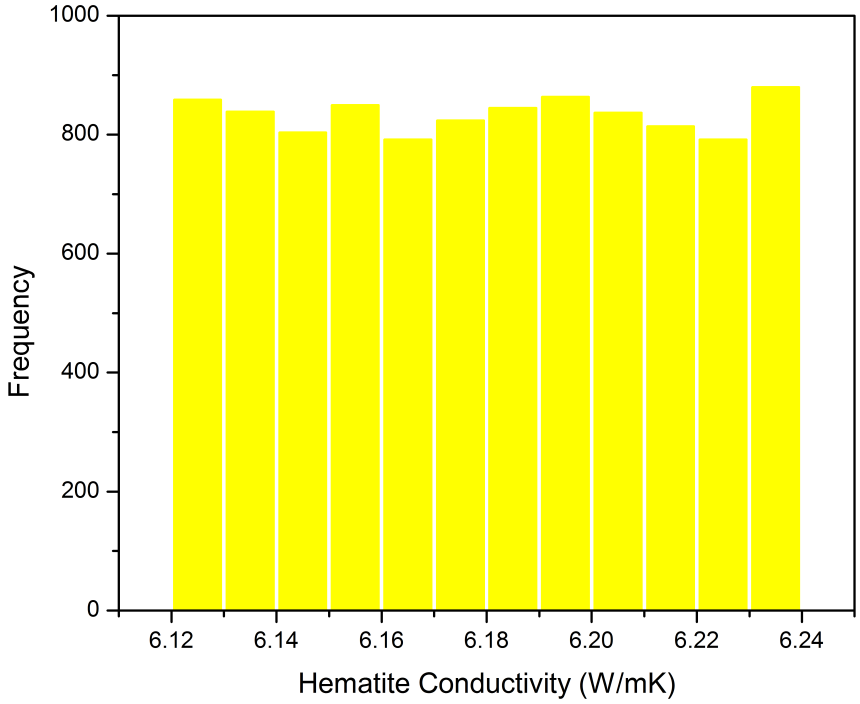

Figure 3.22: Hematite Thermal Conductivity Distribution Function.The distribution is not perfectly rectangular because of the random nature of the Monte Carlo Simulation.

The other major component of the Queenston Formation, sand, is expected to vary between 35 and 55% as a volume fraction. According to Tamulonis (2010), the area of Steuben County where these wells are present is a transition area where the Queenston

is sand-dominated to the east and sand and silt-dominated to the west. This definition of sandstone will include the quartz grains and lithic fragments. For the purposes of this model, calcite and quartz cement are also included in the sand fraction because those minerals contribute to the conductivity similar to the framework grains. The remaining fraction will be shale and modeled by the shale conductivity histogram of Case 1 (Figure 3.8). The hematite fraction is found in both the more sand rich units and the more silty and shaley units. Therefore it is not distinguished in which (sand or shale) the hematite is concentrated, rather it is assumed to be 10 to 20% of the total volume regardless. As with the Syracuse, a volume weighted conductivity was then calculated and a histogram of that model is presented in Figure 3.23.

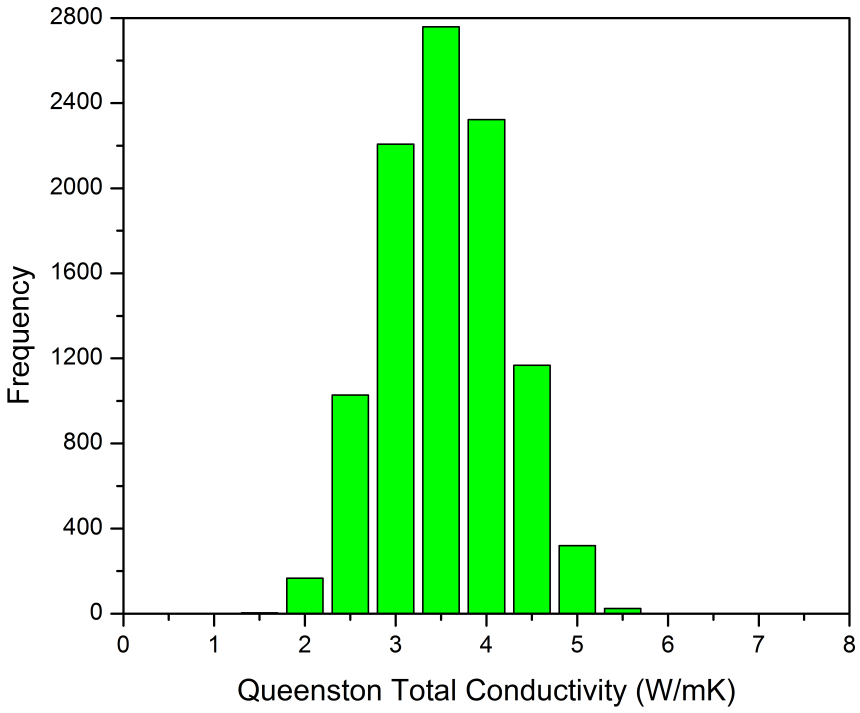

Figure 3.23: Queenston Total Thermal Conductivity Distribution Function

For Case 3, the Hamilton, Syracuse, and Queenston properties described here were combined with the other properties explored in Case 2. Ten thousand distinct Monte Carlo simulations were conducted, with the output of surface heat flow. The sensitivity

of the surface heat flow to the Case 3 input parameters are shown in Figure 3.24.

Below are the sensitivity plots for the input parameters for Case 3. Because the Hamilton was left undifferentiated with the exception of the Marcellus, it contributes a high degree of uncertainty for every well. For this Case there are 112 possible input parameters, but only 22 of these are displayed for each well. This was expanded from 15, as in Case 1 and 2, to show not only the top overall correlated parameters, but also those specific to the Hamilton, Syracuse, and Queenston.

3.10.4 Case 3 Uncertainty

With the refinements as described in Case 3, the uncertainty in the predicted temperature at 6 km can be seen in Table 3.7 and in Figure 3.24, the box and whisker plot for each well.

The uncertainty in the temperature at 6 km depth is again reduced from Case 2 to Case 3 for every well in this study. All wells now have an uncertainty of 20% or less, with the deepest well achieving results under 10%.

In Case 3 it again appears that the benefits gained from the revision to the thermal conductivity for the Hamilton, Syracuse, and Queenston have the most affect on the shallowest well. This well, # 00170, now fits with wells # 23190 and # 23040 , which again from Figure 3.2 are very close in latitude. Again wells # 23038 and # 22861 have median values close to one another as in Case 2. In Case 3 the most anomalous well is # 22963, the deepest. It's mean predicted temperature is in the middle of the 6 wells, but it is the furthest south (Figure 3.2). This may negate the prospect of a spatial correlation.

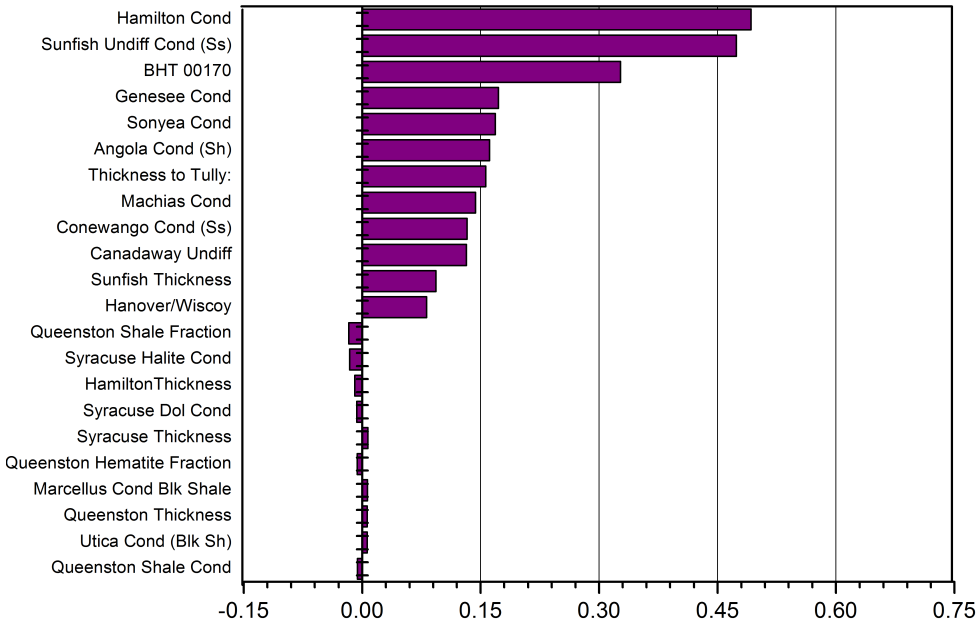

Well # 00170 Sensitivity Case 3

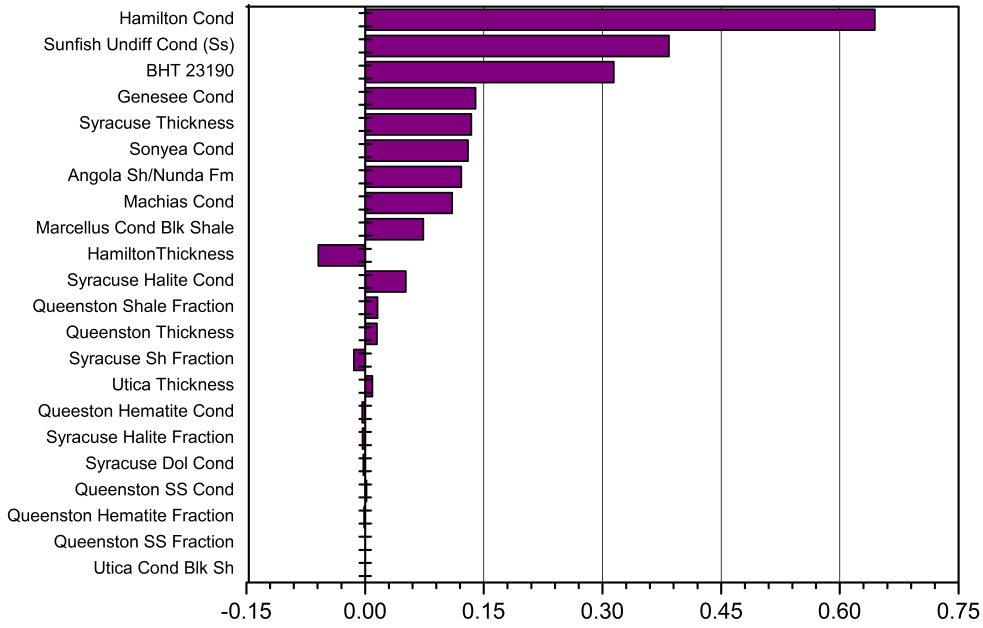

Well # 23190 Sensitivity Case 3

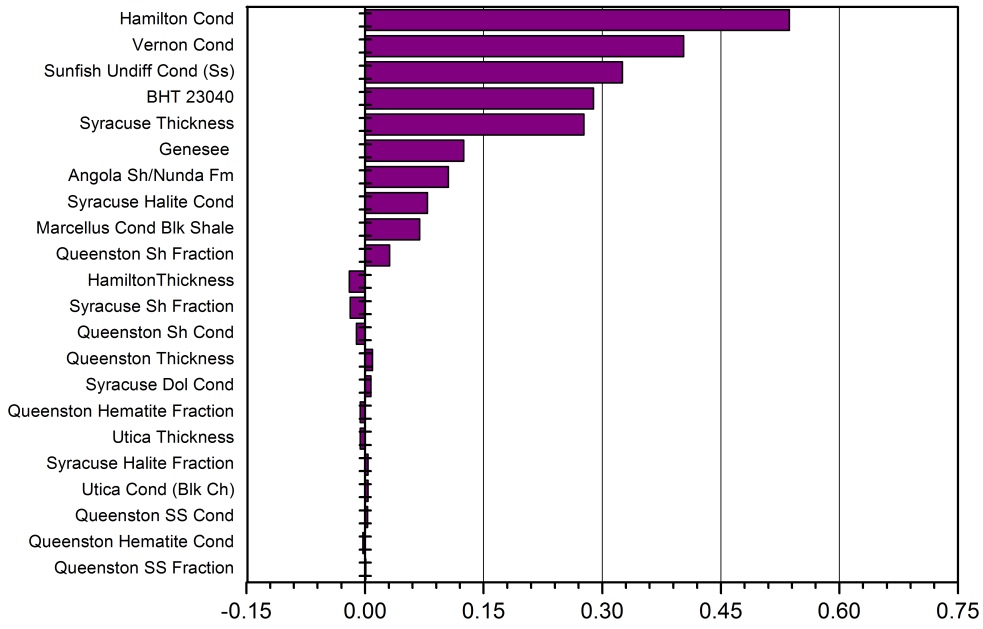

Well # 23040 Sensitivity Case 3

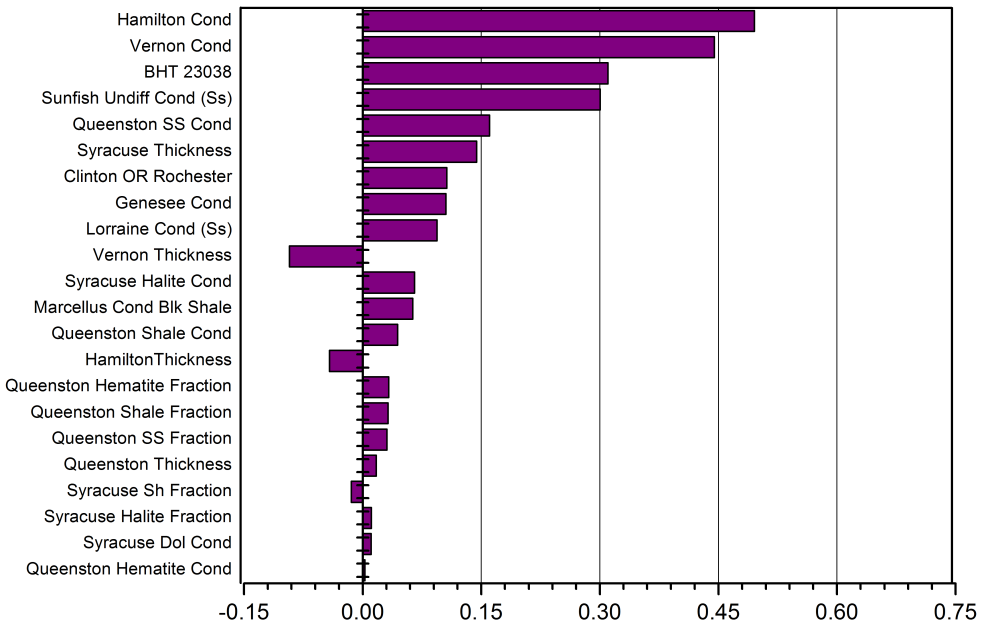

Well #23038 Sensitivity Case 3

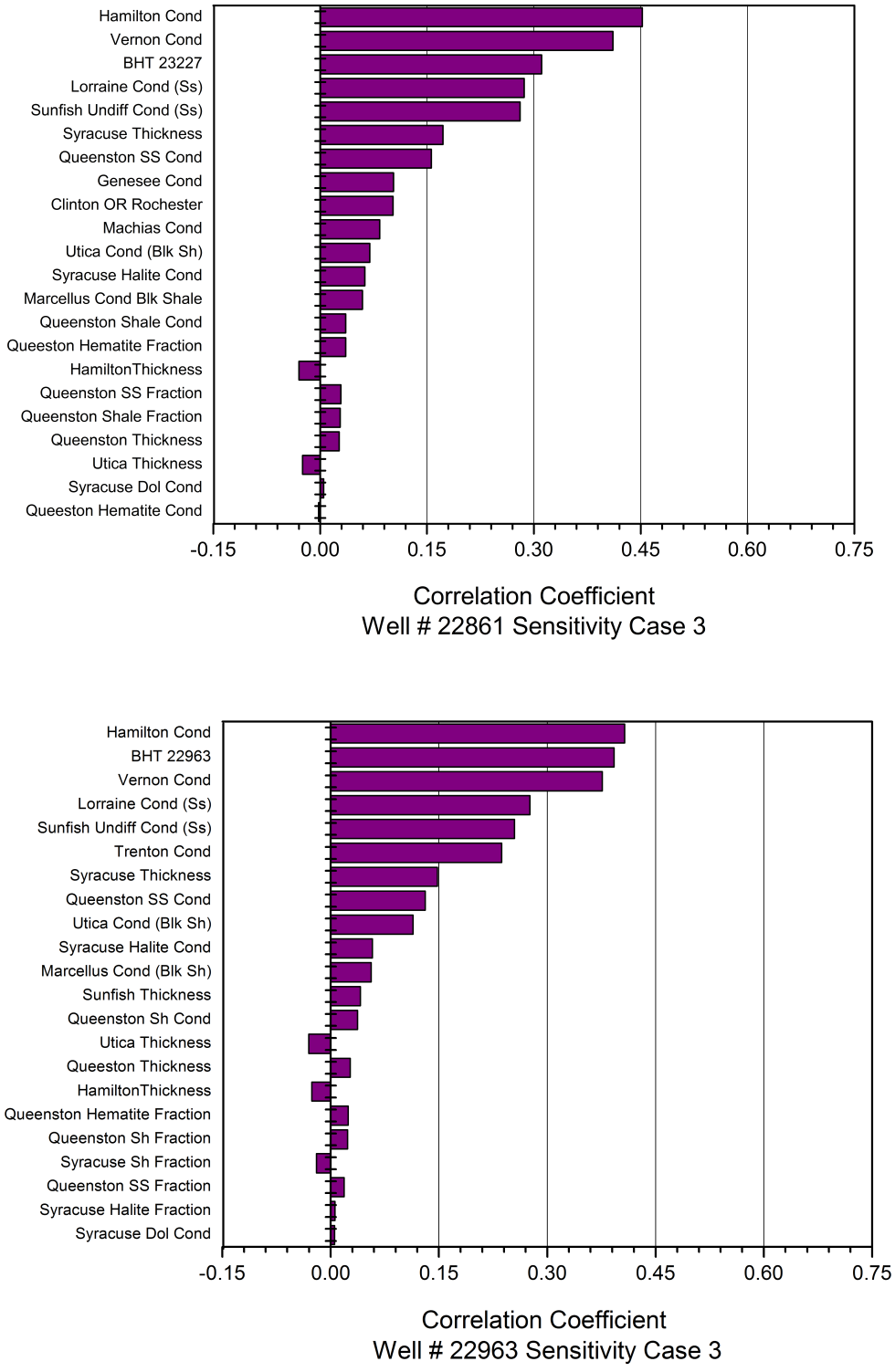

Figure 3.24: Diagram of sensitivity of the calculated surface heat flow to the parameters tested for each of the 6 wells in Steuben County, NY with the conductivity refinements for the Syracuse, Hamilton, and Queenston formations as described in Case 3.

Table 3.7: Statistical Summary Data for Case 3. The mean, standard deviation, P95 and P5 values refer to the anticipated temperature at 6 km based on the BHT data acquired from each well and processed via the model presented by Chapter 2.

Well:	**00170**		**23190**		**23040**		**23038**		**22861**		**22963**	
Depth (m)	1177		1776		2287		2879		3206		3560	
Mean (°C)	147		147		146		158		154		152	
Std. Dev (°C)	17.19		14.29		11.93		11.94		14.33		12.94	
P95 (°C)	177	20%	172	17%	167	14%	177	12%	172	11%	165	9%
P5 (°C)	121	18%	126	15%	128	12%	142	10%	140	10%	139	8%

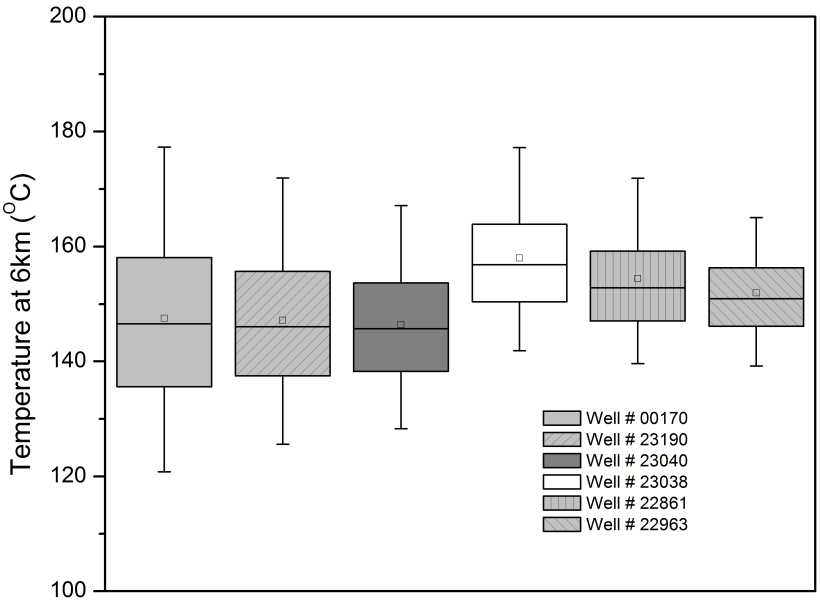

Figure 3.25: Box and whisker plot for the Case 3 uncertainty. The box represents the median 50%, the small square the mean, and the whiskers the P95 and P5 values.

3.11 Additional Uncertainties

There are two additional model inputs unrelated to the sedimentary section: the assumed thermal conductivity of the basement rock and the radiogenic heat generation of the basement rock. These two topics will be briefly discussed here.

3.11.1 Basement Rock Thermal Conductivity

For all previous Cases the basement was assumed to have a thermal conductivity of 2.7 W/mK. This is a simplified attempt in the model to take into account the temperature dependence of thermal conductivity. The temperature-dependent conductivity and the range of possible average values that could be assumed for these 6 wells in Steuben

County, NY will be analyzed here.

For this study, 2.7 W/mK was adopted as the conductivity for all basement rock between 4,000 meters and 6,000 meters depth. The temperatures for those depths range from approximately 100 to 175 °C. Based on the work of Sibbitt et al. (1979) using data for the thermal conductivity of basement rocks sampled in cores from the Jemez Mountains in Northern New Mexico, the thermal conductivity range over the stated temperature range is effectively 2.05 W/mK to 3.05 W/mK. These values are in good agreement with temperature dependent values found by Clauser and Huenges (1995).

One of the 10,000 trials for Case 3 was randomly selected and the effect of basement thermal conductivity on predicted temperature at 6 km was estimated by comparing the output assuming 2.05 W/mK and 3.05 W/mK to the base case of 2.7 W/mK. The average predicted temperature at 6 km for the base case of 2.7 W/mK was 148 °C, for the 2.05 W/mK it was 160 °C, and 144 °C for the 3.05 W/mK case. The uncertainty then is -3% or +8%.

The results were very similar to those observed for the sedimentary section property variation cases. The uncertainty in the shallow wells was typically larger than for deeper wells, but not in all cases, and uncertainty on the lower possible temperature was less than on the higher possible temperature side. The overall average uncertainty based on this simple approach to the property of basement thermal conductivity was 5%.

3.11.2 Basement Radiogenic Heat Generation

An additional assumption, not addressed previously, is the radiogenic heat generation of the basement rock. Because this property is calculated via Equation (2.7) in Chapter

2 and is subject to the assumptions of mantle heat flow and sediment radiogenic heat generation, it is dependent on these two properties. As stated by Shope et al. (2012), the basement terrain in the Appalachian basin is poorly understood and poorly sampled.

In Williams and DeAngelo (2011), data on the variation in heat production in basement terrains in California, Nevada, and Oregon can be found, based on data taken primarily from Monroe and Sass (1974). The heat generation distribution from that work was compared to the calculated heat production for all wells in the database used in Shope et al. (2012). Probability histograms for the two data sets can be seen in Figure 3.26 and cumulative distribution functions in Figure 3.27.

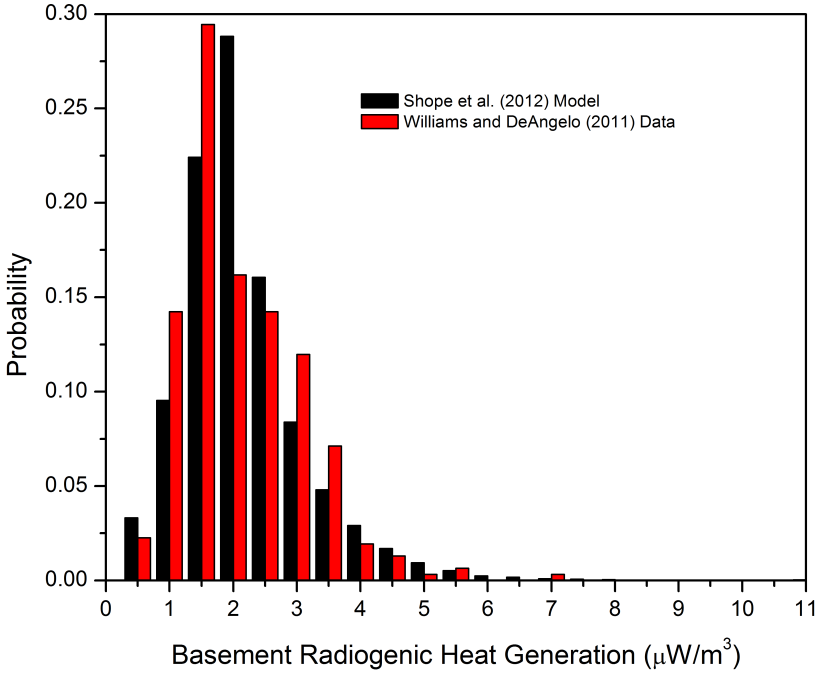

Figure 3.26: Histogram of basement rock heat generation (μW/m^3) from measurements in California, Nevada, and Oregon compared to calculated values by Shope et al. (2012).

The distribution for the actual values are in very good agreement with those calculated by Shope et al. (2012). Both have an average of 1.90, a median of 1.70, and a standard deviation of 0.96 μW/m^3. Because of this match in distributions, it is be-

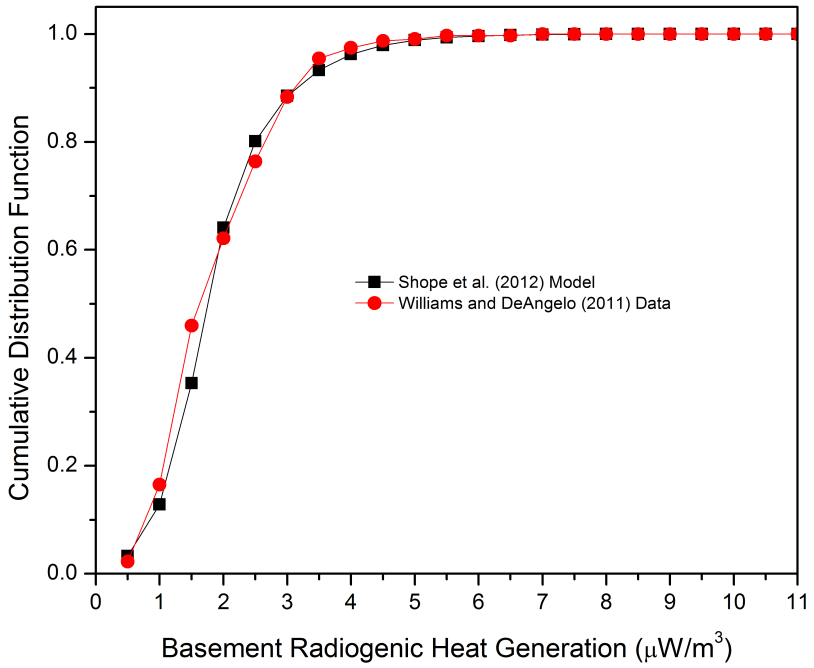

Figure 3.27: Cumulative distribution functions for basement rock heat generation from measurements in CA, NV, and OR compared to calculated values by Shope et al. (2012).

lieved the variation in the model is closely matching natural variation. Therefore the assumptions of mantle heat flow and average sediment radiogenic generation were not considered for this uncertainty analysis.

3.12 Accuracy Validation

The previous 3 cases involving Monte Carlo simulations help to gauge uncertainty or precision in the model. From Case 3 we can say that the precision is 8-20% on the predicted temperature at 6 km depth, but this may still be inaccurate. In Chapter 2 accuracy was attempted to be validated by the application of equilibrium well data (Figure 1.1, Figure 2.5, and Figure 2.6). However equilibrium data are scarce in this area of

New York; therefore two other checks are presented here. First the difference between the corrected BHT from each Monte Carlo simulation in Case 3 will be compared to the model predicted temperature at the total depth. Second a basic calculation given assumptions for average thermal properties to 6 km will be performed.

For each of the 10,00 Monte Carlo simulations in Case 3, a BHT for each well was generated based on a modeled distribution function such as in Figure 3.3. One way to check model accuracy is to compare the calculated temperature at the well total depth to the observed BHT at that depth. Performing this analysis, average predicted temperatures were 1.9% lower than the observed corrected BHT. The average for well # 00170 was 0.8% lower and 2.5% lower for well # 22963, the shallowest and deepest well respectively. This confirms that the model is accurately predicting temperatures over the total depth span of the wells to within 0.8 to 2.5 %.

In order to perform one final check on the validity of the model, a basic calculation of the predicted temperature at 6 km was computed given reasonable assumptions for the thermal properties within the basin using Equation (2.5) and (2.14). The following assumptions were used: sediment conductivity = 2.0 W/mK, sediment radiogenic heat generation = 1.0 μW/m^3, sediment thickness = 4000 m, corrected BHT = 104 °C, mantle heat flow = 30 mW/m^2, basement conductivity = 2.7 W/mK, basement radiogenic heat generation initial = 2.8 W/mK, and b = 9000 m. The result was 150 °C, which is at most 10 °C or 7% different from any mean predicted temperature for any well in all Cases, with the exception of well #00170 in Case 1. This simple calculation shows that if the properties are well constrained by *a priori* knowledge, similar results to the model output may be achieved and that the model is accurately predicting expected temperatures. When the specified parameters given above are not well known, an uncertainty analysis will help to identify the properties which are most sensitive in controlling model output.

3.13 Conclusions and Future Work

Overall the model is performing as intended. From Case 1 it is apparent that uncertainty can be large, but as areas of high heat flow are revealed and focused on, uncertainty or precision of less than 10% can be achieved by refining the model input parameters. Additionally, if the thermal properties of interest are well constrained, accuracy of under 10% appears achievable. However with the lack of deep equilibrium temperature data over most of New York and Pennsylvania, this level of accuracy cannot be validated to 6 km depth.

Based on this study, variation in the sedimentary section can account for 15% of the uncertainty in the anticipated temperature at 6 km depth using the model developed and presented in Chapter 2. This is the average uncertainty in Case 2 of this study, the case that most closely matches the procedure applied by Shope et al. (2012). However, the uncertainty based on any single well may range from 10-25% without stratigraphic refinement, as evidenced in Case 2 and 3. Additionally, based on the results for the shallowest well (# 00170) in Case 1, care and attention must always be given to the inherent limitations of such a model.

The model developed in Chapter 2 and then used by Shope et al. (2012) was primarily to identify areas of aberrantly high heat flow. While predicted temperature at depth is the ultimate goal, the heat flow maps generated will suffer from much lower values of uncertainty. While the uncertainty is not specifically calculated here for heat flow, because the majority of wells in the Cornell database do not penetrate the entire sedimentary section (only 42% of sedimentary cover is penetrated on average) there are fewer unknowns in generating a heat flow map.

Finally, this uncertainty study dealt primarily with the variation in the properties of

the sedimentary section. In the case of New York and Pennsylvania, this deep, complex assemblage of varying rock types will most likely dominate. However, based on the brief analysis of the uncertainty in the basement rock conductivity, 5% uncertainty is expected from this model parameter. Because the methods and procedure used to analyze the uncertainty in sedimentary properties differed from the methods used to analyze uncertainty of the basement properties, these uncertainties cannot simply be added. Therefore a full Monte Carlo style analysis of this parameter should be performed.

REFERENCES

AAPG (1978), Basement map of North America, The American Association of Petroleum Geologists, scale 1:5,000,000.

Beach, R. (1985), "Sedimentary heat flow in the $\delta Q = 0$ region of Alberta," M.Sc. Thesis, University of Alberta, Edmonton, Alberta, (unpublished).

Beach, R. D.W., F.W. Jones, and J.A. Majorowicz (1987), "Heat flow and heat generation estimates for the Churchill basement of the Western Canadian Basin in Alberta, Canada," *Geothermics*, 16, 1987, 1-16.

Beardsmore, G. R., and Cull, J. P. (2001), *Crustal Heat Flow: A Guide to Measurement and Modeling*, New York: Cambridge University Press, 2001. Print.

Blackwell, D. D., Negraru, P. T., and Richards, M. C. (2007), "Assessment of the Enhanced Geothermal System Resource Base of the United States, *Natural Resources Research*, 15, December 2006, 283-308.

Cercone, K. R., D. Deming, and H.N. Pollack (1996), "Insulating effect of coals and black shales in the Appalachian Basin, Western Pennsylvania," *Organic Geochemistry*, 24, 1996, 243-249.

Clauser C., and E. Huenges (1995), "Thermal conductivity of rocks and minerals," *in* Rock Physics and Phase Relations: a Handbook of Physical Constants, Ahrens T. J., ed., Washington, DC: American Geophysical Union; 1995, 105-126.

DEC (1996), "New York State Oil, Gas and Mineral Resources," New York State Department of Environmental Conservation: Division of Mineral Resources, Annual Report 1996.

Empire State Oil and Gas Information System (ESOGIS) (2012), ”Search for wells,” in the New York State Museum, Retrieved April, 2012, from ¡ http://esogis.nysm.nysed.gov/esogis/search.cfm¿.

Harrison, W. E., Luza, K. V., Prater, M. L., and Chueng, P. K. (1983), ”Geothermal resource assessment of Oklahoma,” *Special Publication 83-1*, Oklahoma Geological Survey, 1983.

Jacobi R.D. (1981), ”Peripheral bulge a causal mechanism for the Lower/Middle Ordovician unconformity along the western margin of the Northern Appalachians,” *Earth and Planetary Science Letters*, 56, December 1981, 245-251.

Jacobi (2012), ”Dr. Jacobi’s Research Page, Department of Geology, The University at Buffalo, The State University of New York, Accessed March, 20120 at ¡ http://www.glyfac.buffalo.edu/Jacobi/index.html¿

Jones, J. L., and H. Blatt (1984), ”Mineral dispersal patterns in the Pierre Shale,” *Journal of Sedimentary Petrology*, 54, March, 1984, 17-28.

Majorowicz J. A., and A.M. Jessop (1981), Regional heat flow patterns in the Western Canadian Sedimentary Basin, *Tectonophysics*, 74, April 1981, 209-238.

Molgaard, J. and W.W. Smeltzer (1971), ”Thermal Conductivity of Magnetite and Hematite,”*Journal of Applied Physics*, 42, 3644-3647.

Orlo, E. C., et al. (1985), Correlation of stratigraphic units in North America: Correlation chart series, The American Association of Petroleum Geologists.

Quinlin, G.M., and C. Beaumont (1984), ”Appalachian thrusting, lithospheric flexure, and the Paleozoic stratigraphy of the Easter Interior of North America,” *Canadian*

Journal of Earth Sciences, 21, September 1984, 973-996.

Reiter, M., and J. C. Tovar (1982), "Estimates of terrestrial heat flow in northern Chihuahua, Mexico based upon petroleum bottom hole temperature," *Geological Society of America Bulletin*, 93, July 1982, 613-621

Shope, E. N. et al. (2012), "Geothermal Resource Assessment: A Detailed Approach to Low-Grade Resources in the States of New York and Pennsylvania," 37th Stanford Geothermal Workshop, Stanford, CA, January 30 February 1, 2012.

Smith, G. R (2002), "Sequence Stratigraphic Analysis of the Conneaut and Conewango Groups in Western New York State," Final Report Prepared for: The New Your State Energy Research and Development Authority, The University at Buffalo, The State University of New York.

Smith, L. et al. (2005), "Final Report: Systematic Technical Innovations Initiative Brine Disposal in the Northeast," Reservoir Characterization Group, New York State Museum, and Sandia National Laboratories, DF-FC26-01NT41298, January 5, 2005.

Stutz, G. R., et al. (2012), "A Well by Well Method for Estimating Surface Heat Flow to Analyze the Geothermal Energy Resource Potential of the United States," 37th Stanford Geothermal Workshop, Stanford, CA, January 30 February 1, 2012.

Tamulonis, K.L. (2010), "Current Issues in New York State From Carbon Dioxide Storage to Landsliding," PhD. Thesis, Cornell University, Ithaca, NY.

Touloukian, Y. S., Judd, W. R., and Roy, R. F. (1981).Physical properties of rocks and minerals. New York: McGraw-Hill.

USGS (2012), "Geologic Maps of US States," USGS Mineral Resources On-Line Spatial Data. Web. Fall 2011. http://tin.er.usgs.gov/geology/state/

William, C. F., and J. DeAngelo (2011), "Evaluation of Approaches and Uncertainties in the Estimation of Temperatures in the Upper Crust of the Western United States," GRC Transactions, Vol. 35.

Young, W.H. Jr., and W.L. Kreidler (Eds.) (1957), "Guidebook for Geology of S.W. Tier Oil and Gas Fields, Oil Refining Field Trips," New York State Geological Association 29th Annual Meeting, Wellsville, New York, May 9-12, 1957.

Zoth G., and R. Haenel (1988), Appendix: Thermal Conductivity. *in* Handbook of Terrestrial Heat Flow Density Determination, (Ed. Haenel, Rybach and Stegna), 449-466. Kluwer Publishers, Boston.

CHAPTER 4

CONCLUSIONS AND OUTCOMES

Although issues still remain within the model, based on this work it appears that the results are able to aid in mapping surface heat flow and subsurface temperature and provide spatial refinement commensurate with the goals of this study. The maps generated by the Geothermal Resource Assessment group provide support for developers of geothermal energy by reducing the cost and risk associated with resource identification and exploration. The work presented by both Shope et al. (2012) and in this thesis show large-scale refinement and increased granularity in the Appalachian Basin region of New York and Pennsylvania.

Additionally within this thesis, a model or tool and technique have been developed to help with mapping out geothermal resource potential. Using this model an improved resource assessment for the states of New York and Pennsylvania have been created. The maps generated increase spatial accuracy and provide a clearer picture of the available geothermal energy in these two states. Continued collaboration should be pursued with groups, such as the New York State Museum, who can provide very location-specific geologic constraints and help to further refine the assessment. Relatively high flow areas in both NY and PA should be focused in on with this more precise approach.

It is hoped as more researchers gain interest in the topic, they will be able to use the model to incorporate 1000's of additional well data points quickly and provide additional refinement. The work of the current students in the GRA group represents only a small piece of what may be possible with this model if its limitations and power are fully understood and utilized.

Based on progress to date, two recommendations are offered as the next impor-

tant steps with which to improve the model. The first is to rewrite the surface heat flow equation to include formation specific sediment radiogenic heat generation. This would be accompanied by the addition of sediment radiogenic heat generation data on a formation-by-formation basis to the stratigraphic column. Currently the generation of heat within the sedimentary rocks is ignored until the step of calculating the temperature at depth. This simplification was made because most of the available wells are relatively shallow, and typical sediment radiogenic generation contributions are within the uncertainty for calculated surface heat flow itself. The second would be an iterative scheme to calculate the temperature-dependent conductivity of each formation. This would eliminate the specific boundary at 4 km sediment thickness, where a discontinuity in thermal conductivity is imposed (see Figure 2.1).

As a result of this work, a few recommendations can be made. The most important would be to drill deep holes at various locations across the northeast. This would provide data for many issues that still exist. First heat flow measurements could be collected and compared to the modeled values, thus providing further assurance of accuracy. Second rock samples can be collected and thermal conductivity measurements performed to help refine the averages for each lithology within the Appalachian basin. Finally equilibrium temperature data can be compared to the model and also used to generate a region specific BHT correction function. This would allow researchers to replace the Harrison et al. (1983) correction currently being used.

CHAPTER 5
APPENDIX

```
'VBA Thermal Model Code. For a fully
functioning Excel File contact Jeff Tester,
 jwt54@cornell.edu

'George Stutz
'Cornell University
'11/8/2011

Option Explicit

'Dimension variables for calculation
Dim i, Break, d, c As Single
Dim Thick, Thick_Tot, Conductivity_Read,
Cum_Res, R, Resistance, K_Avg, Kbb, Eps, BHT,
T_surf, Gradient, Depth, Sed_Well, Sed_Column,
Base_Cond, K_Base, K_DeepSed, T_Iso,
Sed_Radio, Basement_Radio, Well_Depth,
K_Well, Heat_Flow, Q_Mantle, Depth_Calc, Ts,
Qs, Qm, Db, Dc, Dw, Kb, Ksed, A_s, A_b,
Sum_Unit_Thick, Sum_Res, b, h, j,
l, m, n, o, p, q, t, u, s, z, Unit_Res,
Unit_Thick, Unit_Cond, T_Calc, D_Guess,
delta_T As Double
```

```
'Subroutine that will calculate and fill in gradient
, heat flow, average conductivity, and estimated
temperatures

Sub RunCalc()

'Initialize all counters and values that will be used in the sub
i = 0
BHT = Cells(9, 2).Value
'Read in constant values input by user
Sed_Column = WorksheetFunction.Sum(Sheets("Strat_Column").Range("D3:D12000"))
K_Base = Cells(2, 9).Value
K_DeepSed = Cells(3, 9).Value
T_Iso = Cells(4, 9).Value
Do While BHT > 0

T_surf = Cells(9 + i, 6).Value
Well_Depth = Cells(9 + i, 3).Value
Sed_Well = Cells(9 + i, 5).Value
Sed_Radio = Cells(9 + i, 7).Value
Gradient = (BHT - T_surf) / (Well_Depth / 1000)
d = 0
Break = 0
Thick_Tot = 0
Cum_Res = 0
Eps = 1
c = 0
```

```
'Check if wells are penetrating basement based
on the assumed sediment thickness at that well

If Well_Depth > Sed_Well Then

'Calculate the resistance for all units from surface to basement
Do While Eps > 0.001

Conductivity_Read = Sheets("Strat_Column").Cells(d + 3, 5).Value
Thick = Sheets("Strat_Column").Cells(d + 3, 4).Value * Sed_Well  Sed_Column
Resistance = Thick / Conductivity_Read
Thick_Tot = Thick_Tot + Thick
Cum_Res = Cum_Res + Resistance
d = d + 1

'Eps is a term to exit the loop once the
thicknesses are within 0.1% of each other
eliminating possible rounding and truncation errors
Eps = Abs((Thick_Tot - Sed_Well) / Thick_Tot)

Loop

'Calculate the additional resistance
from the penetration into basement
Thick = Well_Depth - Sed_Well
Resistance = Thick / K_Base
Cum_Res = Cum_Res + Resistance
K_Well = Well_Depth / Cum_Res
Heat_Flow = K_Well * Gradient
```

```
'If the well is not into basement
calculate heat flow using the conductivity
of the sedimentary layers it penetrates

Else

'Do loop with a break set to exit once
the cumulative sediment thickness is greater
than the well depth

Do While Break < 1


'If the current depth is greater than the well
depth, read in the values from the previous scaled depth

If Well_Depth < Thick_Tot Then

'Previous resistance is calculated using the
entire thickness of the next layer, it must be removed and _
adjusted to only incorporate the proportion of the well within  the last layer
Cum_Res = Cum_Res - Resistance
Thick_Tot = Thick_Tot - Thick

'The incremental resistance of the last layer
is calculated from the proportion of the well in that layer
Resistance = (Abs(Well_Depth - Thick_Tot) / Thick) * ((1 / Conductivity_Read) * Thick)
```

```
'Calculate the total resistance to surface
and then the average affective conductivity
Cum_Res = Cum_Res + Resistance
K_Well = Well_Depth / Cum_Res

'Use to average conductivity to calculate the
heat flow based on the calculated gradient
for that well
Heat_Flow = K_Well * Gradient


'Set Break=1 so that the loop will cease
Break = 1

Else

'When the total depth is less that the well depth
calculate the resistance of each layer based on
conductivity and thickness
Conductivity_Read = Sheets("Strat_Column").Cells(d + 3, 5).Value
Thick = Sheets("Strat_Column").Cells(d + 3, 4).Value * Sed_Well / Sed_Column
Resistance = Thick / Conductivity_Read


'Leave break as zero so each layer will be
added until the well depth is exceeded
Break = 0

End If
```

```
'After each check of the depth keep a
running total of the sum resistance
Thick_Tot = Thick_Tot + Thick
Cum_Res = Cum_Res + Resistance
d = d + 1

Loop

End If

Cells(9 + i, 9).Value = Gradient
Cells(9 + i, 10).Value = Heat_Flow
Cells(9 + i, 11).Value = K_Well

Q_Mantle = Cells(9 + i, 4).Value

Do While c <= 5

Depth_Calc = Cells(8, 12 + c).Value

'Note all depth inputs are expected in m, conductivities in W/m/k,
heat flows in mW/m^2, radiogenic heat generation in microW/m^3

'Prepare and convert function inputs to SI
units for use in calculating temperatures
Ts = T_surf
Qm = Q_Mantle * 10 ^ -3
Qs = Heat_Flow * 10 ^ -3
```

```
Db = Sed_Well
Dc = Depth_Calc
Dw = Well_Depth
Kb = K_Base
Ksed = K_DeepSed
A_s = Sed_Radio * 10 ^ -6

'Counters that must be reset before calculation
of each temperature value
Eps = 1
d = 0
Sum_Unit_Thick = 0
Sum_Res = 0
Break = 0

'Varible crustal thickness based on depth of
sedimentary cover
If Db > 3000 Then
b = 13000 - Db
Else
b = 10000
End If

A_b = (Qs - Qm - A_s * Db) / b
Cells(9 + i, 8).Value = A_b * 10 ^ 6
'Series of If Statements to figure out what conditions
the well and calculation parameters fit into and
then loop to calculate the appropriate _
thermal conductivities. Once the conductivities are found use those
```

```
to calculate the expected T at the specified depth.
If Db > 0 Then
If Db > 3000 Then

If Db > 4000 Then

If Dc > 4000 Then
If Db < Dc Then
If Dw < Db Then
If Dw < 4000 Then
l = (Qs * Dw / K_Well - A_s * Dw ^ 2 / (2 * K_Well)) 'Tw

Do While Break < 1

If 4000 < Sum_Unit_Thick Then

Sum_Res = Sum_Res - Unit_Res
Sum_Unit_Thick = Sum_Unit_Thick - Unit_Thick

Unit_Res = (Abs(4000 - Sum_Unit_Thick) / Unit_Thick) * ((1 / Unit_Cond) * Unit_Thick)

Sum_Res = Sum_Res + Unit_Res
K_Avg = 4000 / Sum_Res

Break = 1

Else

Unit_Cond = Sheets("Strat_Column").Cells(d + 3, 5).Value
```

```
Unit_Thick = Sheets("Strat_Column").Cells(d + 3, 4).Value * Db / Sed_Column
Unit_Res = Unit_Thick / Unit_Cond

Break = 0

Sum_Unit_Thick = Sum_Unit_Thick + Unit_Thick
Sum_Res = Sum_Res + Unit_Res

d = d + 1

End If

Loop

Kbb = (K_Avg * 4000 - K_Well * Dw) / (4000 - Dw)

h = (Qs * (4000 - Dw) / Kbb - A_s * (4000 - Dw) ^ 2 / (2 * Kbb)) 'Tw4
j = ((Qs - A_s) * (Db - 4000) / Ksed - A_s * ((Db - 4000) ^ 2) / (2 * Ksed)) 'Tb4
z = (Qm * (Dc - Db) / Kb + A_b * (b) ^ 2 * ((1 - Exp(-(Dc - Db) / (b))) / Kb)) 'Tbx

T_Calc = Ts + l + h + j + z 'Equation 2

Else

Do While Break < 1

If 4000 < Sum_Unit_Thick Then

Sum_Res = Sum_Res - Unit_Res
```

```
Sum_Unit_Thick = Sum_Unit_Thick - Unit_Thick

Unit_Res = (Abs(4000 - Sum_Unit_Thick) / Unit_Thick) * ((1 /  Unit_Cond) * Unit_Thick)

Sum_Res = Sum_Res + Unit_Res
K_Avg = 4000 / Sum_Res

Break = 1

Else

Unit_Cond = Sheets("Strat_Column").Cells(d + 3, 5).Value
Unit_Thick = Sheets("Strat_Column").Cells(d + 3, 4).Value * Db / Sed_Column
Unit_Res = Unit_Thick / Unit_Cond

Break = 0

Sum_Unit_Thick = Sum_Unit_Thick + Unit_Thick
Sum_Res = Sum_Res + Unit_Res

d = d + 1

End If

Loop


m = (4000 * Qs / K_Avg - A_s * 4000 ^ 2 / (2 * K_Avg))  'T4km
j = ((Qs - A_s) * (Db - 4000) / Ksed - A_s * ((Db - 4000) ^ 2) / (2 * Ksed)) 'Tb4
```

```
z = (Qm * (Dc - Db) / Kb + A_b * (b) ^ 2 * ((1 - Exp(-(Dc - Db) / (b))) / Kb)) 'Tb


T_Calc = Ts + m + j + z 'Equation 3
End If

Else
Do While Break < 1

If 4000 < Sum_Unit_Thick Then

Sum_Res = Sum_Res - Unit_Res
Sum_Unit_Thick = Sum_Unit_Thick - Unit_Thick

Unit_Res = (Abs(4000 - Sum_Unit_Thick) / Unit_Thick) * ((1 / Unit_Cond) * Unit_Thick)

Sum_Res = Sum_Res + Unit_Res
K_Avg = 4000 / Sum_Res

Break = 1

Else

Unit_Cond = Sheets("Strat_Column").Cells(d + 3, 5).Value
Unit_Thick = Sheets("Strat_Column").Cells(d + 3, 4).Value * Db / Sed_Column
Unit_Res = Unit_Thick / Unit_Cond

Break = 0
```

```
Sum_Unit_Thick = Sum_Unit_Thick + Unit_Thick
Sum_Res = Sum_Res + Unit_Res

d = d + 1

End If

Loop

m = (4000 * Qs / K_Avg - A_s * 4000 ^ 2 / (2 * K_Avg))  'T4km
j = ((Qs - A_s) * (Dw - 4000) / Ksed - A_s * ((Dw - 4000) ^ 2) / (2 * Ksed)) 'Tb4
z = (Qm * (Dc - Db) / Kb + A_b * (b) ^ 2 * ((1 - Exp(-(Dc - Db) / (b))) / Kb)) 'Tb

T_Calc = Ts + m + j + z 'Equation 4
End If

Else
If Dw < Dc Then
If Dw < 4000 Then
l = (Qs * Dw / K_Well - A_s * Dw ^ 2 / (2 * K_Well)) 'Tw

Do While Break < 1

If 4000 < Sum_Unit_Thick Then

Sum_Res = Sum_Res - Unit_Res
Sum_Unit_Thick = Sum_Unit_Thick - Unit_Thick

Unit_Res = (Abs(4000 - Sum_Unit_Thick) / Unit_Thick) * ((1 / Unit_Cond) * Unit_Thick)
```

```
Sum_Res = Sum_Res + Unit_Res
K_Avg = 4000 / Sum_Res

Break = 1

Else

Unit_Cond = Sheets("Strat_Column").Cells(d + 3, 5).Value
Unit_Thick = Sheets("Strat_Column").Cells(d + 3, 4).Value * Db / Sed_Column
Unit_Res = Unit_Thick / Unit_Cond

Break = 0

Sum_Unit_Thick = Sum_Unit_Thick + Unit_Thick
Sum_Res = Sum_Res + Unit_Res

d = d + 1

End If

Loop

Kbb = (K_Avg * 4000 - K_Well * Dw) / (4000 - Dw)

h = (Qs * (4000 - Dw) / Kbb - A_s * (4000 - Dw) ^ 2 / (2 * Kbb)) 'Tw4
 n = ((Qs - A_s) * (Dc - 4000) / Ksed - A_s * ((Dc - 4000) ^ 2) / (2 * Ksed)) 'Tb4

T_Calc = Ts + l + h + n 'Equation 5
```

```
Else

Do While Break < 1

If 4000 < Sum_Unit_Thick Then

Sum_Res = Sum_Res - Unit_Res
Sum_Unit_Thick = Sum_Unit_Thick - Unit_Thick

Unit_Res = (Abs(4000 - Sum_Unit_Thick) / Unit_Thick) * ((1 / Unit_Cond) * Unit_Thick)

Sum_Res = Sum_Res + Unit_Res
K_Avg = 4000 / Sum_Res

Break = 1

Else

Unit_Cond = Sheets("Strat_Column").Cells(d + 3, 5).Value
Unit_Thick = Sheets("Strat_Column").Cells(d + 3, 4).Value * Db / Sed_Column
Unit_Res = Unit_Thick / Unit_Cond

Break = 0

Sum_Unit_Thick = Sum_Unit_Thick + Unit_Thick
Sum_Res = Sum_Res + Unit_Res

d = d + 1
```

```
End If

Loop

m = (4000 * Qs / K_Avg - A_s * 4000 ^ 2 / (2 * K_Avg))  'T4km
n = ((Qs - A_s) * (Dc - 4000) / Ksed - A_s * ((Dc - 4000) ^ 2) / (2 * Ksed)) 'Tb4

T_Calc = Ts + m + n 'Equation 6
End If
Else
Do While Break < 1

If 4000 < Sum_Unit_Thick Then

Sum_Res = Sum_Res - Unit_Res
Sum_Unit_Thick = Sum_Unit_Thick - Unit_Thick

Unit_Res = (Abs(4000 - Sum_Unit_Thick) / Unit_Thick) * ((1 / Unit_Cond) * Unit_Thick)

Sum_Res = Sum_Res + Unit_Res
K_Avg = 4000 / Sum_Res

Break = 1

Else

Unit_Cond = Sheets("Strat_Column").Cells(d + 3, 5).Value
Unit_Thick = Sheets("Strat_Column").Cells(d + 3, 4).Value * Db / Sed_Column
Unit_Res = Unit_Thick / Unit_Cond
```

```
Break = 0

Sum_Unit_Thick = Sum_Unit_Thick + Unit_Thick
Sum_Res = Sum_Res + Unit_Res

d = d + 1

End If

Loop

m = (4000 * Qs / K_Avg - A_s * 4000 ^ 2 / (2 * K_Avg))  'T4km
n = ((Qs - A_s) * (Dc - 4000) / Ksed - A_s * ((Dc - 4000) ^ 2) / (2 * Ksed)) 'Tb4

T_Calc = Ts + m + n 'Equation 7
End If
End If

Else
If Dw < Dc Then
l = (Qs * Dw / K_Well - A_s * Dw ^ 2 / (2 * K_Well)) 'Tw

Do While Break < 1

If Dc < Sum_Unit_Thick Then

Sum_Res = Sum_Res - Unit_Res
Sum_Unit_Thick = Sum_Unit_Thick - Unit_Thick
```

```
Unit_Res = (Abs(Dc - Sum_Unit_Thick) / Unit_Thick) * ((1 / Unit_Cond) * Unit_Thick)

Sum_Res = Sum_Res + Unit_Res
K_Avg = Dc / Sum_Res

Break = 1

Else

Unit_Cond = Sheets("Strat_Column").Cells(d + 3, 5).Value
Unit_Thick = Sheets("Strat_Column").Cells(d + 3, 4).Value * Db / Sed_Column
Unit_Res = Unit_Thick / Unit_Cond

Break = 0

Sum_Unit_Thick = Sum_Unit_Thick + Unit_Thick
Sum_Res = Sum_Res + Unit_Res

d = d + 1

End If

Loop

Kbb = K_Avg

o = (Qs * (Dc - Dw) / Kbb - A_s * (Dc - Dw) ^ 2 / (2 * Kbb)) 'Tbb
```

```
T_Calc = Ts + l + o 'Equation 8
Else
Do While Break < 1

If Dc < Sum_Unit_Thick Then

Sum_Res = Sum_Res - Unit_Res
Sum_Unit_Thick = Sum_Unit_Thick - Unit_Thick

Unit_Res = (Abs(Dc - Sum_Unit_Thick) / Unit_Thick) * ((1 / Unit_Cond) * Unit_Thick)

Sum_Res = Sum_Res + Unit_Res
K_Avg = Dc / Sum_Res

Break = 1

Else

Unit_Cond = Sheets("Strat_Column").Cells(d + 3, 5).Value
Unit_Thick = Sheets("Strat_Column").Cells(d + 3, 4).Value * Db / Sed_Column
Unit_Res = Unit_Thick / Unit_Cond

Break = 0

Sum_Unit_Thick = Sum_Unit_Thick + Unit_Thick
Sum_Res = Sum_Res + Unit_Res

d = d + 1
```

```
End If

Loop
p = (Qs * Dc / K_Avg - A_s * Dc ^ 2 / (2 * K_Avg)) 'Tw

T_Calc = Ts + p 'Equation 9
End If

End If

Else

If Db < Dc Then
If Dw < Db Then
l = (Qs * Dw / K_Well - A_s * Dw ^ 2 / (2 * K_Well)) 'Tw

Do While Eps > 0.01

Unit_Cond = Sheets("Strat_Column").Cells(d + 3, 5).Value
Unit_Thick = Sheets("Strat_Column").Cells(d + 3, 4).Value * Db / Sed_Column
Unit_Res = Unit_Thick / Unit_Cond
Sum_Unit_Thick = Sum_Unit_Thick + Unit_Thick
Sum_Res = Sum_Res + Unit_Res

d = d + 1

Eps = (Db - Sum_Unit_Thick) / Db

Loop
```

```
K_Avg = Sum_Unit_Thick / Sum_Res
Kbb = (K_Avg * Db - K_Well * Dw) / (Db - Dw)

q = (Qs * (Db - Dw) / Kbb - A_s * (Db - Dw) ^ 2 / (2 * Kbb)) 'Tbb
z = (Qm * (Dc - Db) / Kb + A_b * (b) ^ 2 * ((1 - Exp(-(Dc - Db) / (b))) / Kb)) 'Tbx


T_Calc = Ts + l + q + z 'Equation 10
Else

Do While Eps > 0.01

Unit_Cond = Sheets("Strat_Column").Cells(d + 3, 5).Value
Unit_Thick = Sheets("Strat_Column").Cells(d + 3, 4).Value * Db / Sed_Column
Unit_Res = Unit_Thick / Unit_Cond
Sum_Unit_Thick = Sum_Unit_Thick + Unit_Thick
Sum_Res = Sum_Res + Unit_Res

d = d + 1

Eps = (Db - Sum_Unit_Thick) / Db

Loop

K_Avg = Sum_Unit_Thick / Sum_Res

l = (Qs * Dw / K_Avg - A_s * Dw ^ 2 / (2 * K_Avg)) 'Tsed
z = (Qm * (Dc - Db) / Kb + A_b * (b) ^ 2 * ((1 - Exp(-(Dc - Db) / (b))) / Kb))  'Tbx
```

```
T_Calc = Ts + l + z 'Equation 11
End If
Else
If Dw < Dc Then

Do While Eps > 0.01

Unit_Cond = Sheets("Strat_Column").Cells(d + 3, 5).Value
Unit_Thick = Sheets("Strat_Column").Cells(d + 3, 4).Value * Db / Sed_Column
Unit_Res = Unit_Thick / Unit_Cond
Sum_Unit_Thick = Sum_Unit_Thick + Unit_Thick
Sum_Res = Sum_Res + Unit_Res

d = d + 1

Eps = (Db - Sum_Unit_Thick) / Db

Loop

K_Avg = Sum_Unit_Thick / Sum_Res
Kbb = (K_Avg * Db - K_Well * Dw) / (Db - Dw)


l = (Qs * Dw / K_Well - A_s * Dw ^ 2 / (2 * K_Well)) 'Tw
o = (Qs * (Dc - Dw) / Kbb - A_s * (Dc - Dw) ^ 2 / (2 * Kbb)) 'Tbbx


T_Calc = Ts + l + o 'Equation 12
```

```
Else
Do While Break < 1

If Dc < Sum_Unit_Thick Then

Sum_Res = Sum_Res - Unit_Res
Sum_Unit_Thick = Sum_Unit_Thick - Unit_Thick

Unit_Res = (Abs(Dc - Sum_Unit_Thick) / Unit_Thick) * ((1 / Unit_Cond) * Unit_Thick)

Sum_Res = Sum_Res + Unit_Res
K_Avg = Dc / Sum_Res

Break = 1

Else

Unit_Cond = Sheets("Strat_Column").Cells(d + 3, 5).Value
Unit_Thick = Sheets("Strat_Column").Cells(d + 3, 4).Value * Db / Sed_Column
Unit_Res = Unit_Thick / Unit_Cond

Break = 0

Sum_Unit_Thick = Sum_Unit_Thick + Unit_Thick
Sum_Res = Sum_Res + Unit_Res

d = d + 1

End If
```

```
Loop


t = (Qs * (Dc) / K_Avg - A_s * (Dc) ^ 2 / (2 * K_Avg))

T_Calc = Ts + t 'Equation 13

End If
End If

End If

Else

If Db < Dc Then

If Dw < Db Then
l = (Qs * Dw / K_Well - A_s * Dw ^ 2 / (2 * K_Well)) 'Tw

Do While Eps > 0.01

Unit_Cond = Sheets("Strat_Column").Cells(d + 3, 5).Value
Unit_Thick = Sheets("Strat_Column").Cells(d + 3, 4).Value * Db / Sed_Column
Unit_Res = Unit_Thick / Unit_Cond
Sum_Unit_Thick = Sum_Unit_Thick + Unit_Thick
Sum_Res = Sum_Res + Unit_Res

d = d + 1
```

```
Eps = (Db - Sum_Unit_Thick) / Db

Loop

K_Avg = Sum_Unit_Thick / Sum_Res
Kbb = (K_Avg * Db - K_Well * Dw) / (Db - Dw)


q = (Qs * (Db - Dw) / Kbb - A_s * (Db - Dw) ^ 2 / (2 * Kbb)) 'Tbb
u = (Qm * (Dc - Db) / Kb + A_b * (b) ^ 2 * ((1 - Exp(-(Dc - Db) / (b))) / Kb)) 'Tbx


T_Calc = Ts + l + q + u 'Equation 14
Else
Do While Eps > 0.01

Unit_Cond = Sheets("Strat_Column").Cells(d + 3, 5).Value
Unit_Thick = Sheets("Strat_Column").Cells(d + 3, 4).Value * Db / Sed_Column
Unit_Res = Unit_Thick / Unit_Cond
Sum_Unit_Thick = Sum_Unit_Thick + Unit_Thick
Sum_Res = Sum_Res + Unit_Res

d = d + 1

Eps = (Db - Sum_Unit_Thick) / Db

Loop
```

```
K_Avg = Sum_Unit_Thick / Sum_Res

s = (Qs * Db / K_Avg - A_s * Db ^ 2 / (2 * K_Avg)) 'Tsed
u = (Qm * (Dc - Db) / Kb + A_b * (b) ^ 2 * ((1 - Exp(-(Dc - Db) / (b))) / Kb)) 'Tb


T_Calc = Ts + s + u 'Equation 15
End If

Else

If Dw < Dc Then

l = (Qs * Dw / K_Well - A_s * Dw ^ 2 / (2 * K_Well)) 'Tw


Do While Break < 1

If Dc < Sum_Unit_Thick Then

Sum_Res = Sum_Res - Unit_Res
Sum_Unit_Thick = Sum_Unit_Thick - Unit_Thick

Unit_Res = (Abs(Dc - Sum_Unit_Thick) / Unit_Thick) * ((1 / Unit_Cond) * Unit_Thick)

Sum_Res = Sum_Res + Unit_Res
K_Avg = Dc / Sum_Res

Break = 1
```

```
Else

Unit_Cond = Sheets("Strat_Column").Cells(d + 3, 5).Value
Unit_Thick = Sheets("Strat_Column").Cells(d + 3, 4).Value * Db / Sed_Column
Unit_Res = Unit_Thick / Unit_Cond

Break = 0

Sum_Unit_Thick = Sum_Unit_Thick + Unit_Thick
Sum_Res = Sum_Res + Unit_Res

d = d + 1

End If

Loop


Kbb = (K_Avg * Dc - K_Well * Dw) / (Dc - Dw)

t = (Qs * (Dc - Dw) / Kbb - A_s * (Dc - Dw) ^ 2 / (2 * Kbb)) 'Tbb


T_Calc = Ts + l + t 'Equation 16

Else
Do While Break < 1
```

```
If Dc < Sum_Unit_Thick Then

Sum_Res = Sum_Res - Unit_Res
Sum_Unit_Thick = Sum_Unit_Thick - Unit_Thick

Unit_Res = (Abs(Dc - Sum_Unit_Thick) / Unit_Thick) * ((1 / Unit_Cond) * Unit_Thick)

Sum_Res = Sum_Res + Unit_Res
K_Avg = Dc / Sum_Res

Break = 1

Else

Unit_Cond = Sheets("Strat_Column").Cells(d + 3, 5).Value
Unit_Thick = Sheets("Strat_Column").Cells(d + 3, 4).Value * Db / Sed_Column
Unit_Res = Unit_Thick / Unit_Cond

Break = 0

Sum_Unit_Thick = Sum_Unit_Thick + Unit_Thick
Sum_Res = Sum_Res + Unit_Res

d = d + 1

End If

Loop
```

```
p = (Qs * Dc / K_Avg - A_s * Dc ^ 2 / (2 * K_Avg)) 'Tw

T_Calc = Ts + p  'Equation 17
End If

End If

End If

Else

T_Calc = Ts + (Qs * Dc / Kb - A_b * Dc ^ 2 / (2 * Kb)) 'Equation 1

End If


Cells(9 + i, 12 + c).Value = T_Calc

c = c + 1
Loop

Secondary Loop to find the depth to an isothermal Surface.

delta_T = 1
D_Guess = (T_Iso / Gradient) * 1000
Do While delta_T > 0.001
```

```
'Note all depth inputs are expected in m,
conductivities in W/m/k, heat flows in mW/m^2,
radiogenic heat generation in microW/m^3

'Prepare and convert function inputs to SI units for use in calculating temperatures
Ts = T_surf
Qm = Q_Mantle * 10 ^ -3
Qs = Heat_Flow * 10 ^ -3
Db = Sed_Well
Dc = D_Guess
Dw = Well_Depth
Kb = K_Base
Ksed = K_DeepSed
A_s = Sed_Radio * 10 ^ -6
A_b = Basement_Radio * 10 ^ -6
'Counters that must be reset before calculation of each temperature value
Eps = 1
d = 0
Sum_Unit_Thick = 0
Sum_Res = 0
Break = 0
'Varible crustal thickness based on depth of sedimentary cover
If Db > 3000 Then
b = 13000 - Db
Else
b = 10000
End If
```

```
'Series of If Statements to figure out what
 conditions the well and calculation
 parameters fit into and then loop to
 calculate the appropriate thermal
 conductivities. Once the conductivities
 are found use those to calculate the
 expected T at the specified depth.
If Db > 0 Then
If Db > 3000 Then

If Db > 4000 Then

If Dc > 4000 Then
If Db < Dc Then
If Dw < Db Then
If Dw < 4000 Then
l = (Qs * Dw / K_Well - A_s * Dw ^ 2 / (2 * K_Well)) 'Tw

Do While Break < 1

If 4000 < Sum_Unit_Thick Then

Sum_Res = Sum_Res - Unit_Res
Sum_Unit_Thick = Sum_Unit_Thick - Unit_Thick

Unit_Res = (Abs(4000 - Sum_Unit_Thick) / Unit_Thick) * ((1 / Unit_Cond) * Unit_Thick)

Sum_Res = Sum_Res + Unit_Res
```

```
K_Avg = 4000 / Sum_Res

Break = 1

Else

Unit_Cond = Sheets("Strat_Column").Cells(d + 3, 5).Value
Unit_Thick = Sheets("Strat_Column").Cells(d + 3, 4).Value * Db / Sed_Column
Unit_Res = Unit_Thick / Unit_Cond

Break = 0

Sum_Unit_Thick = Sum_Unit_Thick + Unit_Thick
Sum_Res = Sum_Res + Unit_Res

d = d + 1

End If

Loop

Kbb = (K_Avg * 4000 - K_Well * Dw) / (4000 - Dw)

h = (Qs * (4000 - Dw) / Kbb - A_s * (4000 - Dw) ^ 2 / (2 * Kbb)) 'Tw4
j = ((Qs - A_s) * (Db - 4000) / Ksed - A_s * ((Db - 4000) ^ 2) / (2 * Ksed)) 'Tb4
z = (Qm * (Dc - Db) / Kb + A_b * (b) ^ 2 * ((1 - Exp(-(Dc - Db) / (b))) / Kb)) 'Tbx

T_Calc = Ts + l + h + j + z 'Equation 2
```

```
Else

Do While Break < 1

If 4000 < Sum_Unit_Thick Then

Sum_Res = Sum_Res - Unit_Res
Sum_Unit_Thick = Sum_Unit_Thick - Unit_Thick

Unit_Res = (Abs(4000 - Sum_Unit_Thick) / Unit_Thick) * ((1 / Unit_Cond) * Unit_Thick)

Sum_Res = Sum_Res + Unit_Res
K_Avg = 4000 / Sum_Res

Break = 1

Else

Unit_Cond = Sheets("Strat_Column").Cells(d + 3, 5).Value
Unit_Thick = Sheets("Strat_Column").Cells(d + 3, 4).Value * Db / Sed_Column
Unit_Res = Unit_Thick / Unit_Cond

Break = 0

Sum_Unit_Thick = Sum_Unit_Thick + Unit_Thick
Sum_Res = Sum_Res + Unit_Res

d = d + 1
```

```
End If

Loop


m = (4000 * Qs / K_Avg - A_s * 4000 ^ 2 / (2 * K_Avg))  'T4km
j = ((Qs - A_s) * (Db - 4000) / Ksed - A_s * ((Db - 4000) ^ 2) / (2 * Ksed)) 'Tb4
z = (Qm * (Dc - Db) / Kb + A_b * (b) ^ 2 * ((1 - Exp(-(Dc - Db) / (b))) / Kb)) 'Tb


T_Calc = Ts + m + j + z 'Equation 3
End If

Else
Do While Break < 1

If 4000 < Sum_Unit_Thick Then

Sum_Res = Sum_Res - Unit_Res
Sum_Unit_Thick = Sum_Unit_Thick - Unit_Thick

Unit_Res = (Abs(4000 - Sum_Unit_Thick) / Unit_Thick) * ((1 / Unit_Cond) * Unit_Thick)

Sum_Res = Sum_Res + Unit_Res
K_Avg = 4000 / Sum_Res

Break = 1

Else
```

```
Unit_Cond = Sheets("Strat_Column").Cells(d + 3, 5).Value
Unit_Thick = Sheets("Strat_Column").Cells(d + 3, 4).Value * Db / Sed_Column
Unit_Res = Unit_Thick / Unit_Cond

Break = 0

Sum_Unit_Thick = Sum_Unit_Thick + Unit_Thick
Sum_Res = Sum_Res + Unit_Res

d = d + 1

End If

Loop

m = (4000 * Qs / K_Avg - A_s * 4000 ^ 2 / (2 * K_Avg))  'T4km
j = ((Qs - A_s) * (Dw - 4000) / Ksed - A_s * ((Dw - 4000) ^ 2) / (2 * Ksed)) 'Tb4
z = (Qm * (Dc - Db) / Kb + A_b * (b) ^ 2 * ((1 - Exp(-(Dc - Db) / (b))) / Kb)) 'Tb

T_Calc = Ts + m + j + z 'Equation 4
End If

Else
If Dw < Dc Then
If Dw < 4000 Then
l = (Qs * Dw / K_Well - A_s * Dw ^ 2 / (2 * K_Well)) 'Tw

Do While Break < 1
```

```
If 4000 < Sum_Unit_Thick Then

Sum_Res = Sum_Res - Unit_Res
Sum_Unit_Thick = Sum_Unit_Thick - Unit_Thick

Unit_Res = (Abs(4000 - Sum_Unit_Thick) / Unit_Thick) * ((1 / Unit_Cond) * Unit_Thick)

Sum_Res = Sum_Res + Unit_Res
K_Avg = 4000 / Sum_Res

Break = 1

Else

Unit_Cond = Sheets("Strat_Column").Cells(d + 3, 5).Value
Unit_Thick = Sheets("Strat_Column").Cells(d + 3, 4).Value * Db / Sed_Column
Unit_Res = Unit_Thick / Unit_Cond

Break = 0

Sum_Unit_Thick = Sum_Unit_Thick + Unit_Thick
Sum_Res = Sum_Res + Unit_Res

d = d + 1

End If

Loop
```

```
Kbb = (K_Avg * 4000 - K_Well * Dw) / (4000 - Dw)

h = (Qs * (4000 - Dw) / Kbb - A_s * (4000 - Dw) ^ 2 / (2 * Kbb)) 'Tw4
n = ((Qs - A_s) * (Dc - 4000) / Ksed - A_s * ((Dc - 4000) ^ 2) / (2 * Ksed)) 'Tb4

T_Calc = Ts + l + h + n 'Equation 5
Else

Do While Break < 1

If 4000 < Sum_Unit_Thick Then

Sum_Res = Sum_Res - Unit_Res
Sum_Unit_Thick = Sum_Unit_Thick - Unit_Thick

Unit_Res = (Abs(4000 - Sum_Unit_Thick) / Unit_Thick) * ((1 / Unit_Cond) * Unit_Thick)

Sum_Res = Sum_Res + Unit_Res
K_Avg = 4000 / Sum_Res

Break = 1

Else

Unit_Cond = Sheets("Strat_Column").Cells(d + 3, 5).Value
Unit_Thick = Sheets("Strat_Column").Cells(d + 3, 4).Value * Db / Sed_Column
Unit_Res = Unit_Thick / Unit_Cond
Break = 0
```

```
Sum_Unit_Thick = Sum_Unit_Thick + Unit_Thick
Sum_Res = Sum_Res + Unit_Res

d = d + 1

End If

Loop

m = (4000 * Qs / K_Avg - A_s * 4000 ^ 2 / (2 * K_Avg))  'T4km
n = ((Qs - A_s) * (Dc - 4000) / Ksed - A_s * ((Dc - 4000) ^ 2) / (2 * Ksed)) 'Tb4

T_Calc = Ts + m + n 'Equation 6
End If
Else
Do While Break < 1

If 4000 < Sum_Unit_Thick Then

Sum_Res = Sum_Res - Unit_Res
Sum_Unit_Thick = Sum_Unit_Thick - Unit_Thick

Unit_Res = (Abs(4000 - Sum_Unit_Thick) / Unit_Thick) * ((1 / Unit_Cond) * Unit_Thick)

Sum_Res = Sum_Res + Unit_Res
K_Avg = 4000 / Sum_Res

Break = 1
```

```
Else

Unit_Cond = Sheets("Strat_Column").Cells(d + 3, 5).Value
Unit_Thick = Sheets("Strat_Column").Cells(d + 3, 4).Value * Db / Sed_Column
Unit_Res = Unit_Thick / Unit_Cond

Break = 0

Sum_Unit_Thick = Sum_Unit_Thick + Unit_Thick
Sum_Res = Sum_Res + Unit_Res

d = d + 1

End If

Loop

m = (4000 * Qs / K_Avg - A_s * 4000 ^ 2 / (2 * K_Avg))  'T4km
n = ((Qs - A_s) * (Dc - 4000) / Ksed - A_s * ((Dc - 4000) ^ 2) / (2 * Ksed)) 'Tb4

T_Calc = Ts + m + n 'Equation 7
End If
End If

Else
If Dw < Dc Then
l = (Qs * Dw / K_Well - A_s * Dw ^ 2 / (2 * K_Well)) 'Tw
```

```
Do While Break < 1

If Dc < Sum_Unit_Thick Then

Sum_Res = Sum_Res - Unit_Res
Sum_Unit_Thick = Sum_Unit_Thick - Unit_Thick

Unit_Res = (Abs(Dc - Sum_Unit_Thick) / Unit_Thick) * ((1 / Unit_Cond) * Unit_Thick)

Sum_Res = Sum_Res + Unit_Res
K_Avg = Dc / Sum_Res

Break = 1

Else

Unit_Cond = Sheets("Strat_Column").Cells(d + 3, 5).Value
Unit_Thick = Sheets("Strat_Column").Cells(d + 3, 4).Value * Db / Sed_Column
Unit_Res = Unit_Thick / Unit_Cond

Break = 0

Sum_Unit_Thick = Sum_Unit_Thick + Unit_Thick
Sum_Res = Sum_Res + Unit_Res

d = d + 1

End If
```

```
Loop

Kbb = K_Avg

o = (Qs * (Dc - Dw) / Kbb - A_s * (Dc - Dw) ^ 2 / (2 * Kbb)) 'Tbb

T_Calc = Ts + l + o 'Equation 8
Else
Do While Break < 1

If Dc < Sum_Unit_Thick Then

Sum_Res = Sum_Res - Unit_Res
Sum_Unit_Thick = Sum_Unit_Thick - Unit_Thick

Unit_Res = (Abs(Dc - Sum_Unit_Thick) / Unit_Thick) * ((1 / Unit_Cond) * Unit_Thick)

Sum_Res = Sum_Res + Unit_Res
K_Avg = Dc / Sum_Res

Break = 1

Else

Unit_Cond = Sheets("Strat_Column").Cells(d + 3, 5).Value
Unit_Thick = Sheets("Strat_Column").Cells(d + 3, 4).Value * Db / Sed_Column
Unit_Res = Unit_Thick / Unit_Cond

Break = 0
```

```
Sum_Unit_Thick = Sum_Unit_Thick + Unit_Thick
Sum_Res = Sum_Res + Unit_Res

d = d + 1

End If

Loop
p = (Qs * Dc / K_Avg - A_s * Dc ^ 2 / (2 * K_Avg)) 'Tw

T_Calc = Ts + p 'Equation 9
End If

End If

Else

If Db < Dc Then
If Dw < Db Then
l = (Qs * Dw / K_Well - A_s * Dw ^ 2 / (2 * K_Well)) 'Tw

Do While Eps > 0.01

Unit_Cond = Sheets("Strat_Column").Cells(d + 3, 5).Value
Unit_Thick = Sheets("Strat_Column").Cells(d + 3, 4).Value * Db / Sed_Column
Unit_Res = Unit_Thick / Unit_Cond
Sum_Unit_Thick = Sum_Unit_Thick + Unit_Thick
Sum_Res = Sum_Res + Unit_Res
```

```
d = d + 1

Eps = (Db - Sum_Unit_Thick) / Db

Loop

K_Avg = Sum_Unit_Thick / Sum_Res
Kbb = (K_Avg * Db - K_Well * Dw) / (Db - Dw)

q = (Qs * (Db - Dw) / Kbb - A_s * (Db - Dw) ^ 2 / (2 * Kbb)) 'Tbb
z = (Qm * (Dc - Db) / Kb + A_b * (b) ^ 2 * ((1 - Exp(-(Dc - Db) / (b))) / Kb)) 'Tbx


T_Calc = Ts + l + q + z 'Equation 10
Else

Do While Eps > 0.01

Unit_Cond = Sheets("Strat_Column").Cells(d + 3, 5).Value
Unit_Thick = Sheets("Strat_Column").Cells(d + 3, 4).Value * Db / Sed_Column
Unit_Res = Unit_Thick / Unit_Cond
Sum_Unit_Thick = Sum_Unit_Thick + Unit_Thick
Sum_Res = Sum_Res + Unit_Res

d = d + 1

Eps = (Db - Sum_Unit_Thick) / Db
```

```
Loop

K_Avg = Sum_Unit_Thick / Sum_Res

l = (Qs * Dw / K_Avg - A_s * Dw ^ 2 / (2 * K_Avg)) 'Tsed
z = (Qm * (Dc - Db) / Kb + A_b * (b) ^ 2 * ((1 - Exp(-(Dc - Db) / (b))) / Kb))  'Tbx

T_Calc = Ts + l + z 'Equation 11
End If
Else
If Dw < Dc Then

Do While Eps > 0.01

Unit_Cond = Sheets("Strat_Column").Cells(d + 3, 5).Value
Unit_Thick = Sheets("Strat_Column").Cells(d + 3, 4).Value * Db / Sed_Column
Unit_Res = Unit_Thick / Unit_Cond
Sum_Unit_Thick = Sum_Unit_Thick + Unit_Thick
Sum_Res = Sum_Res + Unit_Res

d = d + 1

Eps = (Db - Sum_Unit_Thick) / Db

Loop

K_Avg = Sum_Unit_Thick / Sum_Res
Kbb = (K_Avg * Db - K_Well * Dw) / (Db - Dw)
```

```
l = (Qs * Dw / K_Well - A_s * Dw ^ 2 / (2 * K_Well)) 'Tw
o = (Qs * (Dc - Dw) / Kbb - A_s * (Dc - Dw) ^ 2 / (2 * Kbb)) 'Tbbx


T_Calc = Ts + l + o 'Equation 12
Else
Do While Break < 1

If Dc < Sum_Unit_Thick Then

Sum_Res = Sum_Res - Unit_Res
Sum_Unit_Thick = Sum_Unit_Thick - Unit_Thick

Unit_Res = (Abs(Dc - Sum_Unit_Thick) / Unit_Thick) * ((1 / Unit_Cond) * Unit_Thick)

Sum_Res = Sum_Res + Unit_Res
K_Avg = Dc / Sum_Res

Break = 1

Else

Unit_Cond = Sheets("Strat_Column").Cells(d + 3, 5).Value
Unit_Thick = Sheets("Strat_Column").Cells(d + 3, 4).Value * Db / Sed_Column
Unit_Res = Unit_Thick / Unit_Cond

Break = 0
```

```
Sum_Unit_Thick = Sum_Unit_Thick + Unit_Thick
Sum_Res = Sum_Res + Unit_Res

d = d + 1

End If

Loop

t = (Qs * (Dc) / K_Avg - A_s * (Dc) ^ 2 / (2 * K_Avg))

T_Calc = Ts + t 'Equation 13


End If
End If
End If
Else

If Db < Dc Then

If Dw < Db Then
l = (Qs * Dw / K_Well - A_s * Dw ^ 2 / (2 * K_Well)) 'Tw

Do While Eps > 0.01

Unit_Cond = Sheets("Strat_Column").Cells(d + 3, 5).Value
Unit_Thick = Sheets("Strat_Column").Cells(d + 3, 4).Value * Db / Sed_Column
Unit_Res = Unit_Thick / Unit_Cond
```

```
Sum_Unit_Thick = Sum_Unit_Thick + Unit_Thick
Sum_Res = Sum_Res + Unit_Res

d = d + 1

Eps = (Db - Sum_Unit_Thick) / Db

Loop

K_Avg = Sum_Unit_Thick / Sum_Res
Kbb = (K_Avg * Db - K_Well * Dw) / (Db - Dw)


q = (Qs * (Db - Dw) / Kbb - A_s * (Db - Dw) ^ 2 / (2 * Kbb)) 'Tbb
u = (Qm * (Dc - Db) / Kb + A_b * (b) ^ 2 * ((1 - Exp(-(Dc - Db) / (b))) / Kb)) 'Tbx


T_Calc = Ts + l + q + u 'Equation 14
Else
Do While Eps > 0.01

Unit_Cond = Sheets("Strat_Column").Cells(d + 3, 5).Value
Unit_Thick = Sheets("Strat_Column").Cells(d + 3, 4).Value * Db / Sed_Column
Unit_Res = Unit_Thick / Unit_Cond
Sum_Unit_Thick = Sum_Unit_Thick + Unit_Thick
Sum_Res = Sum_Res + Unit_Res

d = d + 1
```

```
Eps = (Db - Sum_Unit_Thick) / Db

Loop

K_Avg = Sum_Unit_Thick / Sum_Res

s = (Qs * Db / K_Avg - A_s * Db ^ 2 / (2 * K_Avg)) 'Tsed
u = (Qm * (Dc - Db) / Kb + A_b * (b) ^ 2 * ((1 - Exp(-(Dc - Db) / (b))) / Kb)) 'Tb


T_Calc = Ts + s + u 'Equation 15
End If

Else

If Dw < Dc Then

l = (Qs * Dw / K_Well - A_s * Dw ^ 2 / (2 * K_Well)) 'Tw


Do While Break < 1

If Dc < Sum_Unit_Thick Then

Sum_Res = Sum_Res - Unit_Res
Sum_Unit_Thick = Sum_Unit_Thick - Unit_Thick

Unit_Res = (Abs(Dc - Sum_Unit_Thick) / Unit_Thick) * ((1 / Unit_Cond) * Unit_Thick)
```

```
Sum_Res = Sum_Res + Unit_Res
K_Avg = Dc / Sum_Res

Break = 1

Else

Unit_Cond = Sheets("Strat_Column").Cells(d + 3, 5).Value
Unit_Thick = Sheets("Strat_Column").Cells(d + 3, 4).Value * Db / Sed_Column
Unit_Res = Unit_Thick / Unit_Cond

Break = 0

Sum_Unit_Thick = Sum_Unit_Thick + Unit_Thick
Sum_Res = Sum_Res + Unit_Res

d = d + 1

End If

Loop


Kbb = (K_Avg * Dc - K_Well * Dw) / (Dc - Dw)

t = (Qs * (Dc - Dw) / Kbb - A_s * (Dc - Dw) ^ 2 / (2 * Kbb)) 'Tbb


T_Calc = Ts + l + t 'Equation 16
```

```
Else
Do While Break < 1

If Dc < Sum_Unit_Thick Then

Sum_Res = Sum_Res - Unit_Res
Sum_Unit_Thick = Sum_Unit_Thick - Unit_Thick

Unit_Res = (Abs(Dc - Sum_Unit_Thick) / Unit_Thick) * ((1 / Unit_Cond) * Unit_Thick)

Sum_Res = Sum_Res + Unit_Res
K_Avg = Dc / Sum_Res

Break = 1

Else

Unit_Cond = Sheets("Strat_Column").Cells(d + 3, 5).Value
Unit_Thick = Sheets("Strat_Column").Cells(d + 3, 4).Value * Db / Sed_Column
Unit_Res = Unit_Thick / Unit_Cond

Break = 0

Sum_Unit_Thick = Sum_Unit_Thick + Unit_Thick
Sum_Res = Sum_Res + Unit_Res

d = d + 1
```

```
End If
Loop

p = (Qs * Dc / K_Avg - A_s * Dc ^ 2 / (2 * K_Avg)) 'Tw
T_Calc = Ts + p  'Equation 17
End If

End If

End If

Else

T_Calc = Ts + (Qs * Dc / Kb - A_b * Dc ^ 2 / (2 * Kb)) 'Equation 1

End If

delta_T = (T_Calc - T_Iso) / T_Iso
D_Guess = (T_Iso / T_Calc) * D_Guess
Loop
Cells(9 + i, 18).Value = D_Guess
i = i + 1
BHT = Cells(9 + i, 2).Value
Loop
End Sub
```